THE ASTROPHYSICAL JOURNAL SUPPLEMENT SERIES, 65:485–541, 1987 December

A 1.49 GHz ATLAS OF SPIRAL GALAXIES WITH $B_T \leq +12$ AND $\delta \geq -45°$

J. J. CONDON
National Radio Astronomy Observatory[1]
Received 1987 April 24; accepted 1987 July 9

ABSTRACT

The VLA has been used in its most compact D- and C/D-configurations to make low-resolution ($\theta \approx 0\rlap{.}'9$ FWHM) 1.49 GHz maps of the spiral galaxies north of $\delta = -45°$ and brighter than $B_T = +12$, the completeness limit of the *Revised Shapley-Ames Catalog*. Most of these maps are confusion-limited at $\sigma \geq 0.1$ mJy per beam, and at least 94% of the galaxies were detected with $S \geq 1$ mJy. The maps have sufficient sensitivity to low-brightness emission that accurate radio "photometry" is possible. An atlas of contour maps, a table of total flux densities plus other radio source parameters, and references to published radio maps are given.

Subject headings: galaxies: structure — radio sources: galaxies

I. INTRODUCTION

There are 335 spiral galaxies in the *Revised Shapley-Ames Catalog* (Sandage and Tammann 1981, hereafter RSA) brighter than its $B_T = +12$ completeness limit (Sandage, Tammann, and Yahil 1979); only 27 of them lie south of $\delta = -45°$. Nearly all should be radio sources at some level, emitting thermal radiation from H II regions and synchrotron radiation from cosmic-ray electrons accelerated by supernova remnants or possibly by X-ray binaries. Yet most have never been mapped, or even detected, at radio wavelengths because their radio emission is both faint (low flux density) and diffuse (low surface brightness). Consequently, observational studies of radio continuum emission from "normal" spiral galaxies have been biased toward those galaxies containing either strong or compact sources; very little is known about the majority of spiral galaxies that are only weak radio emitters.

The 1415 MHz Westerbork fan-beam survey (Hummel 1980) first showed that the continuum emission from the stronger radio sources in a magnitude-limited sample of spiral galaxies typically consists of two major components — one roughly coextensive with the optical disk and, in some galaxies, a much more compact central source. Thus the global radio structures of many spiral galaxies can be defined with moderately low-resolution observations, i.e., FWHM beamwidth θ about equal to the exponential scale length of the optical disk. Unfortunately, filled-aperture telescopes do not have even this much resolving power on any but the nearest galaxies, and two-dimensional aperture-synthesis maps generally have not had the necessary surface brightness sensitivity ($T_B \ll 1$ K at 1.49 GHz) to map the entire disk component.

The NRAO Very Large Array (VLA) in its D- and C/D-configurations *can* make low-resolution ($\theta \approx 0\rlap{.}'9$) 1.49 GHz maps of the brightest spirals north of $\delta = -45°$ with sufficient surface brightness sensitivity. The rms map noise after 8 minutes of integration is only about 0.1 mJy per beam, or 0.02 K. Nearly all of the galaxy flux appears to be contained within contours brighter than the sensitivity limits of such maps, so that accurate total flux densities S and basic structural parameters (source position, size, and orientation) can be obtained. Flux densities from this paper and the supplementary atlas of fainter spiral galaxies with *H*-magnitudes (Condon, Yin, and Burstein 1987) have been used to study the relationship between stellar population and radio continuum emission in spiral galaxies (Burstein, Condon, and Yin 1987).

This paper presents 1.49 GHz continuum maps, total flux densities, and component parameters for the spiral galaxies brighter than $B_T = +12$ and north of $\delta = -45°$.

II. THE OPTICAL GALAXY SAMPLE

The principal sample comprises 307 spiral galaxies with $B_T \leq +12$ and $\delta \geq -45°$ in the RSA, either in the main catalog (Part II) or in the table of missing galaxies brighter than $B_T = +12$ (Part IV). The galaxy NGC 1316 identified with the strong radio source Fornax A was excluded, as it is probably not a spiral galaxy. Seven galaxies (IC 1727, NGC 784, NGC 1337, NGC 1560, NGC 2541, NGC 5023, and NGC 6140) were added to this magnitude-limited sample to complete a diameter-limited sample of 125 galaxies with $D_{25} \geq 6'$ and $\delta \geq -45°$. Table 1 lists all of these galaxies as follows:

Column (1).—Galaxy name.

Columns (2) and (3).—Optical position (equinox 1950.0) taken from Dressel and Condon (1976) for $\delta \geq -2\rlap{.}°5$, from Gallouët, Heidmann, and Dampierre (1975) for $-33° \leq \delta < -2\rlap{.}°5$, or measured with overlays on the Palomar Observatory Sky Survey prints and UK Schmidt Southern Sky Survey film copies. The rms uncertainties in these coordinates are usually 4″, but they can be much bigger for large or irregular galaxies.

Column (4).—Apparent blue (B_T) magnitude from the RSA.

Column (5).—Optical major diameter D_{25} and minor diameter d_{25} of the 25 mag arcsec^{-2} isophote from the

[1]The National Radio Astronomy Observatory is operated by Associated Universities, Inc., under contract with the National Science Foundation.

TABLE 1

OPTICAL DATA

GALAXY NAME	R.A. (1950.0)	Decl. (1950.0)	B_T (mag)	$D_{25} \times d_{25}$	*P.A.*	*D* (Mpc)	$M_{B_T}^{0,i}$ (mag)	RC2 TYPE	RSAC TYPE
NGC 7814	$00^h00^m41^s.1$	+15°52′03″	11.35	6′.3 × 2′.6	135°	25.8	−21.70	.SAS2*/	S(ab)
NGC 0045	00 11 31.8	−23 27 35	11.10	8.1 × 5.8	142	10.7	−19.45	.SAS8..	Scd(s)III
NGC 0055	00 12 24.3	−39 28 28	8.22	32.4 × 6.5	108	3.2	−20.15	.SBS9*/	Sc
IC 0010	00 17 41.4	+59 01 03	11.71	5.1 × 4.3		1.3	−16.20	.IB.9$.	Im?IV
NGC 0134	00 27 53.5	−33 31 23	10.96	8.1 × 2.6	50	31.9	−22.28	.SXS4..	Sbc(s)II-III:
NGC 0150	00 31 47.1	−28 04 50	11.75	4.2 × 2.3	118	32.4	−21.31	.SBT3*.	Sbc(s)II
NGC 0157	00 32 14.4	−08 40 20	11.04	4.3 × 2.9		36.3	−22.19	.SXT4..	Sc(s)I-II
NGC 0210	00 38 03.9	−14 08 48	11.65	5.4 × 3.7		37.5	−21.86	.SXS3..	Sb(rs)I
NGC 0224	00 40 00.3	+41 00 03	4.38	178. × 63.1	35	0.7	−21.61	.SAS3..	SbI-II
NGC 0247	00 44 39.8	−21 01 58	9.51	20.0 × 7.4	174	3.2	−18.62	.SXS7..	Sc(s)III-IV
NGC 0253	00 45 07.6	−25 33 39	8.13	25.1 × 7.4	52	4.2	−20.72	.SXS5..	Sc(s)
NGC 0278	00 49 14.8	+47 16 43	11.51	2.2 × 2.1		18.6	−20.50	.SXT3..	Sbc(s)II.2
NGC 0289	00 50 17.5	−31 28 39	11.81	3.7 × 2.7	130	36.7	−21.41	.SBT4..	SBbc(rs)I-II
NGC 0300	00 52 32.1	−37 57 25	8.70	20.0 × 14.8	111	2.4	−18.59	.SAS7..	ScII.8
IC 1613	01 02 19.8	+01 51 56	9.96	12.0 × 8.9		0.9	−14.81	.IXS9..	ImV
NGC 0428	01 10 21.1	+00 43 05	11.85	4.1 × 3.2	120	26.2	−20.61	.SXS9..	Sc(s)III
NGC 0488	01 19 11.2	+04 59 36	11.15	5.2 × 4.1	15	48.8	−22.86	.SAR3..	Sab(rs)I
NGC 0578	01 28 05.6	−22 55 27	11.48	4.8 × 3.2	110	33.5	−21.59	.SXT5..	Sc(s)I-II
NGC 0598	01 31 04.6	+30 23 40	6.26	61.7 × 38.9	23	0.9	−19.07	.SAS6..	Sc(s)II-III
NGC 0613	01 31 58.7	−29 40 19	10.75	5.8 × 4.6	120	30.7	−22.24	.SBT4..	SBb(rs)II
NGC 0628	01 34 00.7	+15 31 55	9.77	10.2 × 9.5		17.2	−21.75	.SAS5..	Sc(s)I
NGC 0660	01 40 20.7	+13 23 32	11.62	9.1 × 4.1	170	19.6	−20.79	.SBS1P.	
IC 1727	01 44 41.6	+27 04 55	12.13	6.2 × 2.9	150	10.6	−18.66	.SBS9..	
NGC 0672	01 45 04.2	+27 11 05	11.41	6.6 × 2.7	65	12.9	−19.87	.SBS6..	SBc(s)III
NGC 0772	01 56 35.3	+18 45 50	11.10	7.1 × 4.5	130	52.9	−23.29	.SAS3..	Sb(rs)I
NGC 0779	01 57 11.9	−06 12 19	11.86	4.1 × 1.4		29.8	−21.57	.SXR3..	Sb(rs)I-II
NGC 0784	01 58 25.0	+28 35 47	12.26	6.2 × 1.7	0	8.6	−17.93	.SB.7*/	Sdm
NGC 0864	02 12 49.8	+05 46 10	11.55	4.6 × 3.5	20	34.1	−21.50	.SXT5..	Sbc(r)II-III
NGC 0891	02 19 25.2	+42 07 18	10.95	13.5 × 2.8	22	15.6	−21.65	.SAS3$/	Sb on edge
NGC 0908	02 20 46.3	−21 27 42	10.87	5.5 × 2.8	75	31.3	−22.14	.SAS5..	Sc(s)I-II
NGC 0925	02 24 16.6	+33 21 20	10.59	9.8 × 6.0	115	15.8	−21.07	.SXS7..	SBc(s)II-III
NGC 0986	02 31 33.7	−39 15 49	11.80	3.7 × 2.8	150	40.1	−21.81	.SBT2..	SBb(rs)I-II
IC 0239	02 33 20.8	+38 45 08	11.93	4.6 × 4.3		21.3	−20.27	.SXT6..	
NGC 1042	02 37 56.3	−08 38 50	11.49	4.7 × 3.9		28.7	−21.15	.SXT6..	Sc(rs)I-II
NGC 1055	02 39 10.7	+00 13 45	11.42	7.6 × 3.0	105	22.0	−20.92	.SB.3*/	Sbc(s)II
NGC 1068	02 40 06.5	−00 13 32	9.55	6.9 × 5.9	70	24.7	−22.93	RSAT3..	Sb(rs)II
NGC 1073	02 41 05.6	+01 09 55	11.50	4.9 × 4.6		26.4	−20.90	.SBT5..	SBc(rs)II
NGC 1084	02 43 31.8	−07 47 08	11.25	2.9 × 1.5		29.6	−21.62	.SAS5..	Sc(s)II.2
NGC 1087	02 43 51.6	−00 42 19	11.56	3.5 × 2.3	0	32.6	−21.43	.SXT5..	Sc(s)III.3
NGC 1097	02 44 11.5	−30 29 06	10.16	9.3 × 6.6	130	25.7	−22.30	.SBS3..	RSBbc(rs)I-II
NGC 1187	03 00 23.8	−23 03 47	10.93	5.0 × 4.1		28.5	−21.70	.SBR5..	SBbc(s)I-II
NGC 1232	03 07 30.0	−20 46 13	10.50	7.8 × 6.9	108	35.5	−22.57	.SXT5..	Sc(rs)I
NGC 1255	03 11 22.5	−25 54 40	11.60	4.1 × 2.8	117	33.1	−21.42	.SXT4..	Sc(s)II
NGC 1291	03 15 28.7	−41 17 28	9.42	10.5 × 9.1		14.8	−21.68	RSBS0..	SBa
NGC 1300	03 17 25.2	−19 35 29	11.10	6.5 × 4.3	106	30.5	−21.99	.SBT4..	SBb(s)I.2
NGC 1302	03 17 $42^s.3$	−26°14 25	11.38	4′.4 × 4.2		33.3	−21.23	RSBS0..	Sa
NGC 1309	03 19 46.9	−15 34 40	12.00	2.3 × 2.2		42.9	−21.61	.SAS4*.	Sb(rs)II
NGC 1326	03 22 01.3	−36 38 29	11.34	4.0 × 3.0	77°	30.2	−21.06	RLBR+..	RSBa
NGC 1337	03 25 39.8	−08 33 46	12.28	6.8 × 2.0		25.4	−20.52	.SAS6..	Sc(s)I-II
NGC 1350	03 29 09.7	−33 47 53	11.40	4.3 × 2.4	0	30.2	−21.38	PSBR2..	Sa(r)
NGC 1365	03 31 41.4	−36 18 23	10.21	9.8 × 5.5	32	30.2	−22.95	.SBS3..	SBb(s)I
NGC 1371	03 32 52.7	−25 05 54	11.50	5.4 × 4.0	135	28.4	−20.76	.SXT1..	Sa(s)
NGC 1386	03 34 52.3	−36 09 52	12.00	3.5 × 1.5	25	30.2	−21.32	.S..1..	Sa
NGC 1385	03 35 19.9	−24 39 51	11.65	3.0 × 2.0	165	39.4	−21.77	.SBS6..	ScIII:
NGC 1398	03 36 45.0	−26 29 55	10.60	6.6 × 5.2	100	29.4	−22.30	PSBR2..	SBab(r)I
NGC 1421	03 40 09.0	−13 38 53	11.95	3.6 × 1.0		41.6	−21.96	.SXT4*.	ScIII:
NGC 1425	03 40 09.4	−30 03 11	11.60	5.4 × 2.7	129	28.8	−21.53	.SAS3..	Sb(r)II
IC 0342	03 41 58.6	+67 56 26	9.10	17.8 × 17.4		4.7	−20.74	.SXT6..	S(B)cd(rs)
NGC 1448	03 42 52.7	−44 48 07	11.30	8.1 × 1.8	41	20.8	−21.14	.SA.6*/	Sc(II):
NGC 1512	04 02 15.7	−43 29 03	11.38	4.0 × 3.2	90	15.2	−20.14	.SBR1..	SBb(rs)I pec
IC 0356	04 02 34.5	+69 40 46	11.43	5.2 × 4.1	90	20.3	−21.14	.SAS2P.	
NGC 1532	04 10 08.7	−32 59 58	11.53	5.6 × 1.8	33	22.1	−21.33	.SBS2$/	Sab(s)I (tides?)
NGC 1569	04 26 05.8	+64 44 18	11.90	2.9 × 1.5	120	2.9	−16.22	.IB.9..	SmIV
NGC 1560	04 27 08.2	+71 46 29	12.24	9.8 × 2.0	23	4.7	−17.33	.SAS7./	Sd(s)
NGC 1637	04 38 57.5	−02 57 11	11.52	3.3 × 2.9		14.3	−19.72	.SXT5..	SBc(s)II.3
NGC 1744	04 57 55.6	−26 05 46	11.70	6.8 × 4.1	168	12.8	−19.40	.SBS7..	SBcd(s)II-III
NGC 1792	05 03 30.6	−38 02 43	10.85	4.0 × 2.1	137	21.1	−21.39	.SAT4..	Sc(s)II
NGC 1808	05 05 58.7	−37 34 37	10.70	7.2 × 4.1	133	16.4	−20.96	RSXS1..	Sbc pec
NGC 1964	05 31 14.4	−21 58 52	11.60	6.2 × 2.5	32	31.6	−22.01	.SXS3..	SbI-II
NGC 1961	05 36 33.9	+69 21 16	11.81	4.3 × 3.0	85	82.9	−23.68	.SXT5..	Sb(rs)II pec

TABLE 1—*Continued*

GALAXY NAME	R.A. (1950.0)	Decl. (1950.0)	B_T (mag)	$D_{25} \times d_{25}$	*P.A.*	D (Mpc)	$M_{B_T}^{0,i}$ (mag)	RC2 TYPE	RSAC TYPE
NGC 2090	05 45 13.4	−34 16 05	11.85	4.5 × 2.3	13	15.1	−19.72	.SAT5..	Sc(s)II
NGC 2146	06 10 40.1	+78 22 23	11.24	6.0 × 3.8	123	22.1	−21.36	.SBS2P.	SbII pec
NGC 2207	06 14 14.4	−21 21 14	11.35	4.3 × 2.9	141	51.8	−22.97	.SXT4P.	Sc(s)I.2
NGC 2217	06 19 40.3	−27 12 31	11.59	4.8 × 4.4		28.7	−21.23	RLBT+..	SBa(s)
NGC 2280	06 42 49.5	−27 35 10	11.96	5.6 × 3.2	163	34.2	−21.63	.SAS6..	Sc(s)I.2
NGC 2276	07 10 22.0	+85 50 58	11.98	2.6 × 2.5	20	53.0	−22.09	.SXT5..	Sc(r)II-III
NGC 2336	07 18 28.0	+80 16 35	11.12	6.9 × 4.0	178	48.5	−22.95	.SXR4..	SBbc(r)I
NGC 2366	07 23 34.2	+69 18 42	11.46	7.6 × 3.5	25	3.6	−16.73	.IBS9..	SBmIV-V
NGC 2403	07 32 05.5	+65 42 40	8.89	17.8 × 11.0	127	3.6	−19.47	.SXS6..	Sc(s)III
NGC 2541	08 11 01.9	+49 12 53	12.25	6.6 × 3.5	165	12.9	−18.93	.SAS6..	Sc(s)III
Ho II	08 13 53.5	+70 52 13	11.27	7.6 × 6.2	15	3.5	−16.74	.I..9..	ImIV-V
NGC 2613	08 31 11.1	−22 48 01	11.35	7.2 × 2.1	113	28.9	−22.71	.SAS3..	Sb(s)(II)
IC 0520	08 48 20.9	+73 40 46	11.70	2.3 × 1.9	0	73.2	−23.27	.SXT2$.	
NGC 2655	08 49 09.1	+78 24 53	10.95	5.1 × 4.4		31.8	−22.19	..SXS0.	Sa pec
NGC 2683	08 49 34.8	+33 36 23	10.61	9.3 × 2.5	44	8.0	−20.17	.SAT3..	Sb(nearly on edge)
NGC 2681	08 49 58.0	+51 30 16	11.09	3.8 × 3.5		16.0	−20.48	PSXT0..	Sa
NGC 2715	09 01 52.5	+78 17 15	11.98	5.0 × 1.9	22	30.8	−21.21	.SXT5..	Sc(s)II
NGC 2770	09 06 29.7	+33 19 38	11.80	3.7 × 1.3	148	38.2	−21.87	.SAS5*.	
NGC 2775	09 07 41.0	+07 14 35	11.20	4.5 × 3.5	155	23.9	−20.79	.SAR2..	Sa(r)
NGC 2835	09 15 36.6	−22 08 45	10.95	6.3 × 4.4	8	12.5	−20.23	.SBT5..	SBc(rs)I.2
NGC 2805	09 16 17.0	+64 18 55	11.78	6.3 × 5.0	125	36.8	−21.49	.SXT7..	
NGC 2841	09 18 34.9	+51 11 19	10.17	8.1 × 3.8	147	14.3	−21.53	.SAR3*.	Sb
NGC 2903	09 29 19.9	+21 43 19	9.50	12.6 × 6.6	17	9.4	−20.96	.SXT4..	Sc(s)I-II
NGC 2935	09 34 26.3	−20 54 12	12.00	3.5 × 3.0	0	40.1	−21.76	PSXS3..	SBb(s)I.2
NGC 2976	09 43 10.0	+68 08 43	10.85	4.9 × 2.5	143	3.6	−17.51	.SA.5P.	SdIII-IV
NGC 2997	09 43 27.4	−30 57 35	10.32	8.1 × 6.5		16.0	−21.40	.SXT5..	Sc(s)I.3
NGC 2985	09 45 52.6	+72 30 45	11.21	4.3 × 3.4	0	29.0	−21.74	PSAT2..	Sab(s)
NGC 3031	09 51 27.6	+69 18 13	7.86	25.7 × 14.1	157	3.6	−20.75	.SAS2..	Sb(r)I-II
NGC 3034	09 51 45.3	+69 55 11	9.28	11.2 × 4.6	65	3.6	−18.56	.I.0../	Amorphous
DDO 70	09 57 22.9	+05 34 22	11.89	4.6 × 3.3	110	2.6	−15.47	.IBS9..	IBm(s)IV-V
NGC 3079	09 58 35.4	+55 55 11	11.20	7.6 × 1.7	165	24.5	−21.64	.SBS5./	Sc pec:
NGC 3077	09 59 21.9	+68 58 33	10.64	4.6 × 3.6	45	3.6	−17.16	.I.0.P.	Amorphous
NGC 3109	10 00 46.9	−25 54 47	10.39	14.5 × 3.5	93	2.6	−17.28	.SBS9./	SmIV
DDO 75	10 08 34.3	−04 27 39	11.93	4.8 × 4.1		2.3	−15.22	.IB.9..	IBmV
NGC 3166	10 11 09.3	+03 40 25	11.52	5.2 × 2.7	87	23.3	−21.19	.SXT0..	Sa(s)
NGC 3169	10 11 38.7	+03 43 03	11.28	4.8 × 3.2	45	21.3	−21.09	.SAS1P.	Sb(r)I-II (tides)
NGC 3147	10 12 39.3	+73 39 02	11.45	4.0 × 3.5	155	58.0	−22.94	.SAT4..	Sb(s)I.8
NGC 3184	10 15 17.7	+41 40 28	10.43	6.9 × 6.8	135	12.1	−20.28	.SXT6..	Sc(r)II.2
NGC 3190	10 15 20.2	+22 05 01	11.99	4.6 × 1.8	125	27.7	−21.19	.SAS1P/	Sa
NGC 3198	10 16 51.8	+45 48 14	10.94	8.3 × 3.7	35	14.0	−20.39	.SBT5..	Sc(rs)I-II
NGC 3223	10 19 20.0	−34 00 49	11.88	4.1 × 2.6	135	52.4	−22.69	.SAS3..	Sb(s)I-II
NGC 3227	10 20 47.6	+20 07 00	11.55	5.6 × 4.0	155	22.0	−20.80	.SXS1P.	Sb(s)III
IC 2574	10 24 41.3	+68 40 18	11.03	12.3 × 5.9	50	3.5	−17.03	.SXS9..	S(B)m(s)IV-V
NGC 3256	10 25 41.7	−43 38 49	11.98	3.5 × 2.0	100	50.3	−22.80	.P.....	Sb(s) pec
NGC 3310	10 35 40.3	+53 45 45	11.20	3.6 × 3.0		21.5	−20.82	.SXR4P.	Sbc(r) pec
NGC 3319	10 36 15.2	+41 56 56	11.78	6.8 × 3.9	37	15.5	−19.66	.SBT6..	SBc(s)II.4
NGC 3338	10 39 28.1	+14 00 35	11.32	5.5 × 3.7	100	23.4	−20.96	.SAS5..	Sbc(s)I-II
NGC 3344	10 40 46.6	+25 11 10	10.48	6.9 × 6.5		12.5	−20.31	RSXR4..	SBbc(rs)I
NGC 3351	10 41 19.6	+11 58 00	10.52	7.4 × 5.1	13	12.8	−20.66	.SBR3..	SBb(r)II
NGC 3359	10 43 21.1	+63 29 11	10.99	6.8 × 4.3	170	22.8	−21.30	.SBT5..	SBc(s)I.8 pec
NGC 3368	10 44 06.9	+12 05 05	10.11	7.1 × 5.1	5	15.2	−21.41	.SXT2..	Sab(s)II
NGC 3423	10 48 37.4	+06 06 27	11.62	3.9 × 3.5	10	16.9	−19.84	.SAS6..	Sc(s)II-III
NGC 3432	10 49 42.7	+36 53 05	11.73	6.2 × 1.5	38	12.1	−19.50	.SBS9./	Sc(II-III:)
NGC 3486	10 57 40.0	+29 14 40	10.85	6.9 × 5.4	80	12.7	−20.05	.SXR5..	Sc(r)I-II
NGC 3504	11 00 28.1	+28 14 35	11.80	2.7 × 2.2		29.6	−21.11	RSXS2..	Sb(s)/SBb(s)I-II
NGC 3507	11 00 46.3	+18 24 25	11.00	3.5 × 3.0	110	17.7	−20.75	.SBS3..	
NGC 3511	11 00 57.0	−22 49 00	11.56	5.4 × 2.2	76	19.0	−20.56	.SAS5..	Sc(s)II.8
NGC 3513	11 01 19.2	−22 58 28	11.99	2.8 × 2.3	75	16.9	−19.61	.SBT5..	SBc(s)II.2
NGC 3521	11 03 15.1	+00 13 58	9.64	9.5 × 5.0	163	12.5	−21.65	.SXT4..	Sb(s)II-III
NGC 3556	11 08 36.8	+55 56 33	10.71	8.3 × 2.5	80	15.8	−21.02	.SBS6./	Sc(s)III
NGC 3593	11 11 59.2	+13 05 28	11.70	5.8 × 2.5	92	9.9	−19.19	.SAS0*.	Sa pec
NGC 3596	11 12 27.9	+15 03 38	11.64	4.2 × 4.1		21.4	−20.31	.SXT5..	Sc(r)II.2
NGC 3621	11 15 50.4	−32 32 25	10.03	10.0 × 6.5	159	8.7	−20.29	.SAS7..	Sc(s)II.8
NGC 3623	11 16 18.6	+13 22 00	10.24	10.0 × 3.3	174	13.5	−21.48	.SXT1..	Sa(s)II
NGC 3626	11 17 25.9	+18 37 56	11.74	3.1 × 2.2	157	28.1	−20.81	RLAT+..	Sa
NGC 3627	11 17^{m}37.9	+13 16 08	9.74	8.7 × 4.4	173	11.9	−21.48	.SXS3..	Sb(s)II.2
NGC 3628	11 17 39.6	+13 51 48	10.31	14.8 × 3.6	104	14.4	−21.30	.S..3P/	Sbc
NGC 3631	11 18 13.2	+53 26 43	11.03	4.6 × 4.1		24.8	−21.26	.SAS5..	Sc(s)I-II
NGC 3646	11 19 05.2	+20 26 43	11.88	3.9 × 2.6	50	82.0	−23.13	.RING..	Sbc(r)II
NGC 3642	11 19 25.6	+59 21 01	11.53	5.8 × 4.9	105	34.7	−21.69	.SAR4*	Sb(r)I

TABLE 1—*Continued*

GALAXY NAME	R.A. (1950.0)	Decl. (1950.0)	B_T (mag)	$D_{25} \times d_{25}$	*P.A.*	D (Mpc)	$M_{B_T}^{0,i}$ (mag)	RC2 TYPE	RSAC TYPE
NGC 3672	11 22 30.4	−09 31 12	11.66	4.1 × 2.1		32.7	−21.49	.SAS5..	Sc(s)I-II
NGC 3675	11 23 24.2	+43 51 36	10.90	5.9 × 3.2	178	15.8	−20.88	.SAS3..	Sb(r)II
NGC 3686	11 25 07.3	+17 29 56	12.00	3.3 × 2.6	15	20.7	−19.95	.SBS4..	SBbc(s)I-II
NGC 3705	11 27 31.5	+09 33 09	11.77	5.0 × 2.3	122	17.4	−20.32	.SXR2..	Sab(r)I-II
NGC 3718	11 29 50.7	+53 20 33	11.26	8.7 × 4.5	15	21.6	−21.24	.SBS1P.	Sa pec?
NGC 3726	11 30 38.3	+47 18 13	10.95	6.0 × 4.5	10	18.2	−20.74	.SXR5..	Sc(r)I-II
NGC 3729	11 31 05.3	+53 24 11	12.00	3.1 × 2.1	15	22.3	−20.16	.SBR1P.	SB(ring) pec
NGC 3810	11 38 23.5	+11 44 55	11.36	4.3 × 3.1	15	17.2	−20.22	.SAT5..	Sc(s)II
NGC 3877	11 43 29.4	+47 46 18	11.78	5.4 × 1.5	35	18.8	−20.35	.SAS5*.	ScII.2
NGC 3887	11 44 32.4	−16 34 36	11.60	3.3 × 2.7		18.3	−20.32	.SBR4..	Sb(r)I-II
NGC 3893	11 46 01.1	+48 59 20	11.10	4.4 × 2.8	165	20.5	−20.91	.SXT5*.	Sc(s)I.2
NGC 3898	11 46 36.3	+56 21 42	11.70	4.4 × 2.6	107	25.2	−21.04	.SAS2..	SaI
NGC 3938	11 50 13.6	+44 24 07	10.91	5.4 × 4.9		16.9	−20.54	.SAS5..	Sc(s)I
NGC 3949	11 51 05.2	+48 08 16	11.40	3.0 × 1.8	120	17.1	−20.23	.SAS4*.	Sc(s)III
NGC 3953	11 51 12.9	+52 36 20	10.79	6.6 × 3.6	13	20.7	−21.30	.SBR4..	SBbc(r)I-II
NGC 3982	11 53 52.3	+55 24 10	11.91	2.5 × 2.2		23.9	−20.30	.SXR3*.	Sbc(r)II-III
NGC 3992	11 55 01.0	+53 39 13	10.64	7.6 × 4.9	68	22.7	−21.83	.SBT4..	SBb(rs)I
NGC 4013	11 55 57.1	+44 13 30	12.00	5.2 × 1.3	66	17.3	−20.02	.S..3./	Sbc:
NGC 4027	11 56 56.5	−18 59 23	11.65	3.0 × 2.3		28.4	−21.06	.SBS8..	Sc(s)III
NGC 4030	11 57 50.3	−00 49 22	11.07	4.3 × 3.2	27	26.4	−21.42	.SAS4..	Sbc(r)I
NGC 4038	11 59 19.0	−18 35 05	11.30	2.6 × 1.8		27.8	−21.40	.SBS9P.	Sc pec
NGC 4041	11 59 38.7	+62 25 03	11.64	2.8 × 2.7		27.2	−20.83	.SAT4*.	Sc(s)II-III
NGC 4051	12 00 35.9	+44 48 48	10.93	5.0 × 4.0	135	14.9	−20.31	.SXT4..	Sbc(s)II
NGC 4062	12 01 30.2	+32 10 23	12.00	4.3 × 2.0	100	14.9	−19.44	.SAS5..	Sc(s)II-III
NGC 4088	12 03 03.1	+50 49 13	11.14	5.8 × 2.5	43	16.4	−20.53	.SXT4..	Sc(s)II-III/SBc
NGC 4096	12 03 28.7	+47 45 13	11.02	6.5 × 2.0	20	12.3	−20.15	.SXT5..	Sc(s)II-III
NGC 4100	12 03 36.4	+49 51 36	11.62	5.2 × 1.9	167	22.7	−20.82	PSAT4..	Sc(s)I-II
NGC 4123	12 05 37.5	+03 09 30	11.84	4.5 × 3.5	135	23.1	−20.35	.SBR5..	SBbc(rs)
NGC 4136	12 06 45.6	+30 12 18	11.58	4.1 × 3.9		8.2	−18.28	.SXR5..	Sc(r)I-II
NGC 4145	12 07 30.5	+40 09 33	11.50	5.8 × 4.4	100	20.6	−20.45	.SXT7..	SBc(r)II
NGC 4151	12 08 00.8	+39 41 11	11.13	5.9 × 4.4		19.6	−20.93	PSXT2*.	Sab
NGC 4157	12 08 34.6	+50 45 51	11.56	6.9 × 1.7	66	17.0	−20.43	.SXS3$/	Sbc
NGC 4178	12 10 13.1	+11 08 30	11.89	5.0 × 2.0	30	21.9	−20.44	.SBT8..	SBc(s)II
NGC 4192	12 11 15.4	+15 10 23	10.92	9.5 × 3.2	155	21.9	−21.85	.SXS2..	SbII:
NGC 4212	12 13 06.4	+14 10 45	11.86	3.0 × 2.1	75	21.9	−20.26	.SA.4$.	Sc(s)II-III
NGC 4214	12 13 08.8	+36 36 19	10.22	7.9 × 6.3		5.8	−18.79	.IXS9..	SBmIII
NGC 4216	12 13 20.3	+13 25 38	10.97	8.3 × 2.2	19	21.9	−21.94	.SXS3*.	Sb(s)
NGC 4217	12 13 21.7	+47 22 12	11.30	5.5 × 1.8	50	21.7	−21.46	.S..3./	Sb:
NGC 4236	12 14 21.8	+69 44 36	10.06	18.6 × 6.9	162	3.6	−18.41	.SBS8..	SBdIV
NGC 4244	12 14 59.9	+38 05 06	10.60	16.2 × 2.5	48	5.0	−18.76	.SAS6*/.	Scd
NGC 4242	12 15^{m}01.3	+45 54 00	11.54	4.8 × 3.8	25	11.3	−19.09	.SXS8..	SBdIII
NGC 4254	12 16 16.9	+14 41 46	10.43	5.4 × 4.8		21.9	−21.59	.SAS5..	Sc(s)I.3
NGC 4258	12 16 29.7	+47 34 55	8.95	18.2 × 7.9	150	10.4	−22.05	.SXS4..	Sb(s)II
NGC 4274	12 17 20.2	+29 53 33	11.30	6.9 × 2.8	102	17.6	−20.87	RSBR2..	Sa(s)
NGC 4293	12 18 41.1	+18 39 36	11.20	6.0 × 3.0	72	21.9	−21.34	RSBS0..	Sa pec
NGC 4303	12 19 21.4	+04 44 58	10.17	6.0 × 5.5		21.9	−21.84	.SXT4..	Sc(s)I.2
NGC 4314	12 20 02.0	+30 10 25	11.35	4.8 × 4.3		17.0	−19.80	.SBT1..	SBa(rs) pec
NGC 4321	12 20 23.2	+16 06 00	10.11	6.9 × 6.2	30	21.9	−21.91	.SXS4..	Sc(s)I
NGC 4388	12 23 14.8	+12 56 18	11.83	5.1 × 1.4	92	21.9	−21.05	.SAS3*/	Sab
NGC 4395	12 23 20.9	+33 49 22	10.69	12.9 × 11.0		6.1	−18.57	.SAS9*.	SdIII-IV
NGC 4394	12 23 24.7	+18 29 30	11.76	3.9 × 3.5		21.9	−20.42	RSBR3..	SBb(sr)I-II
NGC 4414	12 23 58.2	+31 30 05	10.95	3.6 × 2.2	155	14.0	−20.26	.SAT5$.	Sc(sr)II.2
NGC 4438	12 25 13.5	+13 17 11	10.91	9.3 × 3.9	27	21.9	−21.73	.SAS0P*	Sb (tides)
NGC 4449	12 25 45.2	+44 22 15	9.85	5.1 × 3.7	45	5.0	−18.84	.IB.9..	SmIV
NGC 4448	12 25 46.1	+28 53 50	12.00	4.0 × 1.6	94	13.1	−19.54	.SBR2..	Sb(r)I-II
NGC 4450	12 25 58.0	+17 21 40	10.93	4.8 × 3.5	175	21.9	−21.39	.SAS2..	Sab pec
NGC 4457	12 26 26.0	+03 50 51	11.66	3.0 × 2.5		21.9	−20.58	RSXS0..	RSb(rs)II
NGC 4490	12 28 10.5	+41 54 56	10.23	5.9 × 3.1	125	12.0	−20.70	.SBS7P.	ScdIII pec
NGC 4487	12 28 29.2	−07 46 41	11.66	4.1 × 3.0		16.6	−19.83	.SXT6..	SBc(s)II.2
NGC 4496	12 29 05.8	+04 12 56	11.71	3.9 × 3.1	70	21.9	−20.36	.SBT9..	SBcIII-IV
NGC 4501	12 29 28.1	+14 41 50	10.27	6.9 × 3.9	140	21.9	−21.93	.SAT3..	Sbc(s)II
NGC 4504	12 29 42.2	−07 17 20	11.92	4.0 × 2.8		15.9	−19.50	.SAS6..	Sc(s)II
NGC 4517	12 30 11.9	+00 23 32	11.20	10.2 × 1.9	83	19.1	−21.08	.SAS6*/	Sc
NGC 4527	12 31 35.5	+02 55 45	11.32	6.3 × 2.3	67	31.5	−22.19	.SXS4..	Sb(s)II
NGC 4535	12 31 47.9	+08 28 25	10.51	6.8 × 5.0	0	21.9	−21.58	.SXS5..	SBc(s)I.3
NGC 4536	12 31 53.5	+02 27 50	11.01	7.4 × 3.5	130	32.9	−22.15	.SXT4..	Sc(s)I
NGC 4548	12 32 55.1	+14 46 20	10.98	5.4 × 4.4	150	21.9	−21.27	.SBT3..	SBb(rs)I-II
NGC 4559	12 33 28.9	+28 14 23	10.36	10.5 × 4.9	150	15.4	−21.15	.SXT6..	Sc(s)II-III
NGC 4565	12 33 51.8	+26 15 50	10.39	16.2 × 2.8	136	23.4	−22.79	.SAS3$/	Sb
NGC 4568	12 34 03.0	+11 30 45	11.70	4.6 × 2.1	23	21.9	−20.57	.SAT4..	Sc(s)II-III

TABLE 1—*Continued*

Galaxy Name	R.A. (1950.0)	Decl. (1950.0)	B_T (mag)	$D_{25} \times d_{25}$	*P.A.*	*D* (Mpc)	$M_{B_T}^{0,i}$ (mag)	RC2 Type	RSAC Type
NGC 4569	12 34 18.7	+13 26 18	10.23	9.5 × 4.7	23	21.9	−22.31	.SXT2..	Sab(s)I-II
NGC 4571	12 34 25.5	+14 29 33	11.81	3.8 × 3.4	55	21.9	−20.21	.SAR7..	Sc(s)II-III
NGC 4579	12 35 12.6	+12 05 40	10.56	5.4 × 4.4	95	21.9	−21.69	.SXT3..	Sab(s)II
NGC 4593	12 37 04.7	−05 04 16	11.72	4.0 × 3.1		50.1	−22.35	RSBT3..	SBb(rs)I-II
NGC 4594	12 37 22.8	−11 21 00	9.28	8.9 × 4.1		17.5	−22.81	.SAS1/.	Sa+/Sb-
NGC 4596	12 37 24.3	+10 27 01	11.45	3.9 × 2.8	135	21.9	−20.25	.LBR+..	SBa (very early)
NGC 4605	12 37 47.5	+61 53 00	10.96	5.5 × 2.3	125	5.5	−18.34	.SBS5P.	Sc(s)III
NGC 4618	12 39 09.5	+41 25 29	11.20	4.4 × 3.8	25	11.3	−19.39	.SBT9..	SBbc(rs)II.2 pec
NGC 4631	12 39 41.5	+32 48 54	9.84	15.1 × 3.3	86	12.1	−21.44	.SBS7./	Sc on edge
NGC 4651	12 41 12.5	+16 40 05	11.36	3.8 × 2.7	80	21.9	−20.75	.SAT5..	Sc(r)I-II
NGC 4654	12 41 25.7	+13 23 58	11.14	4.7 × 3.0	128	21.9	−21.02	.SXT6..	SBc(rs)II
NGC 4656	12 41 32.8	+32 27 00	10.86	13.8 × 3.3	33	12.5	−20.03	.SBS9P.	Im
NGC 4666	12 42 35.1	−00 11 14	11.56	4.5 × 1.5	42	29.5	−21.49	.SX.5*.	SbcII.3
NGC 4689	12 45 15.3	+14 02 13	11.55	4.0 × 3.5		21.9	−20.48	.SAT4..	Sc(s)II.3
NGC 4691	12 45 39.5	−03 03 28	11.70	3.2 × 2.7		18.8	−20.22	RSBS0P.	SBb pec
NGC 4698	12 45 51.8	+08 45 37	11.53	4.3 × 2.5	170°	21.9	−20.55	.SAS2..	Sa
NGC 4699	12 46 26.5	−08 23 34	10.44	3.5 × 2.7		26.2	−22.24	.SXT3..	Sab(sr)
NGC 4725	12 47 59.9	+25 46 20	9.99	11.0 × 7.9	35	23.3	−22.47	.SXR2P.	Sb/SBb(r)II
NGC 4731	12 48 25.5	−06 07 17	11.55	6.5 × 3.4		26.1	−21.06	.SBS6..	SBc(s)III:
NGC 4736	12 48 32.4	+41 23 28	8.92	11.0 × 9.1	105	6.9	−20.81	RSAR2..	RSab(s)
NGC 4775	12 51 10.8	−06 21 11	11.74	2.2 × 2.1		27.5	−20.76	.SAS7..	Sc(s)II.8
NGC 4781	12 51 46.8	−10 15 54	11.69	3.5 × 1.8		13.8	−19.55	.SBT7..	Sc(s)II.8
NGC 4818	12 54 12.7	−08 15 13	11.89	4.5 × 1.7		17.0	−20.24	.SXS2..	Sab:
NGC 4826	12 54 16.9	+21 57 18	9.37	9.3 × 5.4	115	7.0	−20.61	RSAT2..	Sab(s)II
NGC 4866	12 56 57.9	+14 26 25	11.84	6.5 × 1.5	87	21.9	−21.11	.LAR.*/	Sa
NGC 4902	12 58 21.3	−14 14 41	11.90	3.0 × 2.8		48.5	−22.04	.SBR3..	SBb(s)I-II
NGC 4941	13 01 37.4	−05 17 02	11.90	3.7 × 2.1		17.6	−20.07	RSXR2*.	Sab(s)II
NGC 4939	13 01 37.6	−10 04 22	11.56	5.8 × 3.2		58.1	−22.77	.SAS4..	Sbc(rs)I
NGC 4981	13 06 13.0	−06 30 48	11.83	2.8 × 2.2		29.8	−20.91	.SXR4..	SBbc(sr)II
NGC 4984	13 06 18.2	−15 15 01	11.71	2.8 × 2.2		20.8	−20.49	RLXT+..	Sa(s)
NGC 4995	13 07 04.4	−07 34 02	11.90	2.5 × 1.7		32.9	−21.10	.SXT3..	Sbc(s)II
NGC 5005	13 08 37.6	+37 19 25	10.64	5.4 × 2.7	65	20.8	−21.78	.SXT4..	Sb(s)II
NGC 5023	13 09 58.0	+44 18 13	12.90	6.5 × 1.0	28	7.5	−17.05	.S..5*/	Sc
NGC 5033	13 11 09.7	+36 51 30	10.63	10.5 × 5.6	170	17.9	−21.16	.SAS5..	Sbc(s)I-II
NGC 5055	13 13 34.9	+42 17 55	9.33	12.3 × 7.6	105	11.0	−21.34	.SAT4..	Sbc(s)II-III
NGC 5054	13 14 18.1	−16 22 17	11.51	5.0 × 3.1		30.5	−21.67	.SAS4..	Sb(s)I-II
NGC 5068	13 16 12.4	−20 46 35	10.53	6.9 × 6.3		6.9	−19.05	.SXT6..	SBc(s)II-III
NGC 5101	13 19 00.7	−27 10 06	11.58	5.5 × 4.9		32.2	−21.06	RSBT0..	SBa
NGC 5112	13 19 41.5	+38 59 55	11.82	3.9 × 2.9	130	20.0	−20.07	.SBT66.	Sc(rs)II
NGC 5161	13 26 24.0	−32 54 56	11.98	5.4 × 2.3	77	42.3	−21.89	.SAS5*.	Sc(s)I
NGC 5170	13 27 07.3	−17 42 24	11.88	8.1 × 1.3	127	25.7	−21.56	.SAS5*/	Sb:
NGC 5204	13 27 43.8	+58 40 32	11.75	4.8 × 3.0	5	7.6	−18.11	.SAS9..	SdIV
NGC 5194	13 27 46.9	+47 27 16	8.98	11.0 × 7.8		10.8	−21.60	.SAS4P.	Sbc(s)I-II
NGC 5236	13 34 10.2	−29 36 49	8.51	11.2 × 10.2		6.9	−21.12	.SXS5..	SBc(s)II
NGC 5248	13 35 02.4	+09 08 23	10.80	6.5 × 4.9	110	21.0	−21.19	.SXT4..	Sbc(s)I-II
NGC 5247	13 35 20.9	−17 37 50	11.10	5.4 × 4.7		22.9	−21.09	.SAS4..	Sc(s)I-II
NGC 5253	13 37 05.2	−31 23 21	11.11	4.0 × 1.7	45	6.9	−18.22	.I.0.P.	Amorphous
NGC 5300	13 45 44.3	+04 12 00	11.93	3.9 × 2.7	150	20.9	−20.09	.SXR5..	Sc(s)II
NGC 5334	13 50 20.2	−00 52 05	11.90	4.4 × 3.3	15	24.7	−20.55	.SBT5*.	SB:
NGC 5371	13 53 34.2	+40 42 23	11.40	4.4 × 3.6	0	52.3	−22.78	.SXT4..	Sb(rs)I/SBb(rs)I
NGC 5364	13 53 41.1	+05 15 33	11.05	7.1 × 5.0	30	22.8	−21.15	.SAT4P.	Sc(r)I
NGC 5377	13 54 18.0	+47 28 55	12.00	4.6 × 2.7	20	37.7	−21.62	RSBS1..	SBa or Sa
NGC 5457	14 01 26.6	+54 35 25	8.18	26.9 × 26.3		7.6	−21.51	.SXT6..	Sc(s)I
NGC 5474	14 03 15.3	+53 54 05	11.31	4.5 × 4.2		7.6	−18.39	.SAS6P.	Scd(s)IV pec
NGC 5530	14 15 17.7	−43 09 27	11.98	4.1 × 2.2	127	18.9	−20.24	.SAT4..	Sc(s)II.8
NGC 5556	14 17 38.5	−29 01 08	11.88	3.1 × 2.7	148	23.3	−20.41	.SXT7..	SBc(sr)II-III
NGC 5566	14 17 49.4	+04 09 42	11.35	6.5 × 2.4	35	29.4	−21.99	.SBR2..	SBa(r)II
NGC 5585	14 18 12.9	+56 57 32	11.37	5.5 × 3.7	30	7.6	−18.46	.SXS7..	Sd(s)IV
NGC 5584	14 19 49.9	−00 09 34	11.95	3.3 × 2.6	140	30.4	−20.84	.SXT6..	Sc(s)I-II
NGC 5643	14 29 27.7	−43 57 13	10.89	4.6 × 4.1		18.9	−21.20	.SXT5..	SBc(s)II-III
NGC 5669	14 30 17.1	+10 06 37	12.00	4.1 × 3.2	50	26.1	−20.46	.SXT6..	Sc/SBc(r)I-II
NGC 5676	14 31 01.4	+49 40 37	11.68	3.9 × 2.0	47	44.8	−22.11	.SAT4..	Sc(s)II
NGC 5701	14 36 41.5	+05 34 50	11.80	4.7 × 4.5		28.5	−20.47	RSBT0..	(PR)SBa
NGC 5713	14 37 37.6	−00 04 35	12.00	2.8 × 2.5	10	35.5	−21.07	.SXT4P.	Sbc(s) pec
NGC 5746	14 42 24.2	+02 09 53	11.55	7.9 × 1.7	170	32.8	−22.34	.SXT3$/	Sb(s)
NGC 5792	14 55 48.2	−00 53 26	11.72	7.2 × 2.1	84	37.8	−22.35	.SBT3..	SBb(s)I.3
NGC 5850	15 04 35.5	+01 44 17	11.71	4.3 × 3.9	140	48.6	−22.23	.SBR3..	SBb(sr)I-II
NGC 5907	15 14 34.8	+56 30 33	11.15	12.3 × 1.8	155	15.6	−20.68	.SAS5*/	Sc (on edge)
NGC 5921	15 19 27.2	+05 14 53	11.53	4.9 × 4.2	130	28.6	−21.14	.SBR4..	SBbc(s)I-II
NGC 5985	15 38 36.3	+59 29 35	11.80	5.5 × 3.2	13	53.9	−22.65	.SXR3..	SBb(r)I

TABLE 1—*Continued*

Galaxy Name	R.A. (1950.0)	Decl. (1950.0)	B_T (mag)	$D_{25} \times d_{25}$	P.A.	D (Mpc)	$M_{B_T}^{0,i}$ (mag)	RC2 Type	RSAC Type
NGC 6015	15 50 39.7	+62 27 30	11.73	5.4 × 2.3	28	20.4	−20.48	.SAS6..	Sc(s)II-III
NGC 6118	16 19 12.6	−02 09 57	11.91	4.7 × 2.3	58	30.7	−21.20	.SAS6..	Sc(s)I.3
NGC 6140	16 20 36.0	+65 30 30	12.40	6.2 × 4.7	95	22.8	−19.85	.SBS5P.	
NGC 6217	16 35 05.1	+78 18 05	11.86	3.1 × 2.7		32.0	−21.11	RSBT4..	RSBbc(s)II
NGC 6340	17 11 16.9	+72 21 55	11.90	3.4 × 3.0	120	29.4	−21.05	.SAS0..	Sa(r)I
NGC 6384	17 29 59.0	+07 05 43	11.29	6.0 × 4.3	30	34.7	−22.28	.SXR4..	Sb(r)I
NGC 6503	17 49 58.7	+70 09 26	10.93	6.2 × 2.3	123	6.1	−18.76	.SAS6..	Sc(s)II.8
NGC 6643	18 21 13.3	+74 32 43	11.74	3.9 × 2.1	38	34.9	−21.64	.SAT5..	Sc(s)II
NGC 6822	19 42 06.4	−14 55 23	9.35	10.2 × 9.5		0.7	−15.25	.IBS9..	ImIV-V
NGC 6907	20 22 07.7	−24 58 18	12.00	3.4 × 3.0	46	63.8	−22.49	.SBS4..	SBbc(s)II
NGC 6946	20 33 48.8	+59 58 50	9.68	11.0 × 9.8		6.7	−20.30	.SXT6..	Sc(s)II
NGC 7177	21 58 18.5	+17 29 50	11.95	3.3 × 2.3	90	28.4	−21.10	.SXR3..	Sab(r)II.2
NGC 7184	21 59 53.3	−21 03 18	11.67	5.8 × 1.8	62	54.1	−23.10	.SBR5..	Sb(r)II
NGC 7217	22 05 37.6	+31 06 53	11.08	3.7 × 3.2	95	24.7	−21.66	RSAR2..	Sb(r)II-III
NGC 7314	22 33 00.2	−26 18 32	11.65	4.6 × 2.3	3	29.8	−21.26	.SXT4..	Sc(s)III
NGC 7331	22 34 47.7	+34 09 35	10.39	10.7 × 4.0	171	22.3	−22.60	.SAS4..	Sb(rs)I-II
NGC 7410	22 52 10.7	−39 55 43	11.30	5.5 × 2.0	45	34.5	−22.40	.SBS1..	SBa
NGC 7418	22 53 47.9	−37 17 44	12.00	3.3 × 2.8	139	29.0	−20.66	.SXT6..	Sc(rs)I.8
IC 5267	22 54 22.3	−43 39 49	11.39	5.0 × 4.1	140	33.8	−21.53	.LAT0*.	Sa(r)
NGC 7424	22 54 27.4	−41 20 19	10.99	7.6 × 6.8		18.5	−20.67	.SXT6..	Sc(s)II.3
IC 5273	22 56 38.9	−37 58 22	11.90	2.9 × 2.1	56	25.9	−20.56	.SBT6*.	SBc(s)II-III
NGC 7479	23 02 26.8	+12 03 06	11.70	4.1 × 3.2	25	52.6	−22.33	.SBS6..	SBbc(s)I-II
NGC 7496	23 06 59.3	−43 41 58	11.78	3.5 × 2.8		28.9	−20.89	.SBS3..	SBc(s)II.8
NGC 7552	23 13 24.7	−42 51 28	11.40	3.5 × 2.5	1	31.3	−21.49	PSBS2..	SBbc(s)I-II
NGC 7582	23 15 38.6	−42 38 40	11.46	4.6 × 2.2	157	29.5	−21.75	PSBS2..	SBab(rs)
NGC 7606	23 16 29.1	−08 45 33	11.55	5.8 × 2.6		46.5	−22.69	.SAS3..	Sb(r)I
NGC 7640	23 19 42.6	+40 34 16	11.44	10.7 × 2.5	167	13.4	−20.30	.SBS5..	SBc(s)II:
IC 5332	23 31 47.7	−36 22 37	11.25	6.6 × 5.1		14.3	−19.90	.SAS7..	Sc(s)II-III
NGC 7713	23 33 35.6	−38 12 55	11.65	4.3 × 2.0	168	13.7	−19.60	.SBR7*.	Sc(s)II-III
NGC 7723	23 36 21.3	−13 14 13	11.85	3.6 × 2.6		39.5	−21.75	.SBR3..	SBb(rs)I-II
NGC 7727	23 37 19.1	−12 34 09	11.55	4.2 × 3.4		39.5	−21.98	.SXS1P.	Sa pec
NGC 7741	23 41 22.7	+25 47 53	11.88	4.0 × 2.8	170	20.6	−20.20	.SBS6..	SBc(s)II.2
NGC 7793	23 55 15.5	−32 52 03	9.65	9.1 × 6.6	98	4.2	−18.85	.SAS8..	Sd(s)IV
DDO 221	23 59 24.2	−15 44 33	11.29	10.2 × 4.2		1.6	−15.29	.IBS9..	IBm(s)IV-V

Second Reference Catalogue of Bright Galaxies (de Vaucouleurs, de Vaucouleurs, and Corwin 1976, hereafter RC2).

Column (6).—Optical major-axis position angle from Nilson (1973) for $\delta \geq -2\overset{\circ}{.}5$ and from Lauberts (1982) for $\delta \leq -17\overset{\circ}{.}5$.

Column (7).—Hubble distance D based on $H_0 = 50$ km s^{-1} Mpc^{-1} or, for group members, the group distance given by the RSA or by Kraan-Korteweg and Tammann (1979).

Column (8).—Absolute blue magnitude corrected for Galactic extinction and internal absorption as specified in the RSA.

Columns (9) and (10).—RC2 and RSA morphological types, respectively.

III. VLA OBSERVATIONS AND DATA REDUCTION

All galaxies listed in Table 1 except NGC 4258 were observed with the D- or C/D-arrays of the VLA between 1984 July 13 and 1986 January 30. Nearly all were covered by two or three "snapshots" of ~ 4 minutes duration each and separated by ~ 2 hr to improve (u, v) coverage. First the (u, v) data were edited and calibrated. The amplitude calibration is based on the Baars *et al.* (1977) 1.49 GHz flux densities $S = 15.16$ Jy for 3C 48 and $S = 14.39$ Jy for 3C 286. Numerous point sources with position uncertainties $\ll 1''$ were used to calibrate the phases of program galaxies not more than 10° or 15° away on the sky. Data from both circular polarizations in two passbands of 50 MHz bandwidth each centered on 1.465 and 1.515 GHz were combined to produce 1.49 GHz total-intensity maps. Square maps, usually 512 pixels × 14″/pixel ≈ 2° on a side, were made and fully CLEANed to eliminate aliasing and sidelobe responses from background sources anywhere in the primary beam (FWHM ≈ 30′) or its first sidelobe. (The CLEANed area was restricted on maps containing very extended sources to avoid CLEANing the strongest sidelobes of the synthesized beam). Uniform weighting and Gaussian tapers ranging from 3 to 3.8 kλ at the 30% intensity radius were used to produce nearly circular synthesized beams with FWHM diameters $\theta \approx 0\overset{'}{.}9$. Such a taper is close to "natural" weighting and minimizes the map noise ($\sigma_n \approx 0.1$ mJy). Most maps containing sources with peak flux densities $S_P > 100$ mJy were dynamic-range–limited, so they were self-calibrated. The CLEANed maps were restored with circular Gaussian beams of exactly 0′.8, 0′.9, or 1′.0 FWHM diameter and finally divided by the primary-beam attenuation pattern at $\nu = 1.49$ GHz. The central 128×128-pixel portions of the final maps were written onto a single 1600 BPI FITS format (Wells, Greisen, and Harten 1981) tape. Copies of this tape are available directly from the author for the cost of the blank tape plus shipping (about $15 each).

A typical map (of the field centered on NGC 4123) is shown as a profile plot (Fig. 1) and as a logarithmic contour plot (Fig. 2). The $S = 22.0$ mJy total flux density of NGC 4123 itself is divided almost equally between its unresolved (< 0′.2 FWHM) central source and an extended (1′.8 × 0′.8 FWHM in P.A. = 103°) disk component. The logarithmic

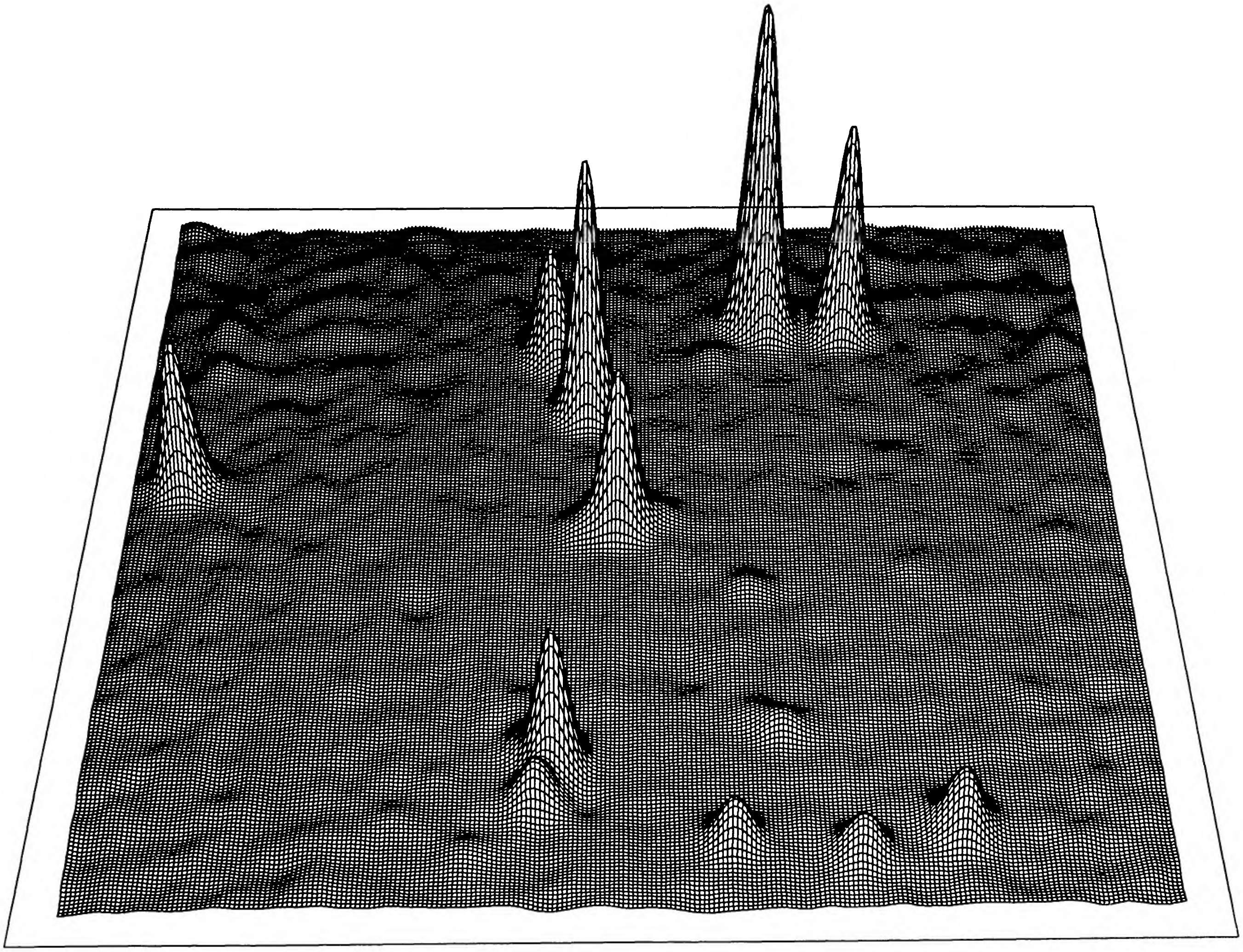

FIG. 1.—Profile plot of the final map centered on NGC 4123. The area covered is the same as that shown in Fig. 2. Height is proportional to peak flux density, reaching 30 mJy for the strongest source shown.

contour plot may make the disk (and other low-brightness sources) appear stronger than they actually are in the linear profile plot. The NGC 4123 map fluctuations in regions free from obvious background, or "confusing," sources increase from $\sigma \approx 0.1$ mJy near the map center to $\sigma \approx 0.2$ mJy in the corners, which lie just outside the primary-beam half-power circle. The variation of σ with primary-beam attenuation is consistent with most of these fluctuations being caused by receiver noise. Maps of fields containing strong ($S \gg 100$ mJy) sources anywhere in the primary beam may be dynamic-range–limited even after self-calibration, and have higher fluctuation levels.

The rms confusion σ_c expected from background sources with a sky density $n(S)\,dS = kS^{-\gamma}\,dS$ is $\sigma_c = [k\Omega_e/(3-\gamma)]^{1/2} D_c^{(3-\gamma)/2}$, where Ω_e is the "effective" beam solid angle and D_c is the cutoff peak flux density above which a discrete source can be recognized as confusion and eliminated (Condon 1974). The effective solid angle of a Gaussian beam is equal to the beam solid angle $\Omega_b = \pi\theta^2/(4\ln 2)$ when $\gamma = 2$. The density of background sources at $\nu = 1.49$ GHz can be approximated by $n(S) \approx 270 S^{-2}$, where S is in janskys (Mitchell and Condon 1985), leading to $\sigma_c \approx (270\Omega_b D_c)^{1/2}$. In "source-free" regions it is appropriate to use $D_c \approx 5\sigma_c$, yielding $\sigma_c \approx 10^{-4}$ Jy $= 0.1$ mJy for $\theta = 0\rlap{.}'9$. (Note that σ_c is directly proportional to Ω_b when $\gamma = 2$, so the rms confusion brightness temperature is approximately 0.02 K at $\nu = 1.49$ GHz *independent* of the beam area. This irreducible "sky noise" is a significant limit for mapping the low-brightness disk emission of spiral galaxies.) The profile plot (Fig. 1) makes it clear that there is a good chance that a fairly strong confusing source will lie directly behind some portion of the galaxy disk. A confusing source behind the disk component of NGC 4123 would have to be about as bright as the disk itself ($D_c \approx 3$ mJy peak flux density) to be recognized as such. Thus $\sigma_c \gg 0.1$ mJy in the galaxy sources themselves; the present maps are effectively confusion-limited.

Galaxy flux densities S determined simply by integrating over the optical disk regions on the radio maps may have quite large confusion errors. The rms confusion uncertainty σ_S in S may be reduced by subtracting the flux densities of

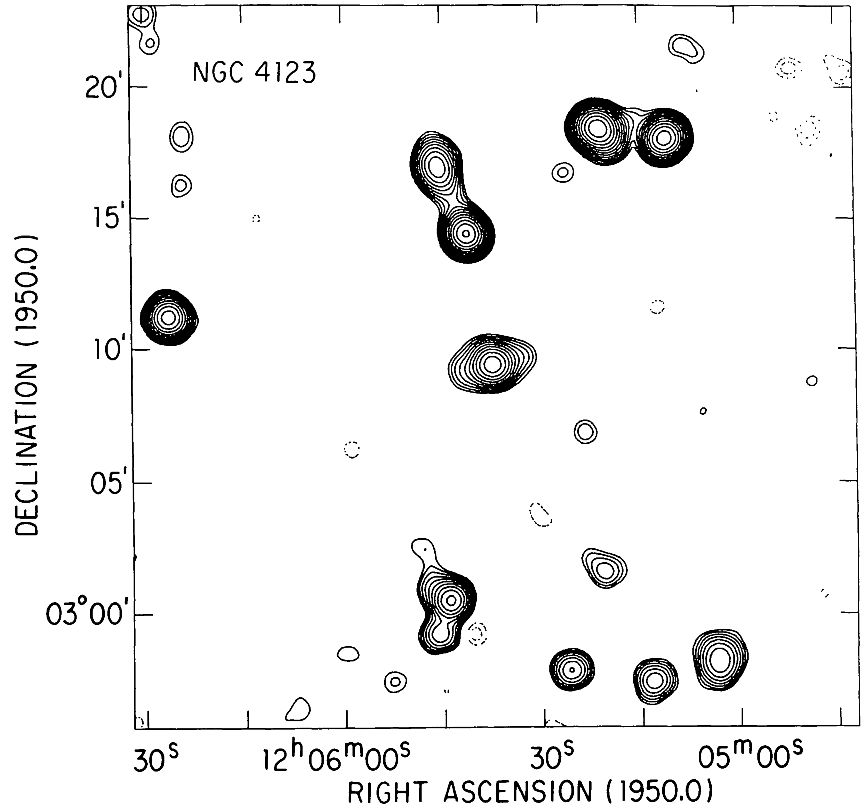

FIG. 2.—Contour plot of the NGC 4123 map. The faintest contours are ± 0.5 mJy per beam solid angle; higher contours are separated by multiples of $2^{1/2}$ in brightness.

recognizable confusing sources. Strong confusing sources behind the galaxy disk can usually be recognized because most are unresolved and do not lie exactly on the galaxy optical position, while the galaxy radio sources are generally well centered and symmetrically extended (cf. NGC 0150 in Fig. 7). Confusion is much more difficult to recognize in the maps of dwarf irregular galaxies, whose radio emission may be dominated by discrete sources in H II regions and supernova remnants spread throughout the galaxy (cf. NGC 0247 in Fig. 6). Genuine radio asymmetries or extranuclear "hot spots" in galaxy disks usually coincide with anomalously bright spiral arms, bars, H II regions, etc., easily visible on the sky survey prints (e.g., the northwestern radio extension on the Fig. 7 map of NGC 0772 is produced by an optically bright arm); radio emission from very young supernova remnants (cf. Rupen *et al.* 1987) being the principal exception to this rule. In addition, most background sources are either unresolved by the $\theta \approx 0\rlap{.}'9$ beam or appear as doubles with nearly equal point components. I have therefore compared the radio and optical images of the atlas galaxies and subtracted the flux densities of all extranuclear point sources and compact double sources lacking optical counterparts. The flux densities and positions of all such excluded sources are given in the notes to Table 2 in § IV*a*. After these obvious confusing sources have been removed, the value of σ_S may be approximated by treating the integrated flux density S as the sum of the *peak* flux densities S_P in the beams covering the source. The confusion uncertainty in each independent beam is the larger of $(270\Omega_b S_P)^{1/2}$ or $(270\Omega_b \times 5\sigma_c)^{1/2}$ (the latter applies only if the integration area includes regions with no detectable flux). Thus for integrations over simply connected sources, $\sigma_S \approx (270\Omega_b S)^{1/2}$ *independent* of the source area. Consequently, future radio surveys of fainter galaxies with smaller angular sizes will tend to be confusion-limited as well. There are no obvious confusing sources behind the simple source NGC 4123, so the rms confusion uncertainty in its total flux density is $\sigma_S \approx 0.7$ mJy.

Total flux densities S of all but the most extended galaxies were obtained by direct integration over their optical areas on the corrected maps, followed by subtraction of the flux densities of any recognizable confusing sources. The flux densities of sources too extended to be mapped accurately by the D-array (25–50 m minimum projected baselines) were estimated from flux densities measured at nearby frequencies with the NRAO 91 m filled-aperture telescope. Many of the observed galaxy brightness distributions could be approximated by one or two elliptical Gaussians. In these cases their Gaussian center positions (α, δ), peak flux densities S_P, integrated flux densities S_I, FWHM axes (θ_M, θ_m), and major-axis position angles PA (measured east from north) were determined. Some of the remaining galaxies contain non-Gaussian central peaks whose positions and peak flux densities only were estimated.

The present total flux densities S can be compared with the total flux densities of galaxies in overlapping samples observed independently with the Westerbork Synthesis Radio

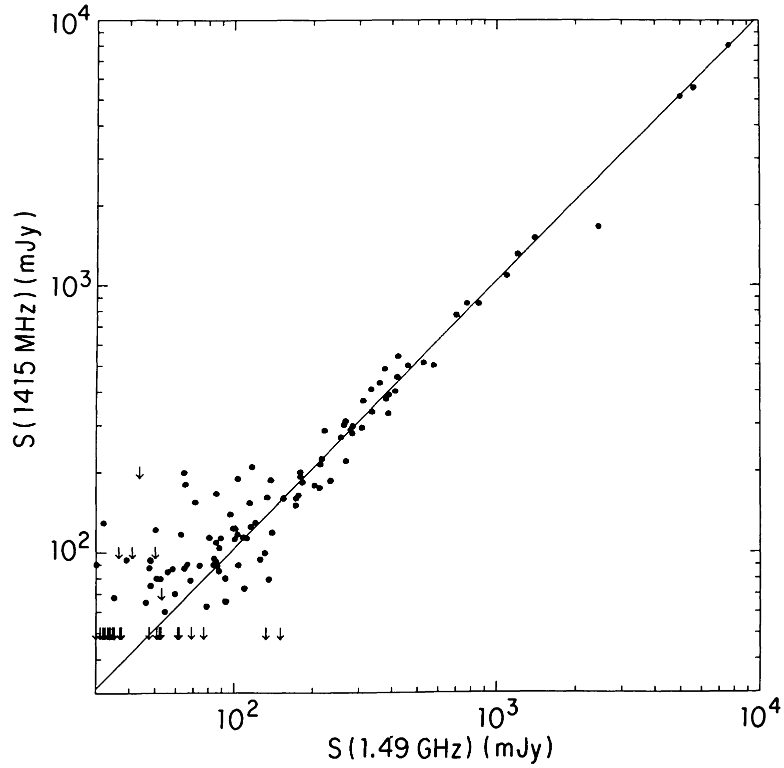

FIG. 3.—Comparison with WSRT fan-beam survey flux densities. The solid line corresponds to perfect agreement assuming that all galaxies have spectral indices $\alpha = +0.75$. *Abscissa*: VLA 1.49 GHz total flux densities from the present survey (mJy). *Ordinate*: WSRT 1415 MHz flux densities (mJy).

Telescope (WSRT) and the VLA C- and D-arrays. The largest overlapping sample is from the 1415 MHz WSRT fan-beam survey (Hummel 1980) of all galaxies with $B(0) \leq +12, \delta \geq -30°$ or $B(0) \leq +13, \delta \geq +30°$. That survey is noise-limited with $\sigma_n \approx 10$ mJy for extended emission, and it is complete to $S \approx 50$ mJy. Figure 3 compares the 1415 MHz WSRT and 1.49 GHz VLA flux densities. The overall scale linearity is good, and the scatter of individual points is generally consistent with the quoted errors. The discrepant point at (2445 mJy, 1650 mJy) comes from NGC 5236, a very extended galaxy at the southern limit of the WSRT survey. Only two sources with S(1.49 GHz) > 100 mJy (NGC 1087 and NGC 4030) were not detected at 1415 MHz. Their declinations ($\delta = -00°42'19''$ and $\delta = -00°49'22''$) suggest that they were missed only because they were inadvertently observed at $\delta = +00°$. The WSRT fan-beam survey completeness is otherwise excellent.

The VLA C-array was used to map 88 bright Sbc galaxies at 1.465 GHz (Hummel *et al.* 1985). The resulting flux-flux diagram (Fig. 4) extends to lower flux densities with smaller scatter, as expected from the lower noise levels. Those galaxies for which S(1.465 GHz) $\ll S$(1.49 GHz) are quite extended, and the missing flux can be explained by the lack of short spacings in the C-array (Hummel *et al.* 1985).

Finally, Gioia and Fabbiano (1987) mapped a sample of 46 early- and late-type spiral galaxies in the declination range $+20° < \delta < +60°$ with the VLA D-array at 1.49 GHz. Their flux densities are compared with the present results in Figure 5. The most discrepant point is from NGC 4395 at (21.5 mJy, 49 mJy). It results from a difference in interpretation (should the $S_P = 28.1$ mJy source at $\alpha = 12^h23^m30\overset{s}{.}9$, $\delta = +33°50'20''$ be included in the galaxy flux density or not?), not a difference between the maps. Otherwise the agreement is quite good and confirms that the VLA D-array has sufficient surface brightness sensitivity to detect most nearby spiral galaxies well above the noise level.

IV. THE RADIO ATLAS AND SOURCE TABLE

The results of the radio observations are presented as an atlas of contour maps and a table of source parameters. The contour plots are divided into two groups: Figure 6 for sources with large angular sizes and Figure 7 for the smaller maps. Within each figure the galaxies are ordered by increasing right ascension. The optical position of each galaxy is indicated by a cross with 8″ arm radius. Both positive (continuous) and negative (broken) contours have been plotted at levels $\pm 2^{n/2}, \pm 2^{(n+1)/2}, \pm 2^{(n+2)/2}, \ldots$ mJy per restoring beam solid angle. The contours are separated by factors $2^{1/2}$ in brightness, or $1.25 \log 2 \approx 0.38$ mag. The value of n listed in Table 2 specifies the faintest contour level plotted; e.g., $n = -3$ means ≈ 0.35 mJy per beam. A brightness of 1 mJy per beam at $\nu = 1.49$ GHz is equivalent to Rayleigh-Jeans brightness temperatures $T_B \approx 0.24$, 0.19, and 0.15 K for FWHM beamwidths $\theta = 0\overset{'}{.}8$, $0\overset{'}{.}9$, and $1\overset{'}{.}0$, respectively. The table of radio source parameters (Table 2) is

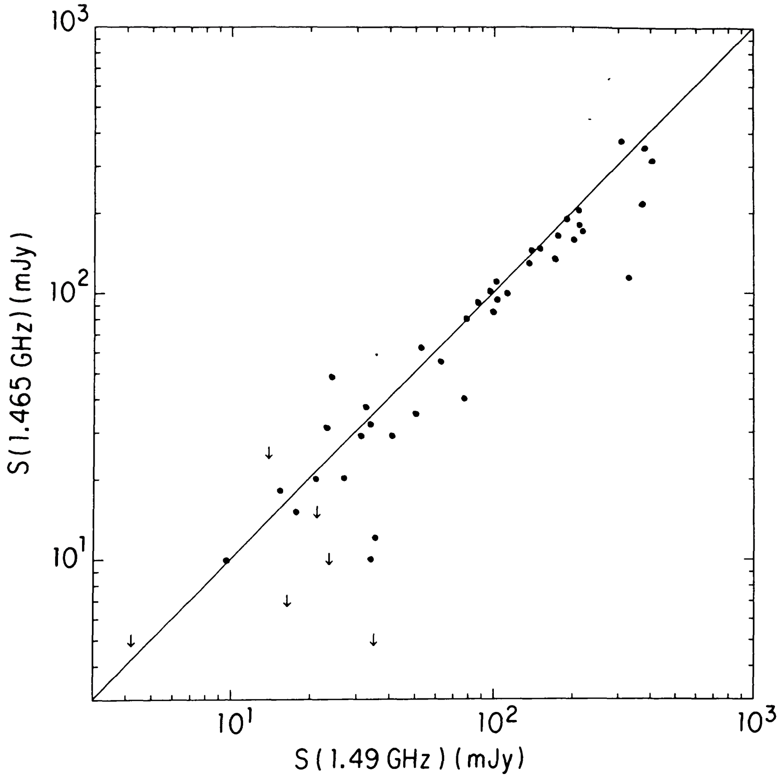

FIG. 4.—Comparison with VLA C-array flux densities. The solid line corresponds to perfect agreement assuming that all galaxies have spectral indices $\alpha = +0.75$. *Abscissa*: VLA 1.49 GHz total flux densities from the present survey (mJy). *Ordinate*: VLA C-array 1.465 GHz flux densities (mJy).

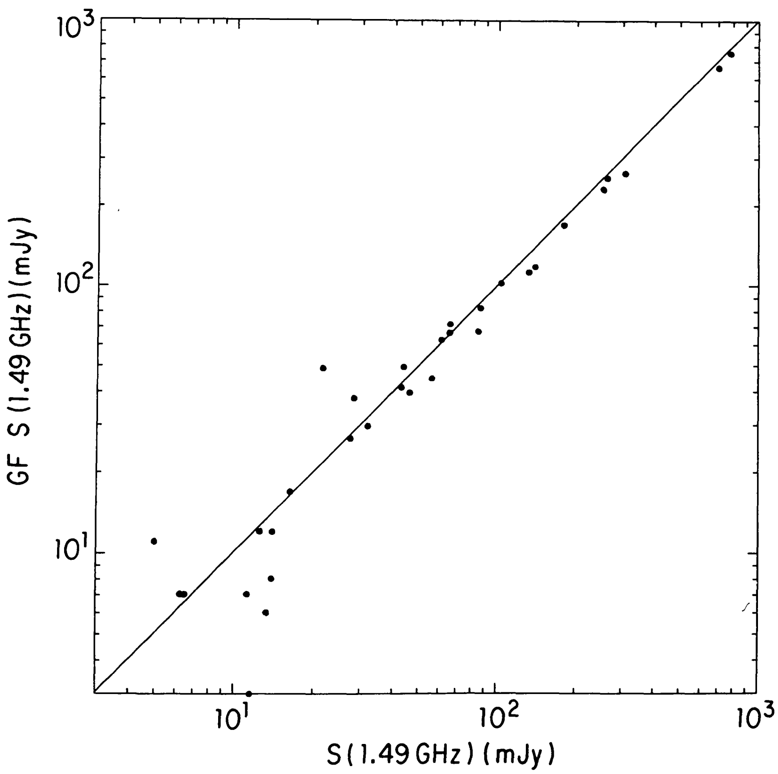

FIG. 5.—Comparison with the VLA D-array flux densities of Gioia and Fabbiano (1987). The solid line corresponds to perfect agreement. *Abscissa*: VLA 1.49 GHz total flux densities from the present survey (mJy). *Ordinate*: VLA D-array 1.49 GHz flux densities (mJy) from Gioia and Fabbiano (1987).

1987ApJS...65..485C

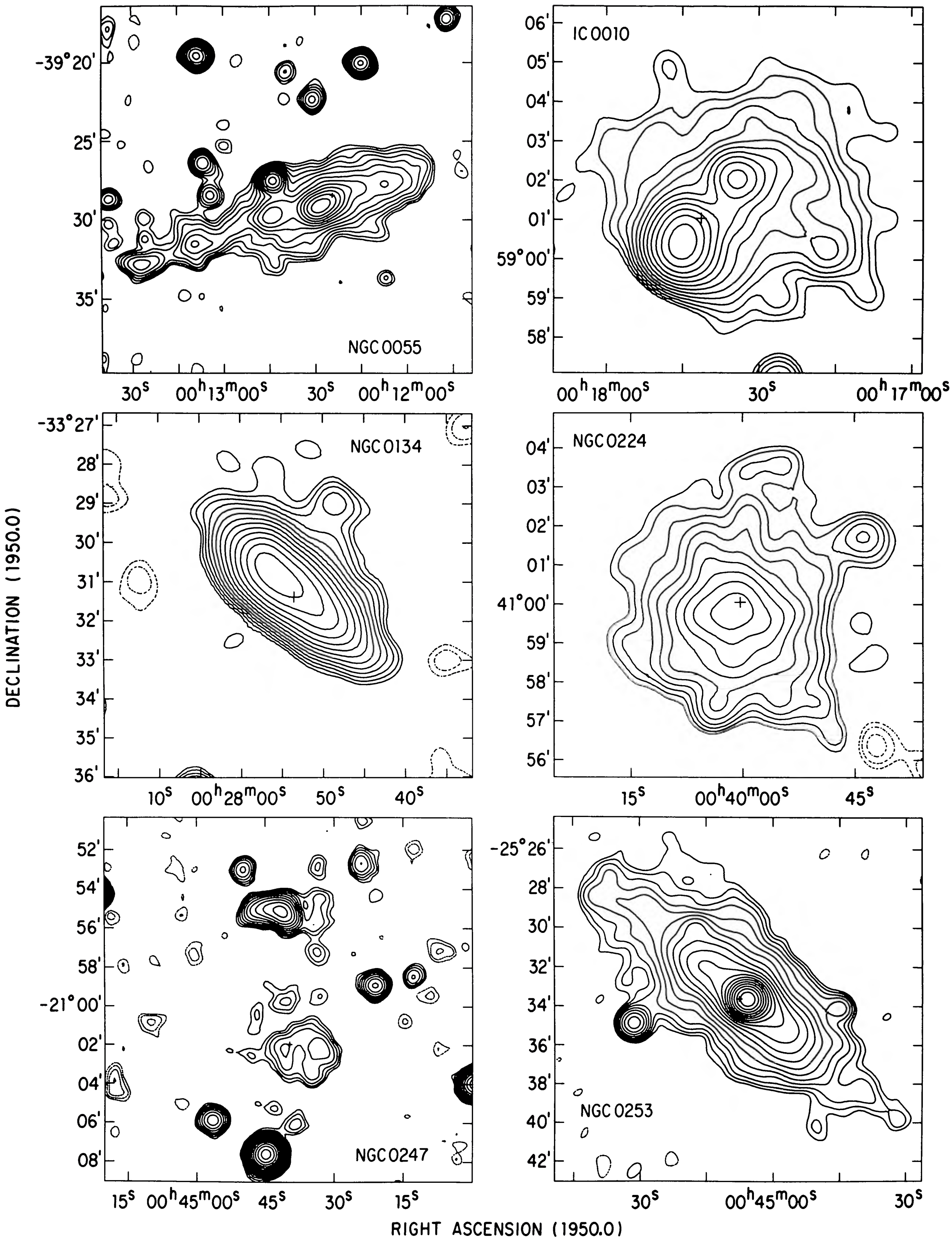

FIG. 6.—Large contour maps, in order of increasing right ascension. The optical position of each galaxy is indicated by a cross. Contour levels are plotted at $\pm 2^{n/2}, \pm 2^{(n+1)/2}, \pm 2^{(n+2)/2}, \ldots$ mJy per restoring beam solid angle. The value of n for each galaxy is listed in Table 2.

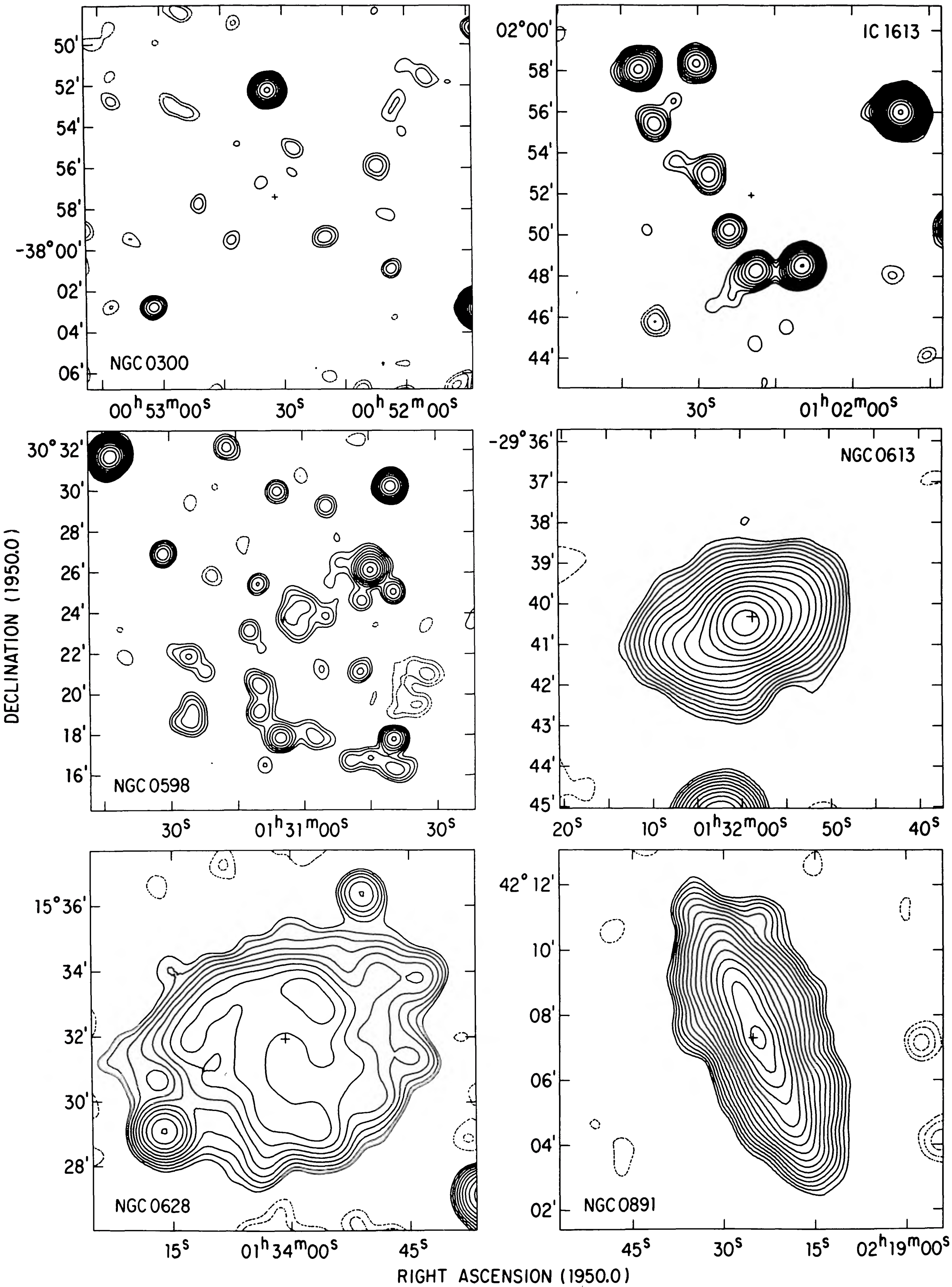

FIG. 6—*Continued*

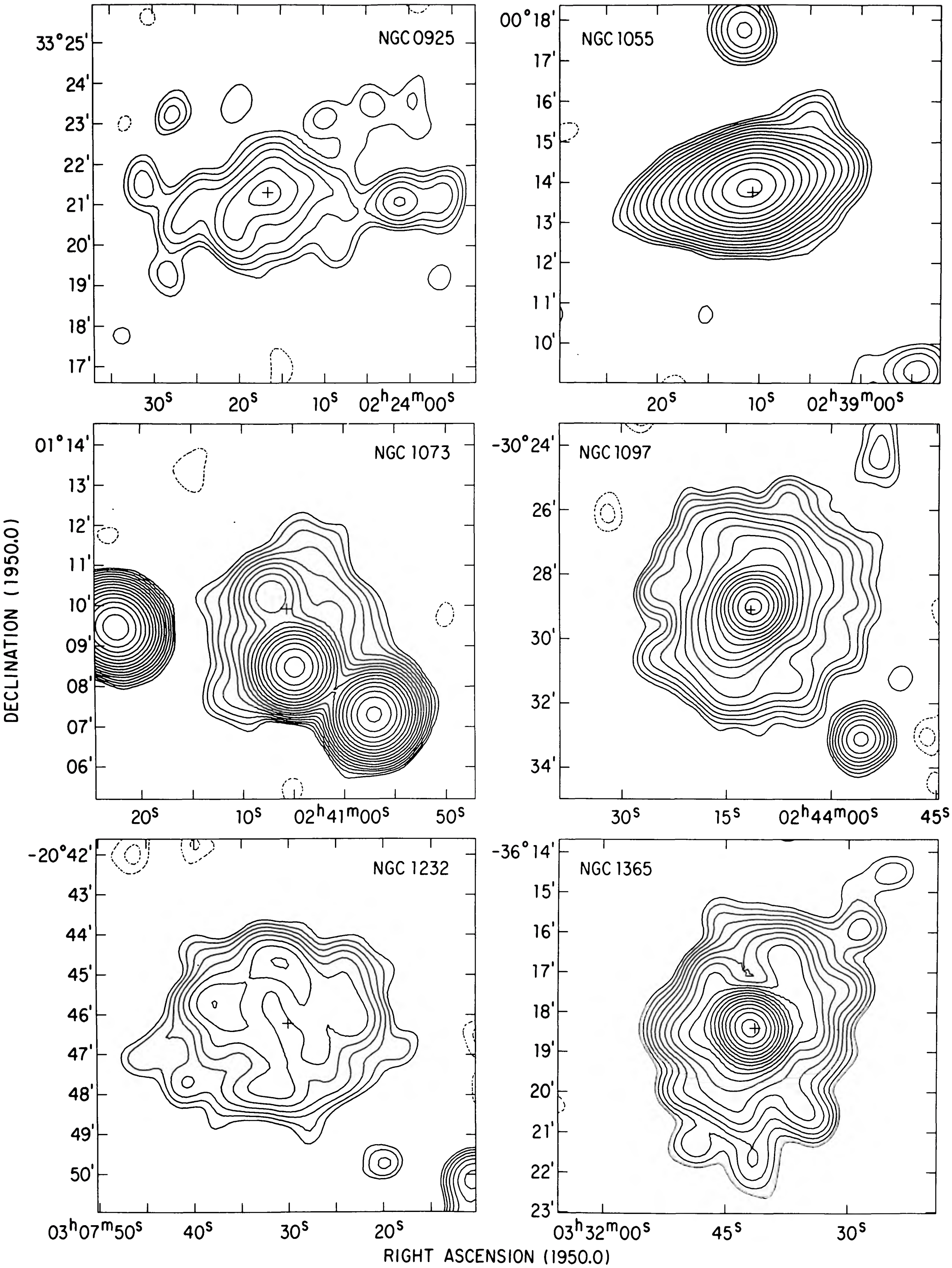

FIG. 6—*Continued*

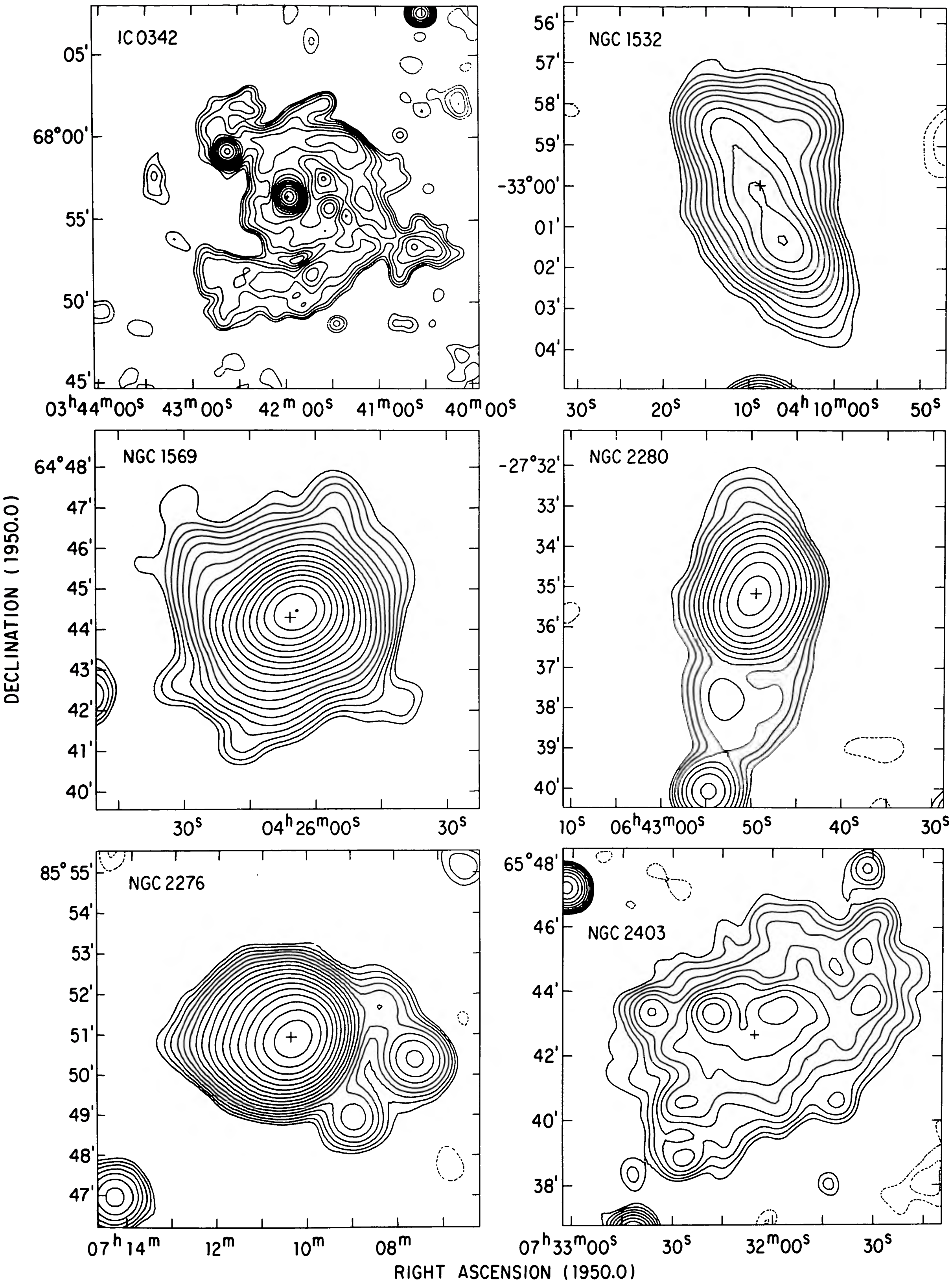

FIG. 6—*Continued*

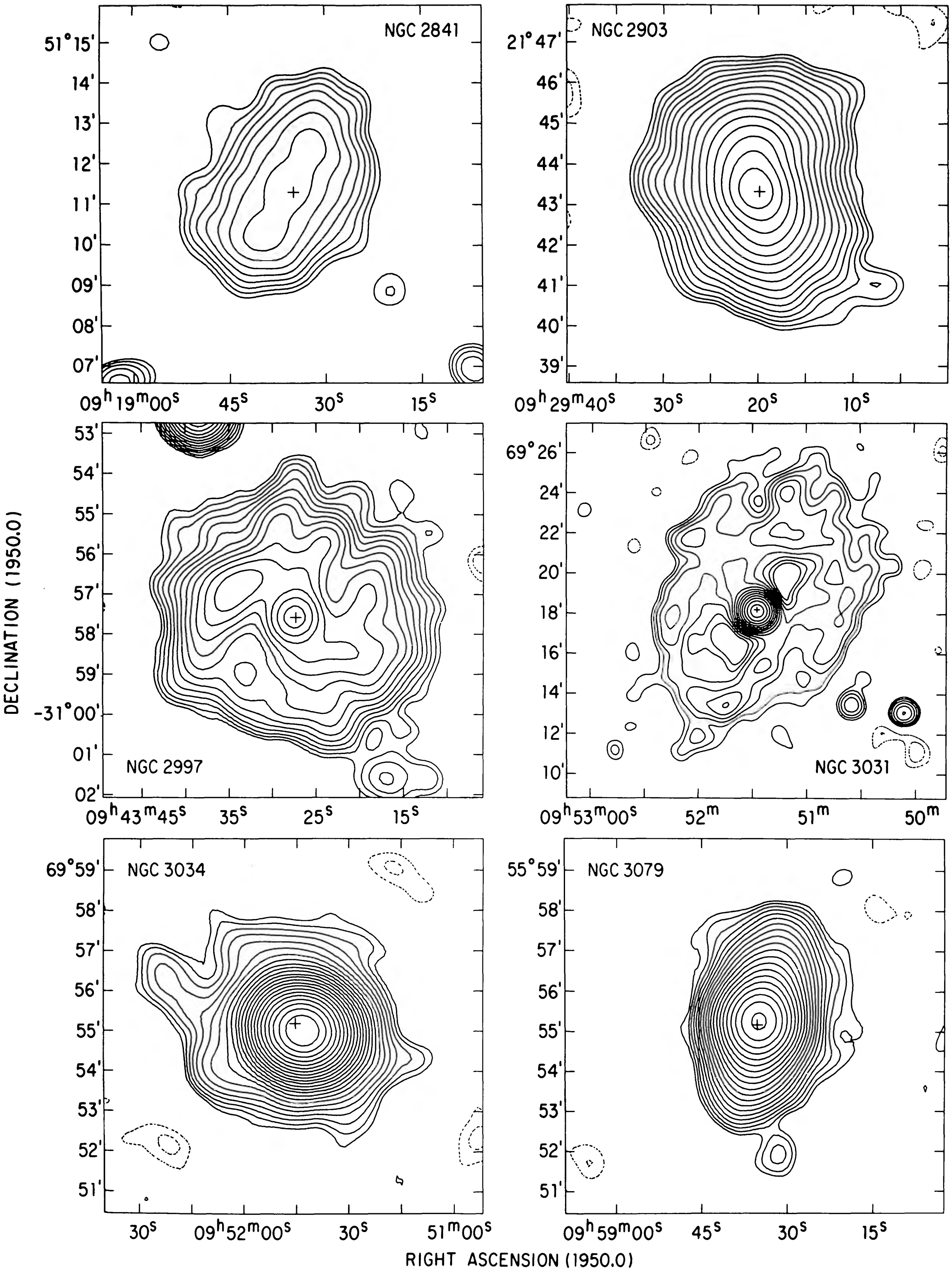

FIG. 6—*Continued*

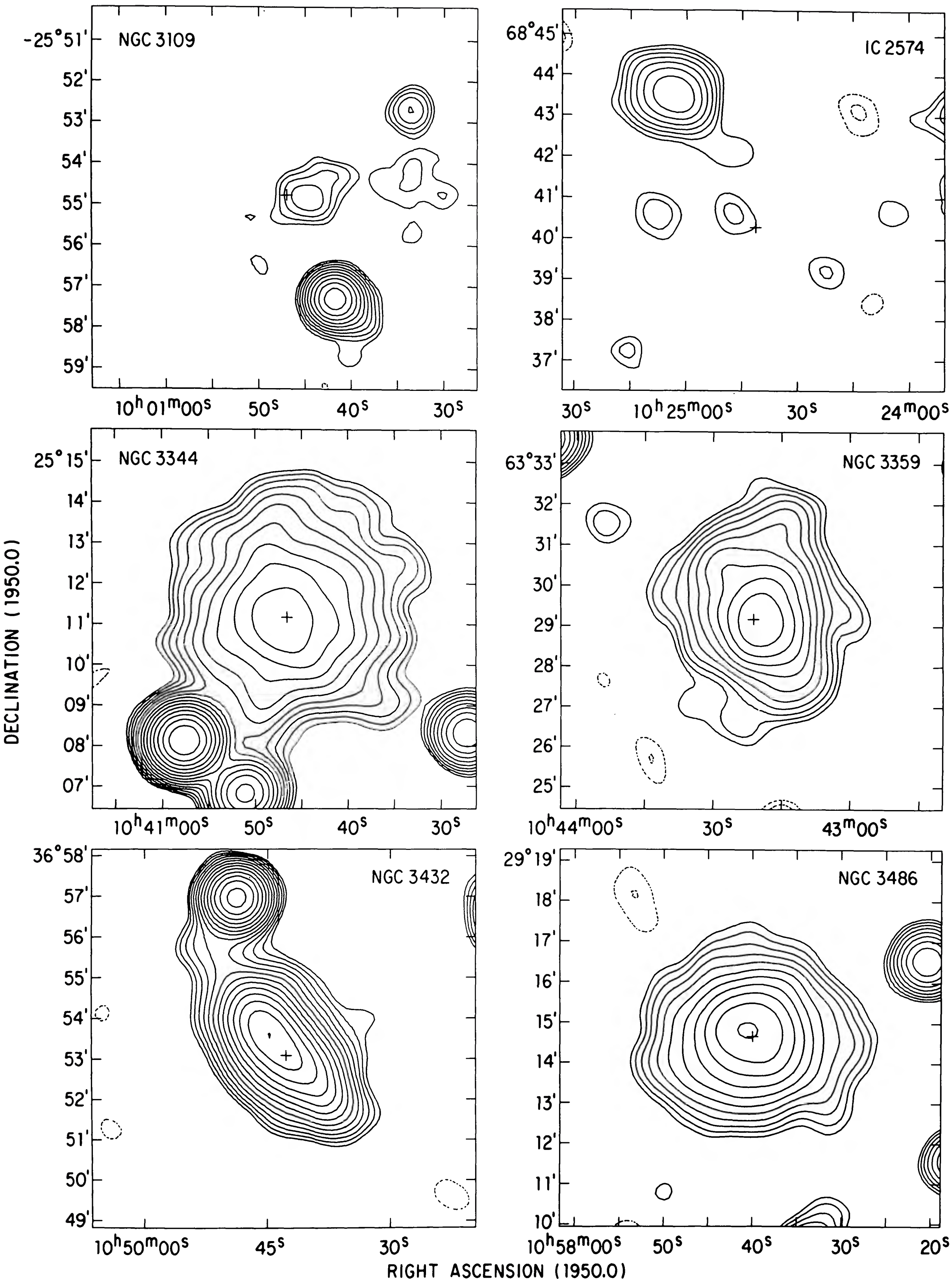

FIG. 6—*Continued*

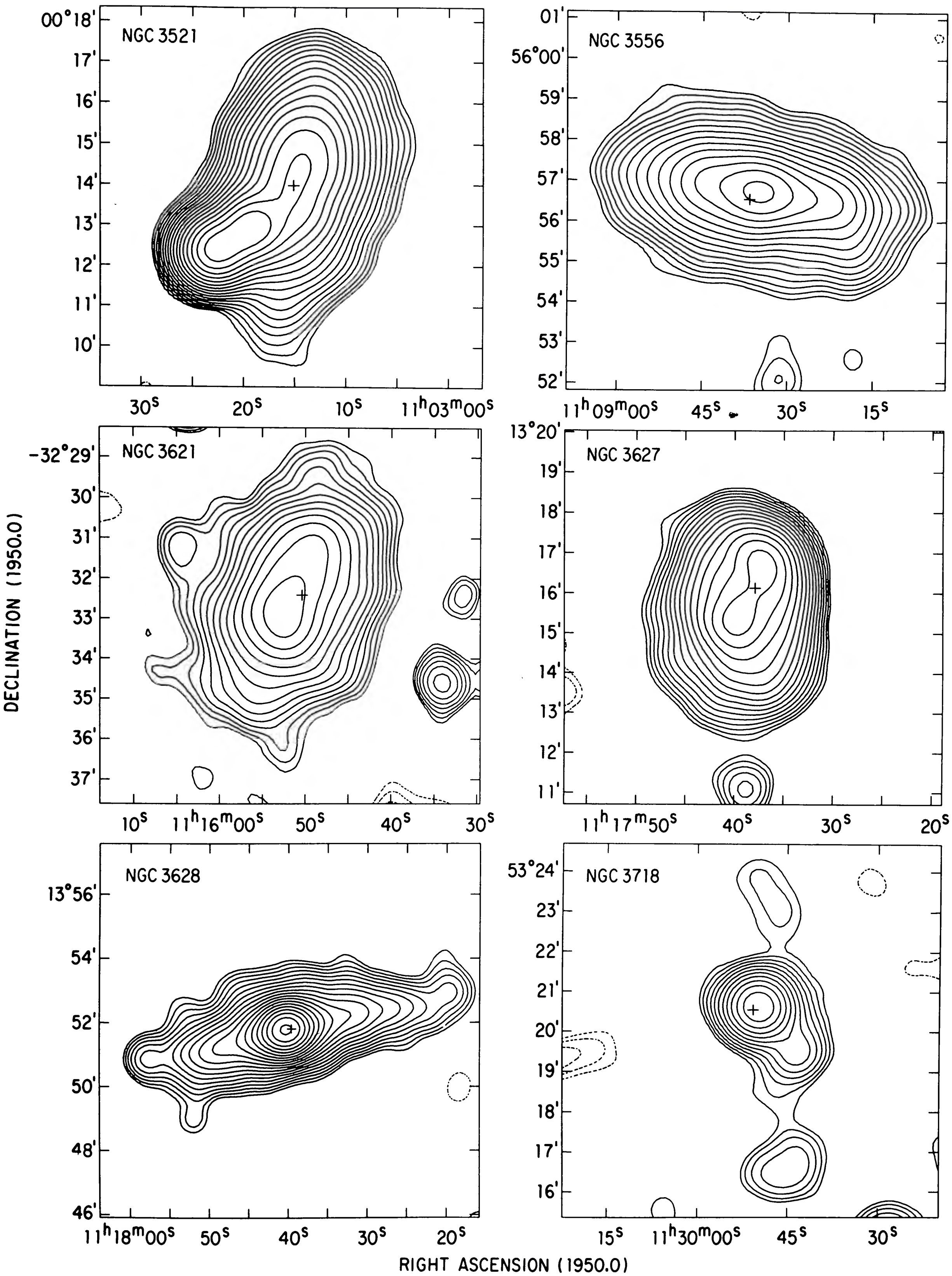

FIG. 6—*Continued*

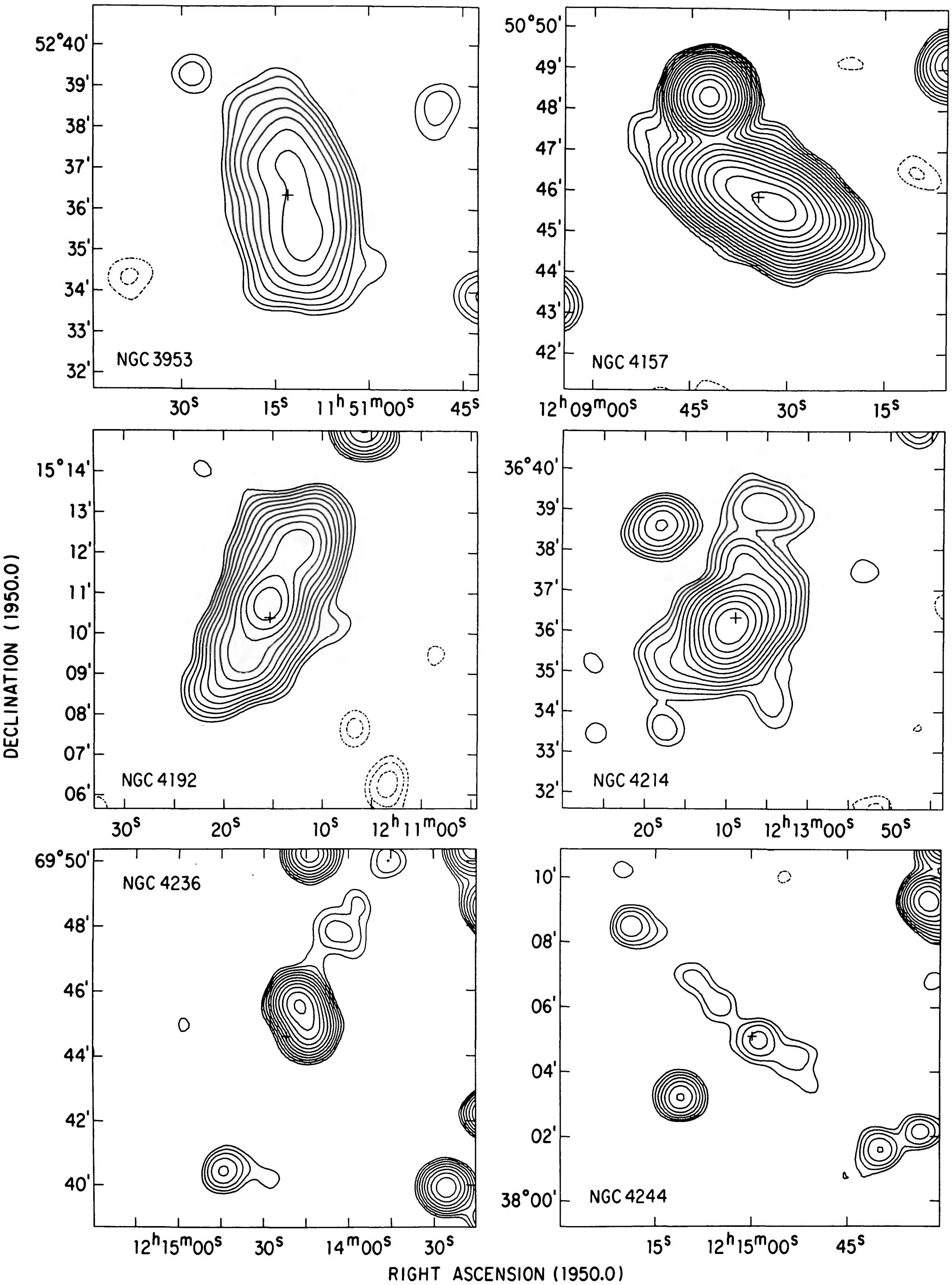

FIG. 6—*Continued*

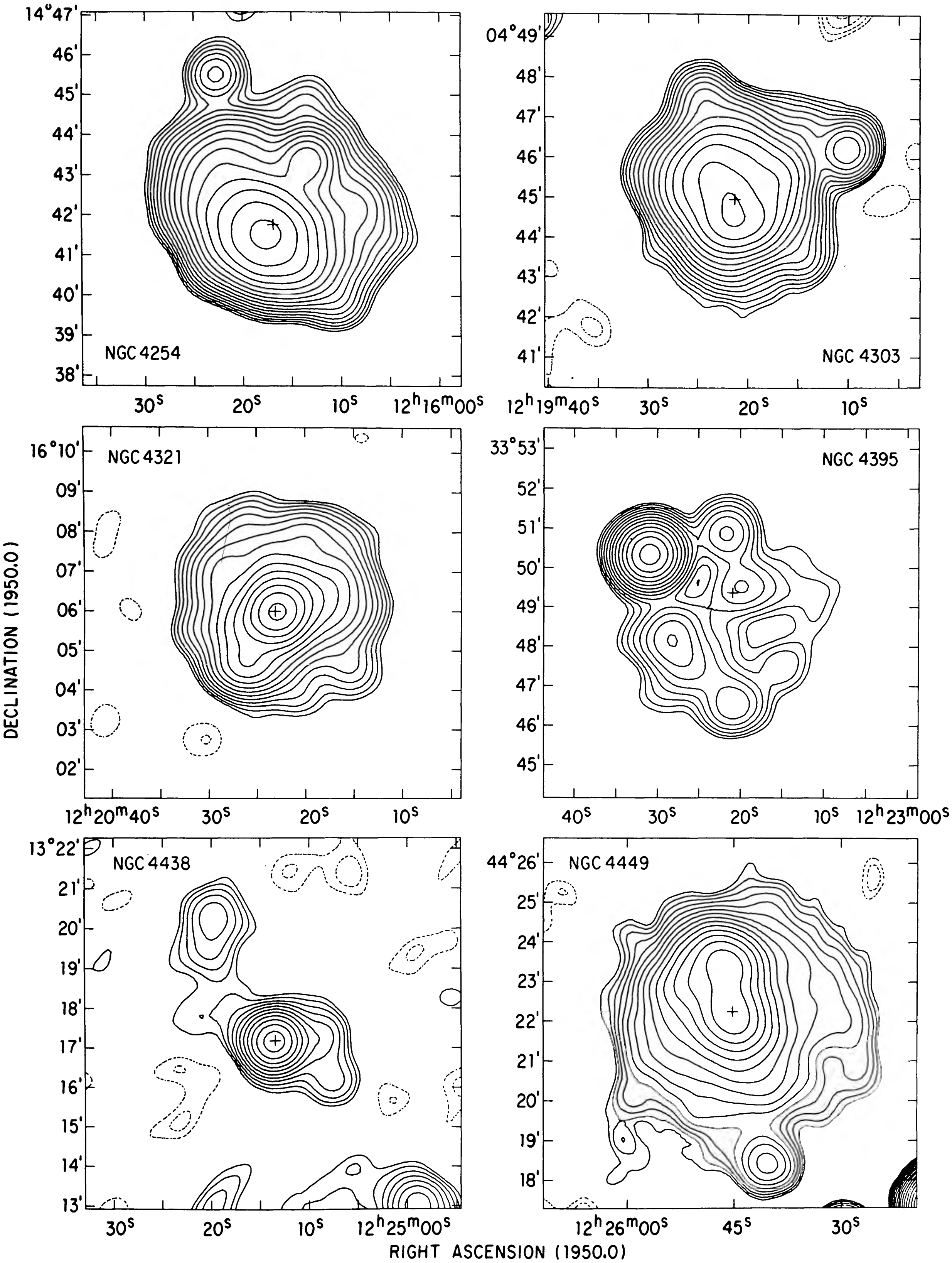

FIG. 6—*Continued*

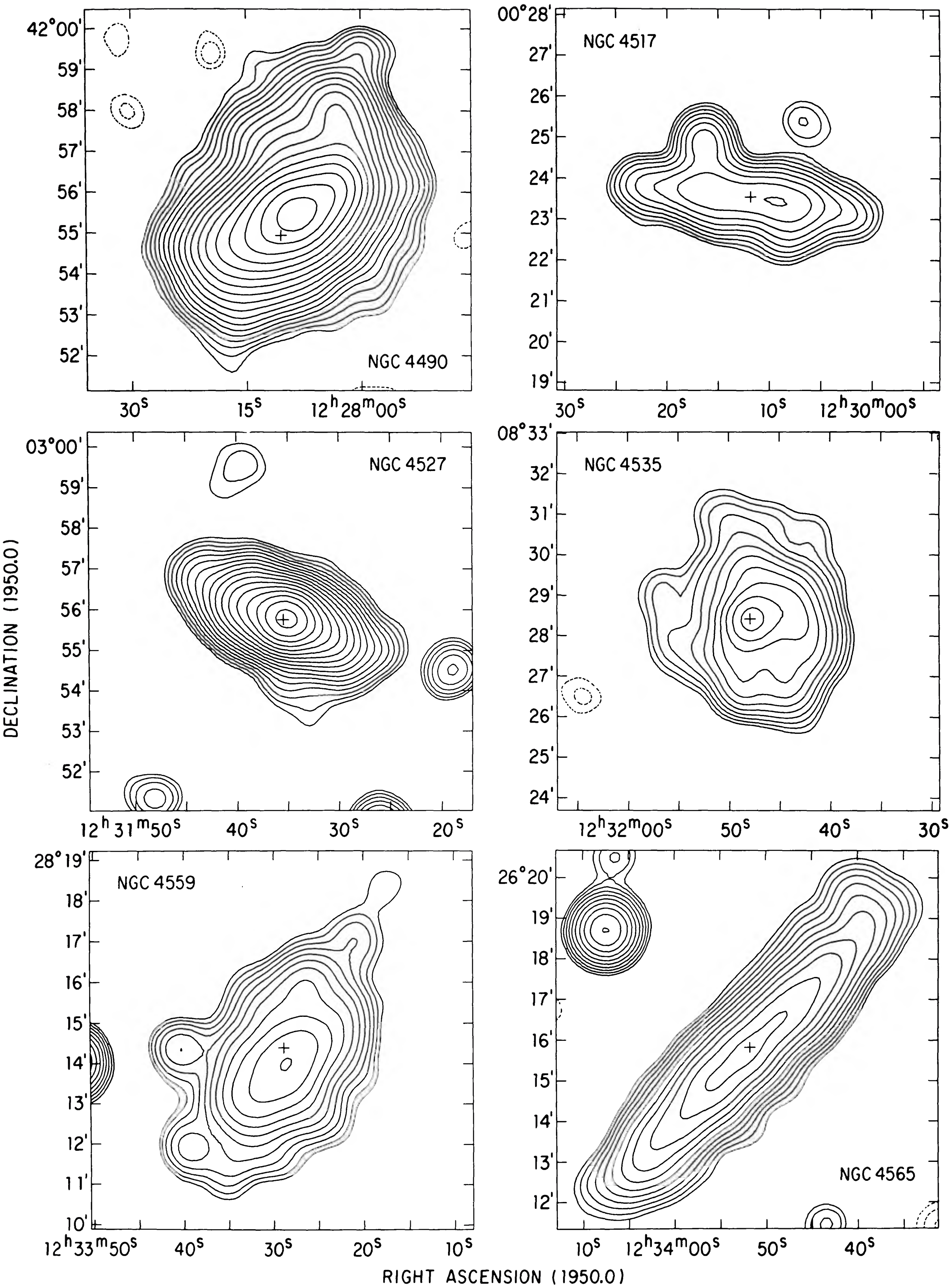

FIG. 6—*Continued*

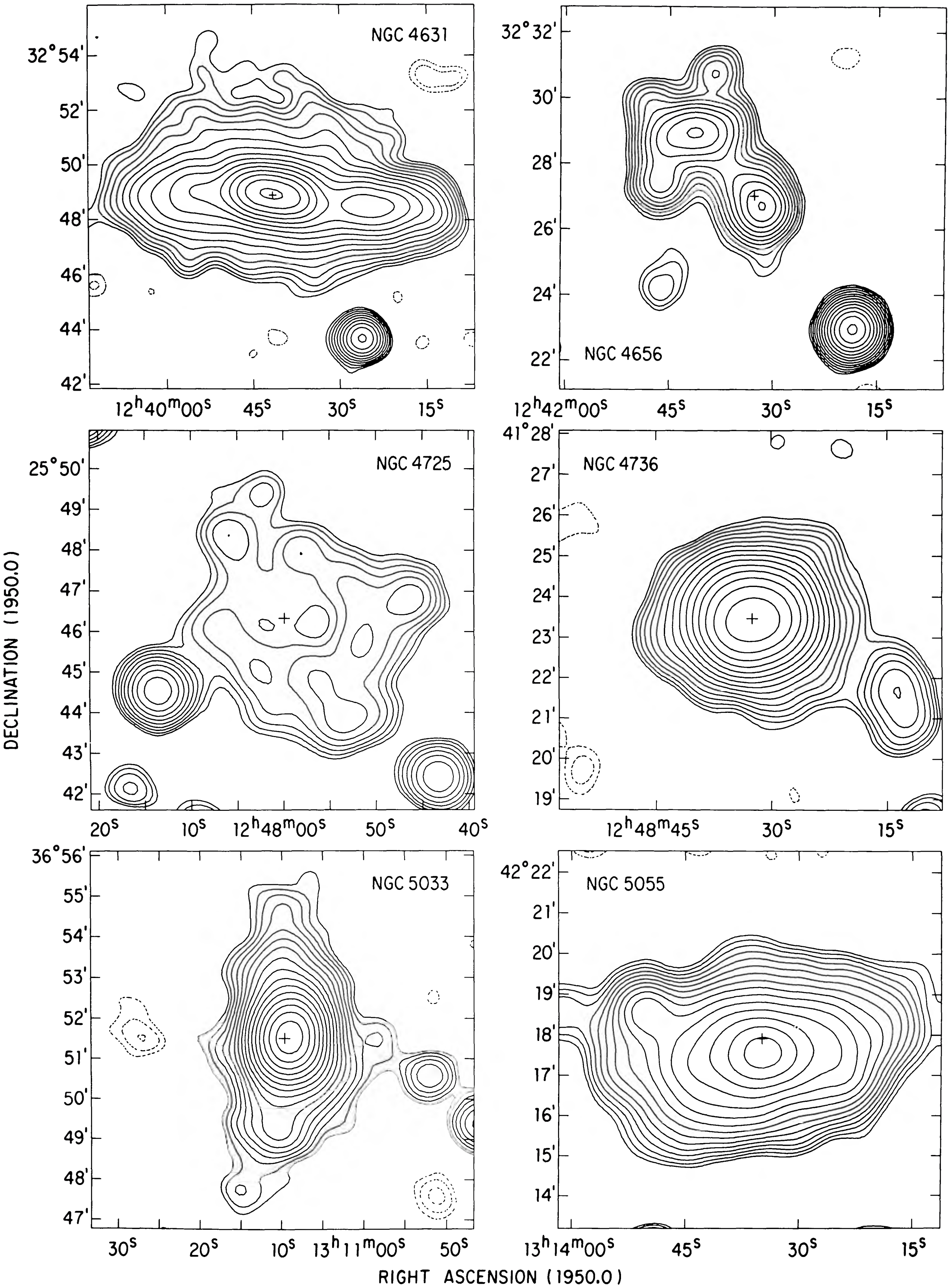

FIG. 6—*Continued*

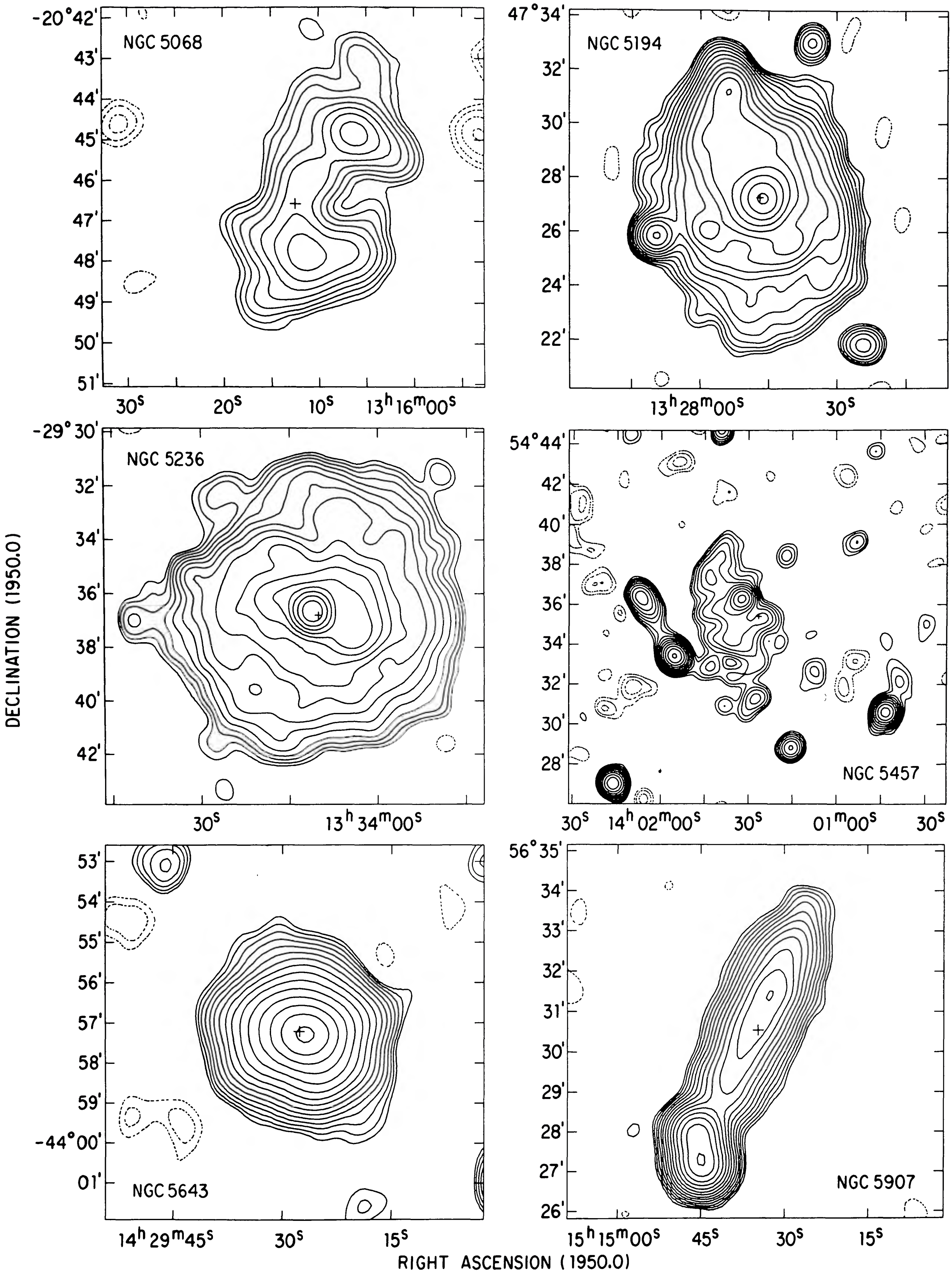

FIG. 6—*Continued*

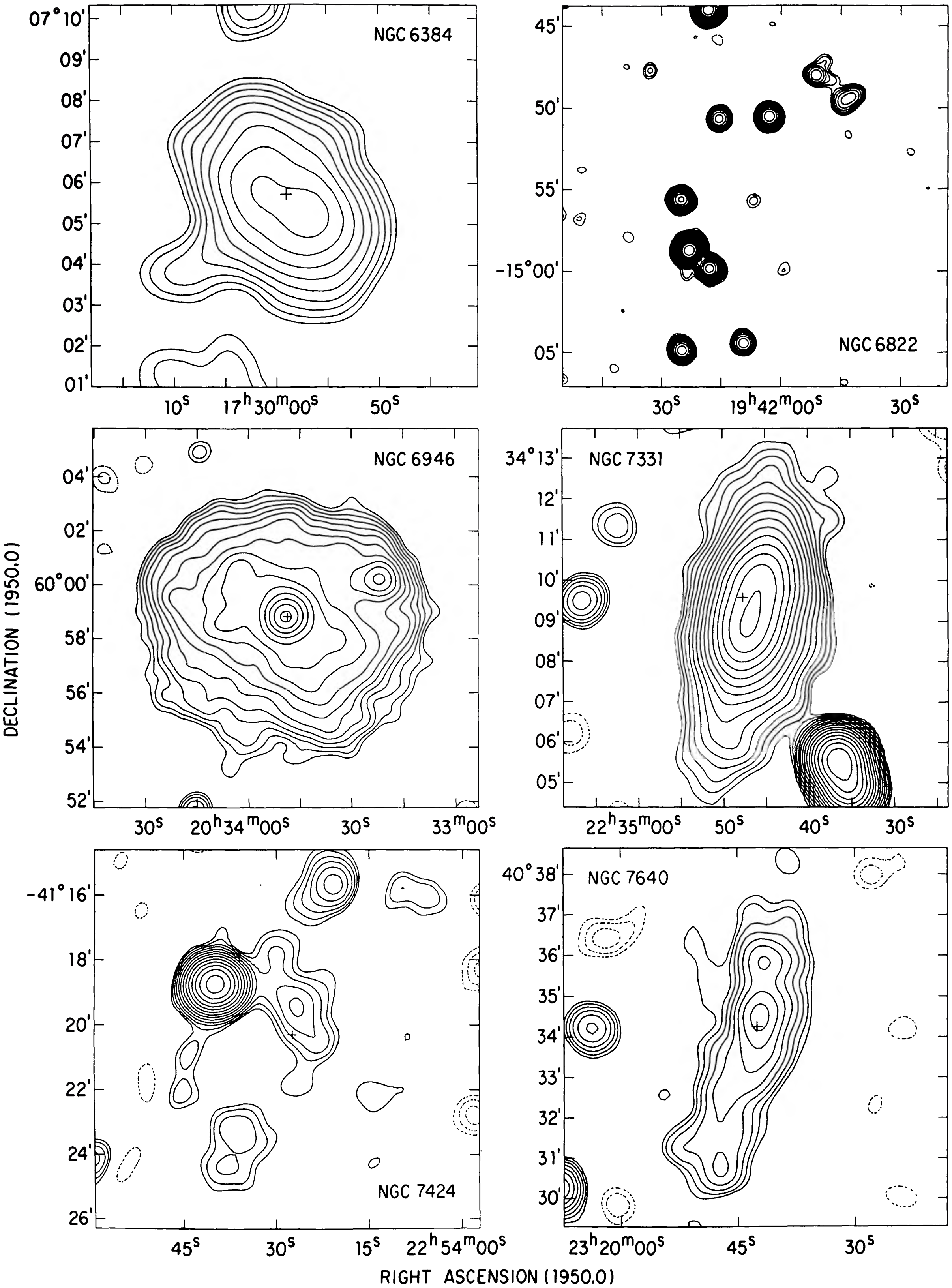

FIG. 6—*Continued*

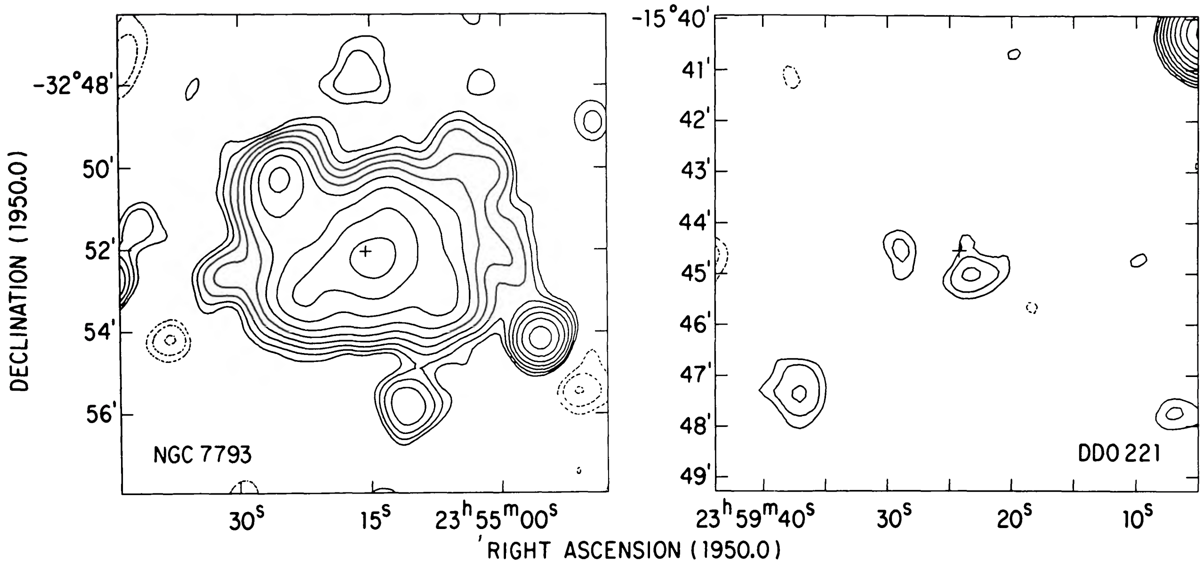

FIG. 6—*Continued*

arranged as follows:

Column (1).—Galaxy name.

Column (2).—Restoring beamwidth θ (FWHM).

Column (3).—The value of n that specifies the faintest contour level plotted, $2^{n/2}$ mJy per beam solid angle.

Column (4).—Total 1.49 GHz flux density S, obtained by direct integration on the map and corrected for recognizable confusion. Uncertain values are indicated by parentheses, and values estimated from filled-aperture observations are enclosed in brackets. Usually the integration area is obvious from the contour map; if not, it is described in the notes to Table 2 in § IV*a*.

Column (5).—The 1.49 GHz absolute spectral luminosity calculated from $L = 4\pi D^2(1+z)^{1+\alpha}S$ assuming $\alpha \approx +0.75$.

The next six columns do not describe the whole source directly but give parameters of Gaussian fits to one or more components of the source. If just the right ascension, declination, and peak flux density S_P are specified, only the source peak was fitted. For full Gaussian fits down to the baseline level, the Gaussian integrated flux densities S_I are also listed. If a component was clearly resolved, its deconvolved major and minor FHWM diameters (θ_M, θ_m) and its major-axis position angle (P.A.) are given.

Columns (6) and (7).—Right ascension and declination (equinox 1950.0).

Column (8).—The 1.49 GHz peak flux density.

Column (9).—The 1.49 GHz integrated flux density.

Column (10).—FWHM major- and minor-axis diameters.

Column (11).—Major-axis position angle.

Column (12).—Notes.

a) *Notes to Individual Galaxies Listed in Table 2*

NGC 7814.—S is the flux density of the component centered on the galaxy only; including the western extensions would increase S to 3.3 mJy.

NGC 0045.—Not detected?

NGC 0055.—S does not include the $S_P = 26.9$ mJy source at $\alpha = 00^h12^m43\overset{s}{.}7$, $\delta = -39°27'32''$ or the $S_P = 3.4$ mJy source at $\alpha = 00^h13^m04\overset{s}{.}3$, $\delta = -39°28'26''$. [1.42 and 4.8 GHz VLA C/D-array maps in Hummel, Dettmar, and Wielebinski (1986); 843 MHz MOST map in Harnett and Reynolds (1985).]

IC 0010.—[10.7 GHz 100 m telescope map in Klein, Gräve, and Wielebinski (1983); 24.5 GHz map in Klein and Gräve (1986).]

NGC 0134.—Asymmetric central component, resolved in the 1.465 GHz VLA C-array map of Hummel *et al.* (1985). S does not include the $S_P = 1.9$ mJy source at $\alpha = 00^h27^m48\overset{s}{.}5$, $\delta = -33°29'00''$.

NGC 0150.—S does not include the $S_I = 55.7$ mJy source at $\alpha = 00^h31^m47\overset{s}{.}8$, $\delta = -28°03'03''$.

NGC 0157.—Asymmetric source; the peak at $\alpha = 00^h32^m13\overset{s}{.}5$, $\delta = -08°40'29''$ is resolved in the 1.465 GHz VLA C-array map of Hummel *et al.* (1985). The southeastern radio extension coincides with an optically bright spiral arm, H II regions.

NGC 0210.—Confused? S does not include the faint northern extensions (with 3.6 mJy total flux density).

NGC 0224.—Contour plot of central region only. The total flux density $S = [8400]$ mJy for the entire galaxy was estimated from the $S = 8.6 \pm 1.1$ Jy at 1410 MHz and $\alpha \approx +0.5$ measured with the NRAO 91 m telescope by Dennison *et al.* (1975). The 1412 MHz WSRT maps and references to earlier maps can be found in Walterbos, Brinks, and Shane (1985).

NGC 0247.—Low T_B, very uncertain S. S does not include the $S_P = 4.5$ mJy source at $\alpha = 00^h44^m21\overset{s}{.}1$, $\delta = -20°58'55''$; the $S_P = 9.9$ mJy source at $\alpha = 00^h44^m41\overset{s}{.}6$, $\delta = -20°55'10''$; the $S_P = 41.0$ mJy source at $\alpha = 00^h44^m44\overset{s}{.}9$, $\delta = -21°07'36''$; or the $S_P = 3.8$ mJy source at $\alpha = 00^h44^m56\overset{s}{.}5$, $\delta = -21°05'51''$. Gaussian fit to the central (?) component only.

NGC 0253.—S does not include the $S_P = 19.5$ mJy source at $\alpha = 00^h44^m45\overset{s}{.}2$, $\delta = -25°34'07''$ or the $S_P = 53.0$ mJy

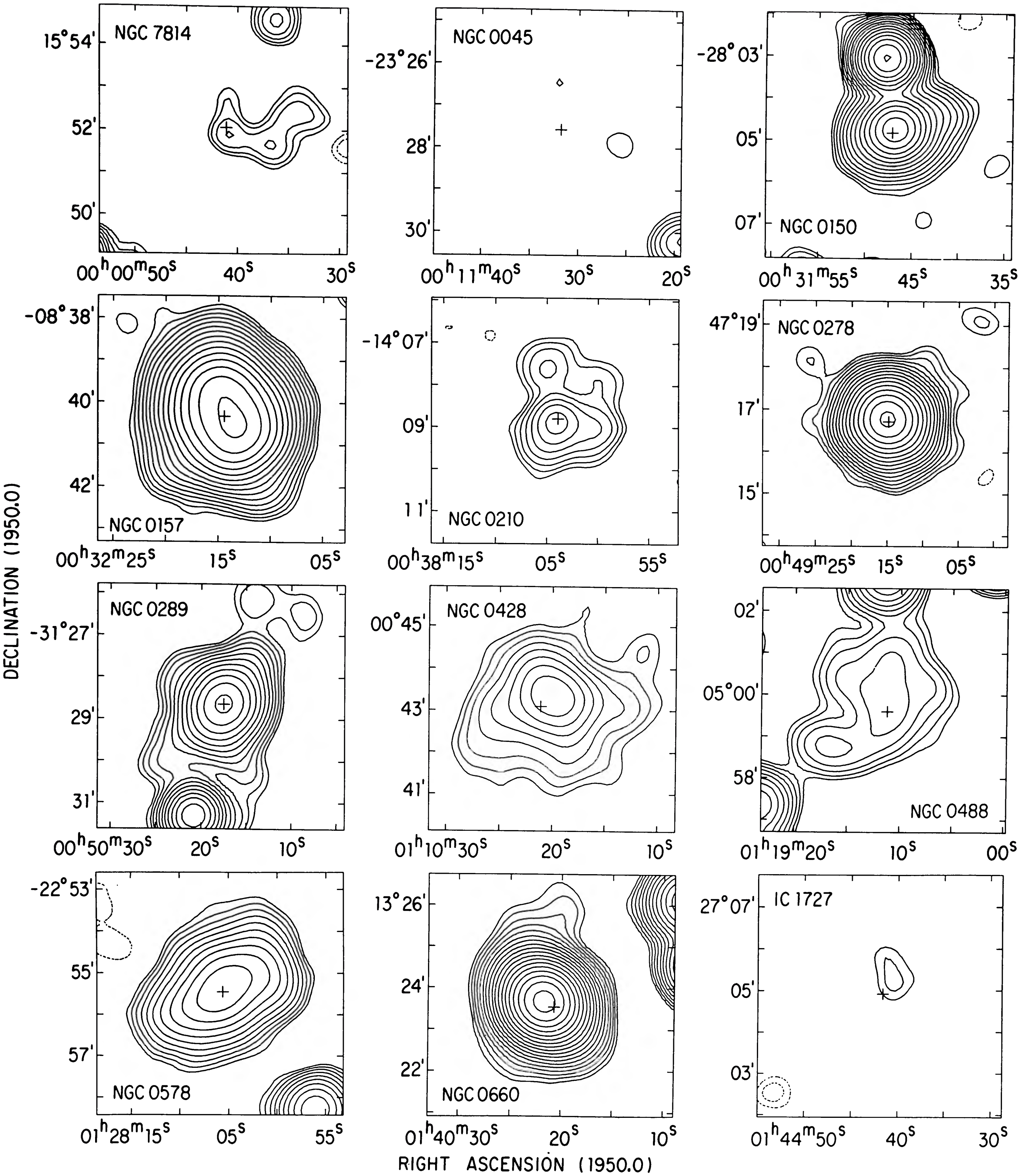

FIG. 7.—Small contour maps, as in Fig. 6

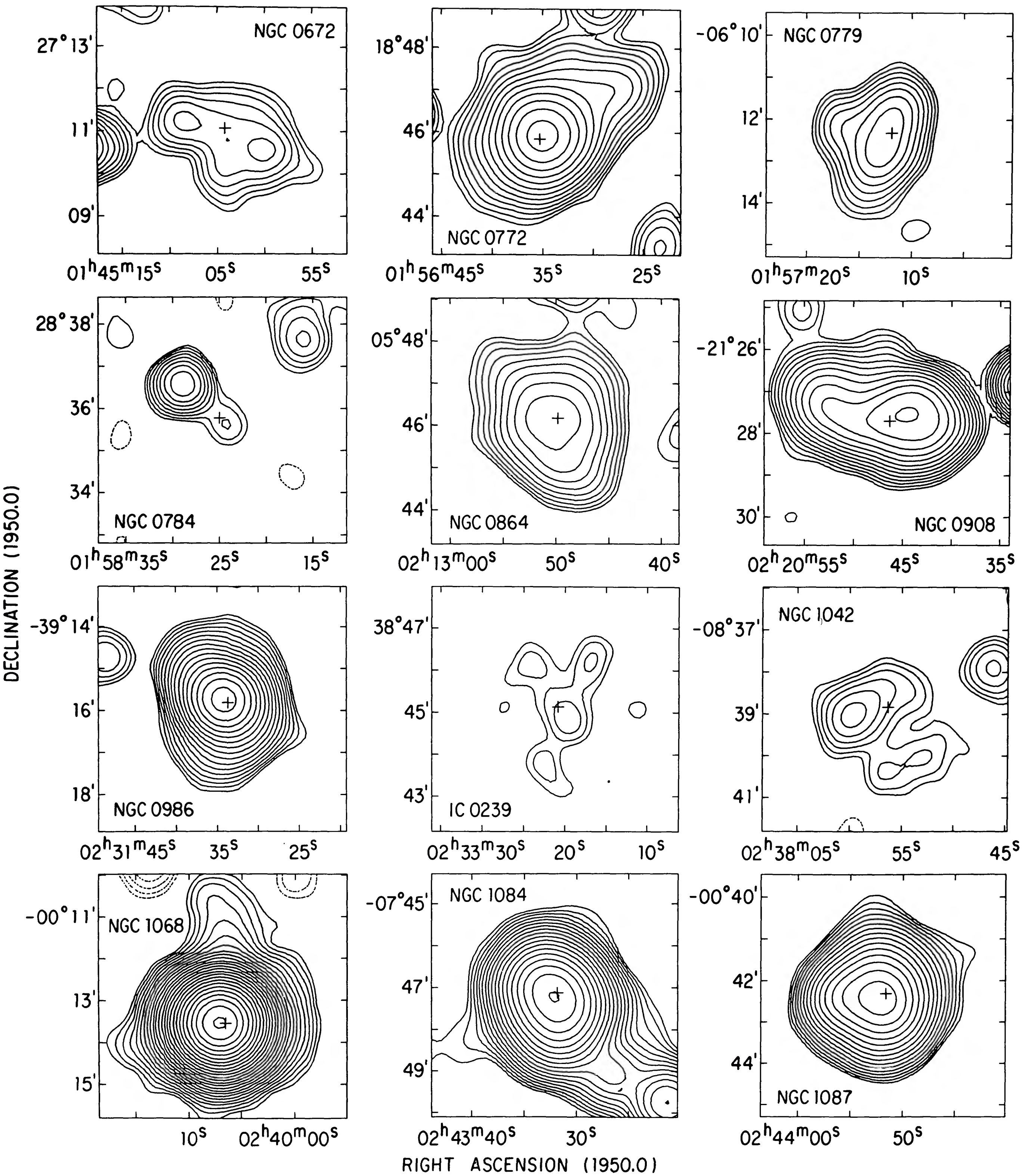

FIG. 7—*Continued*

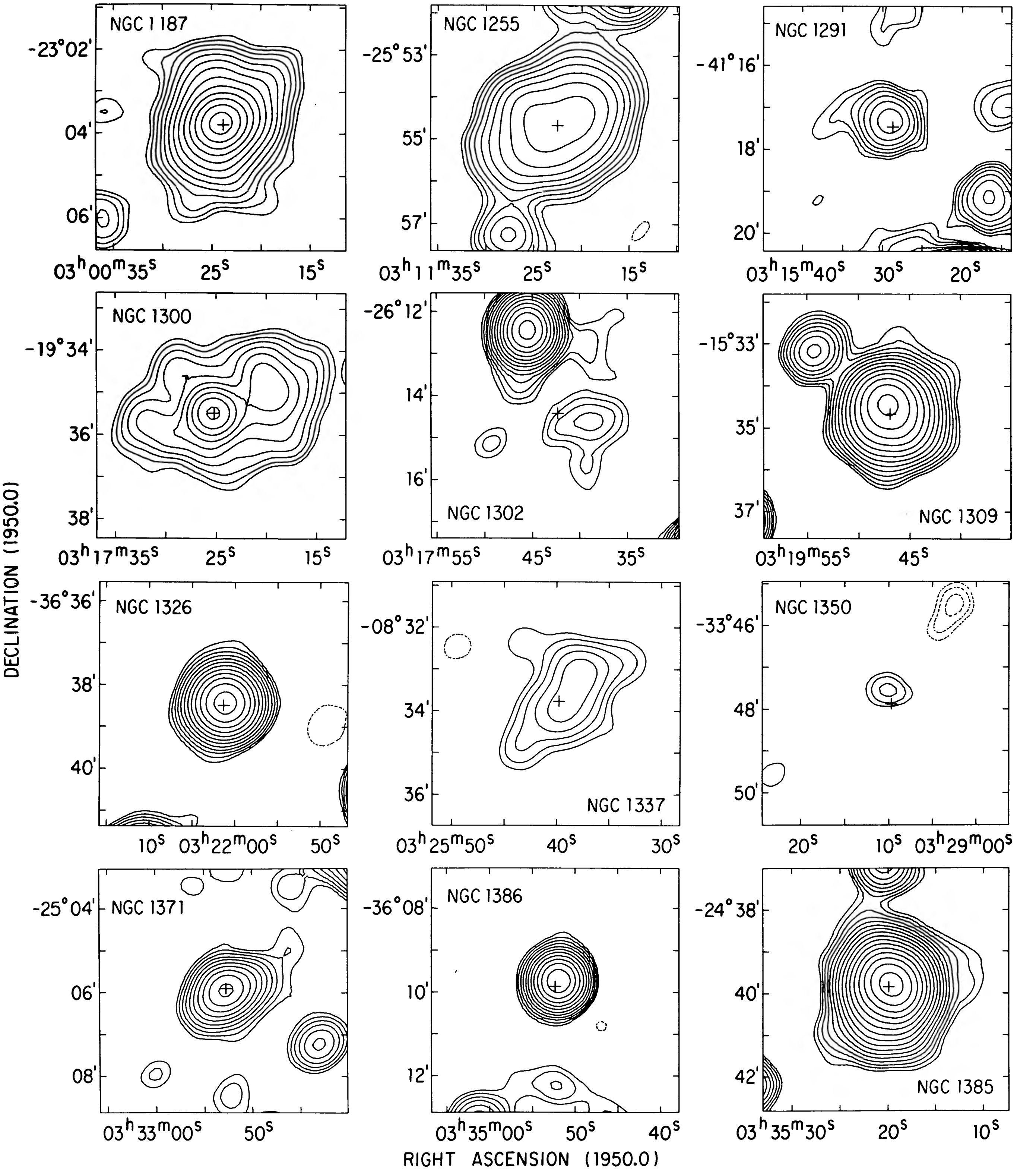

FIG. 7—*Continued*

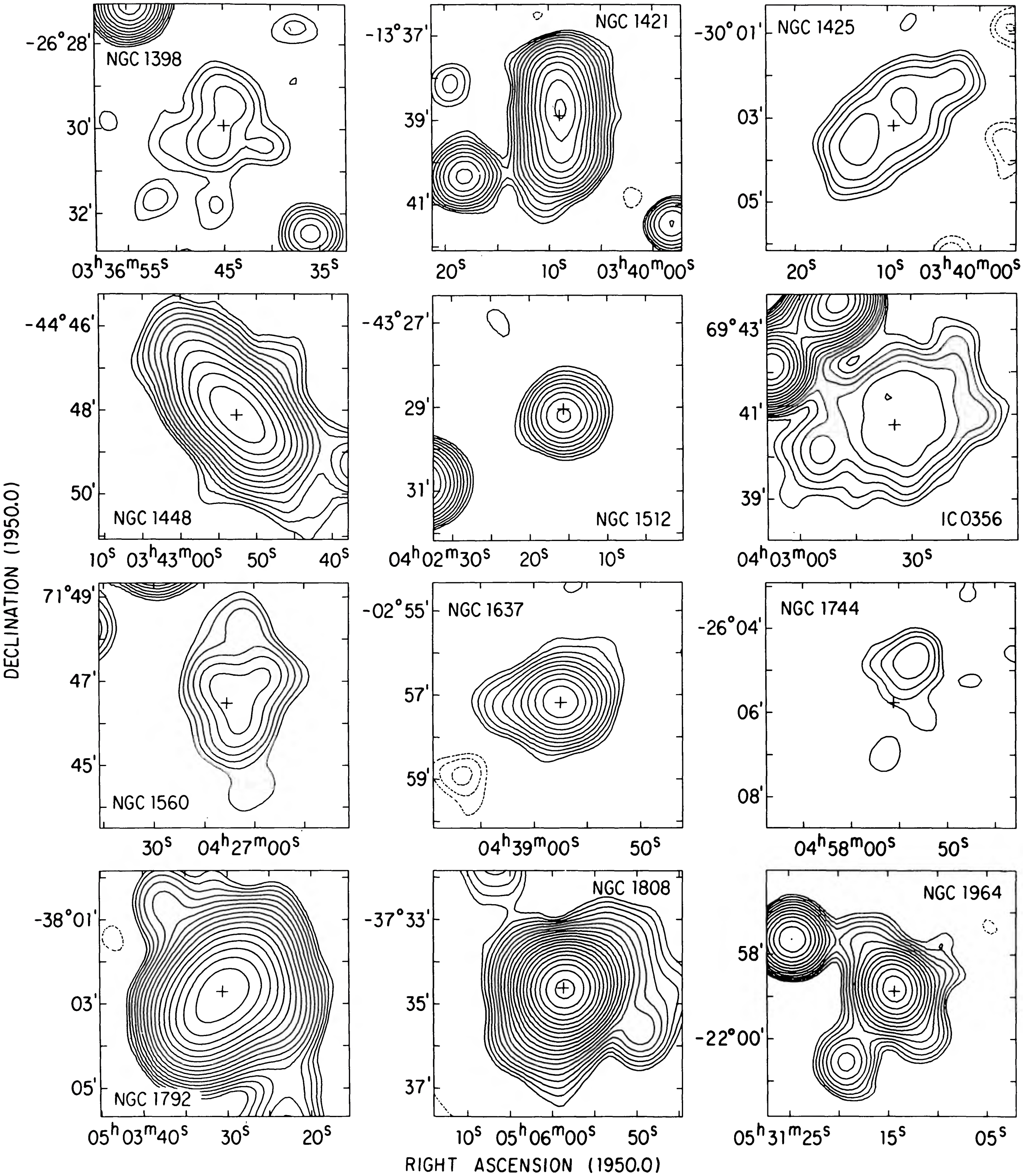

FIG. 7—*Continued*

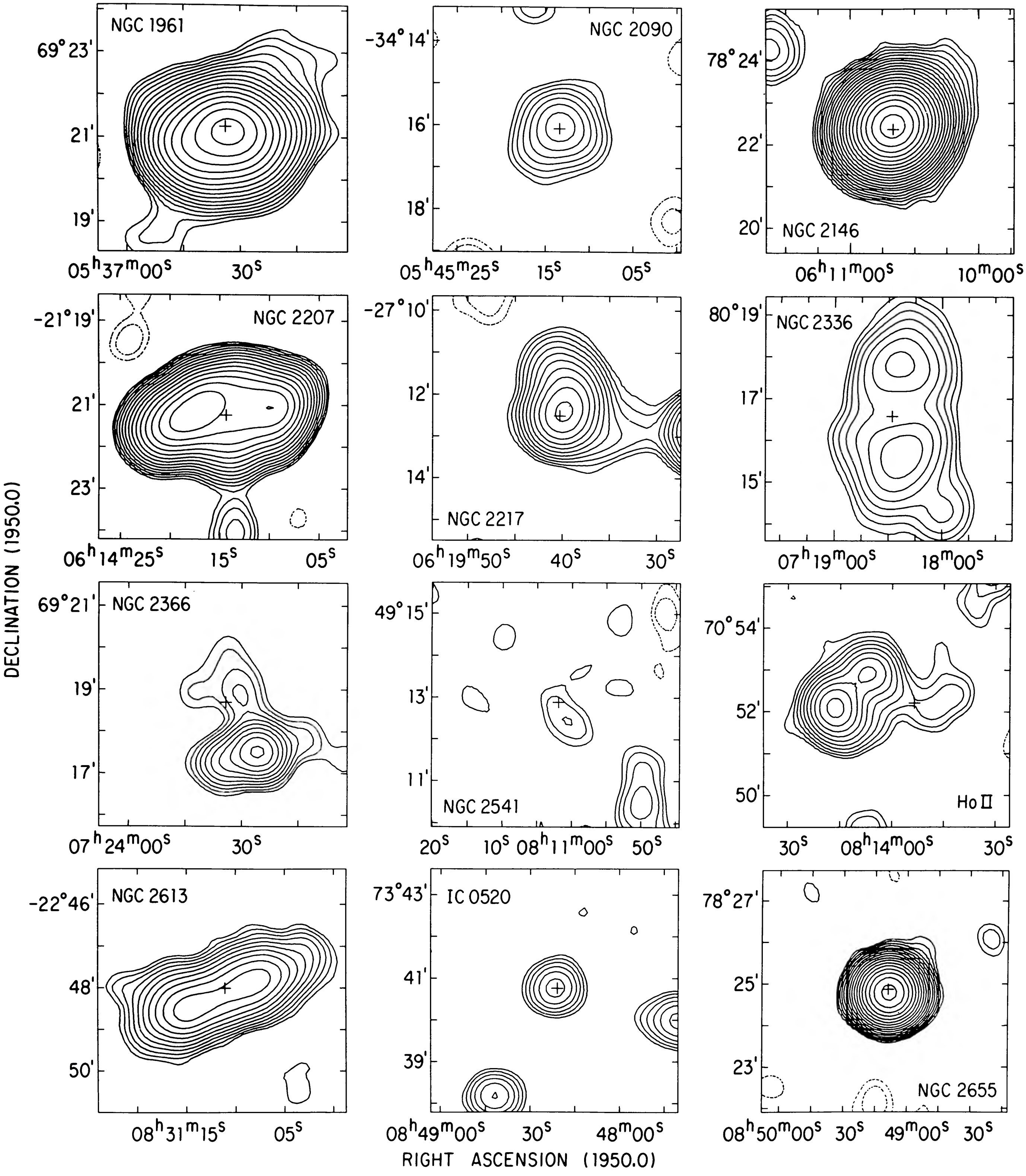

FIG. 7—*Continued*

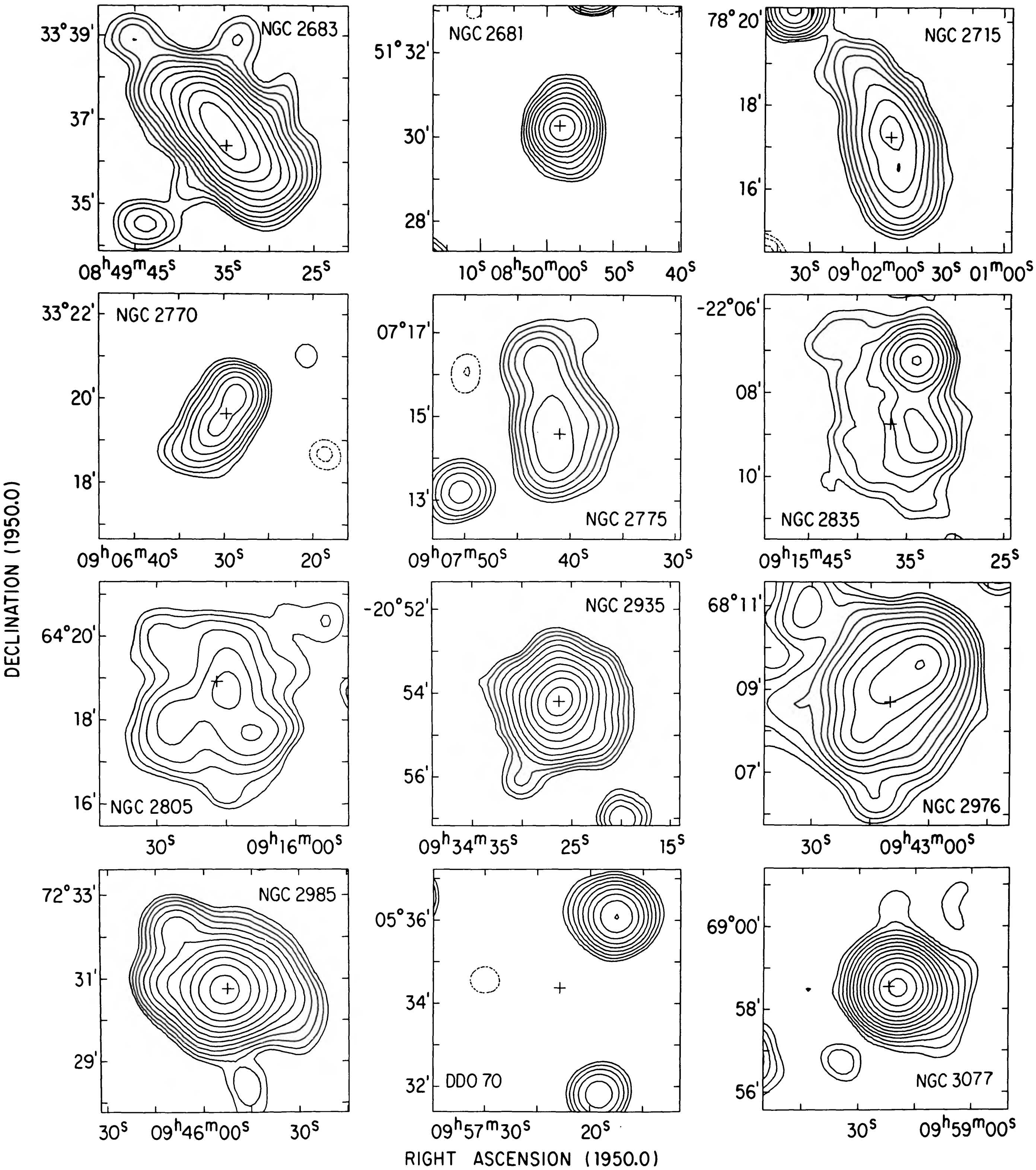

FIG. 7—*Continued*

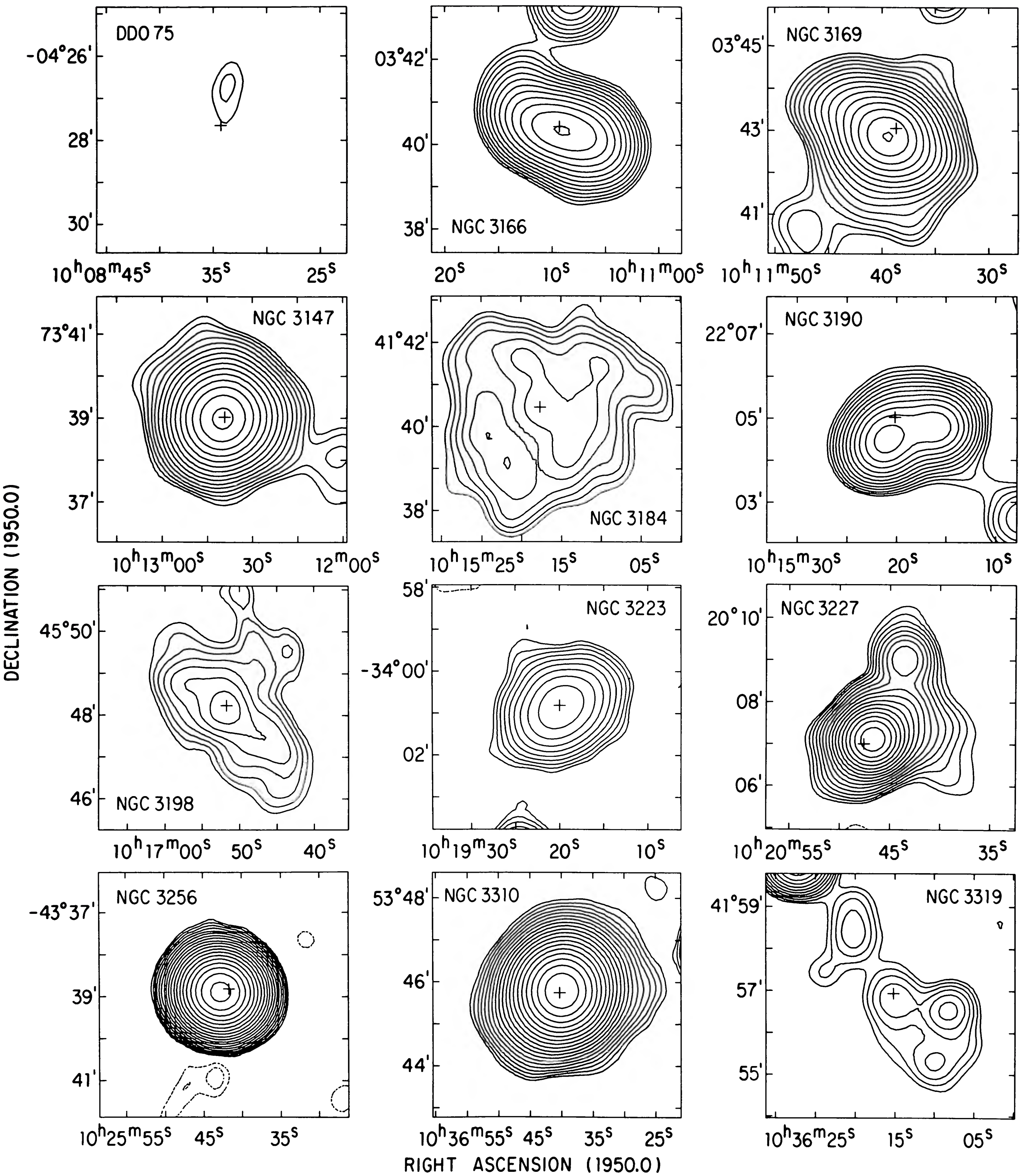

FIG. 7—*Continued*

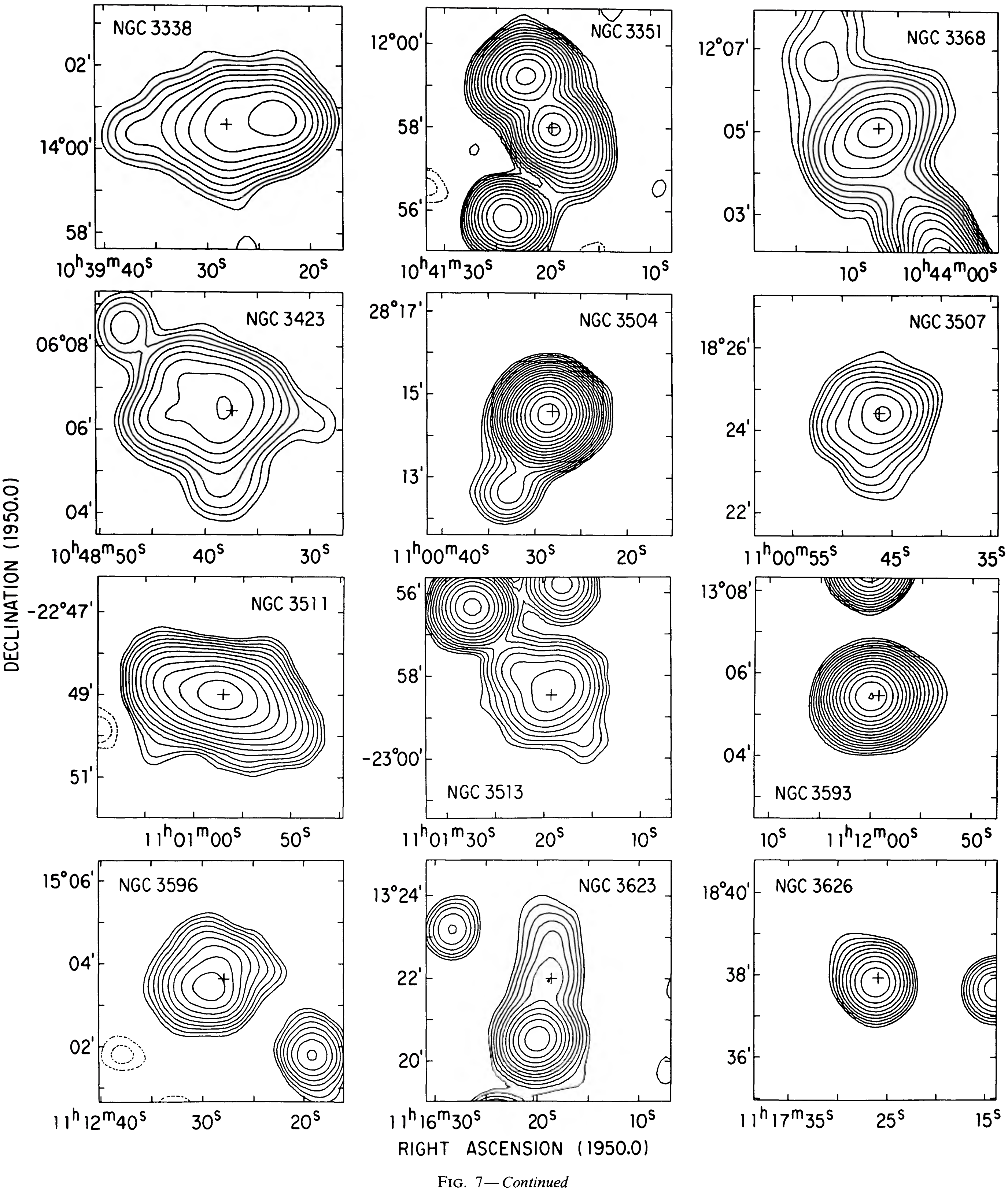

FIG. 7—*Continued*

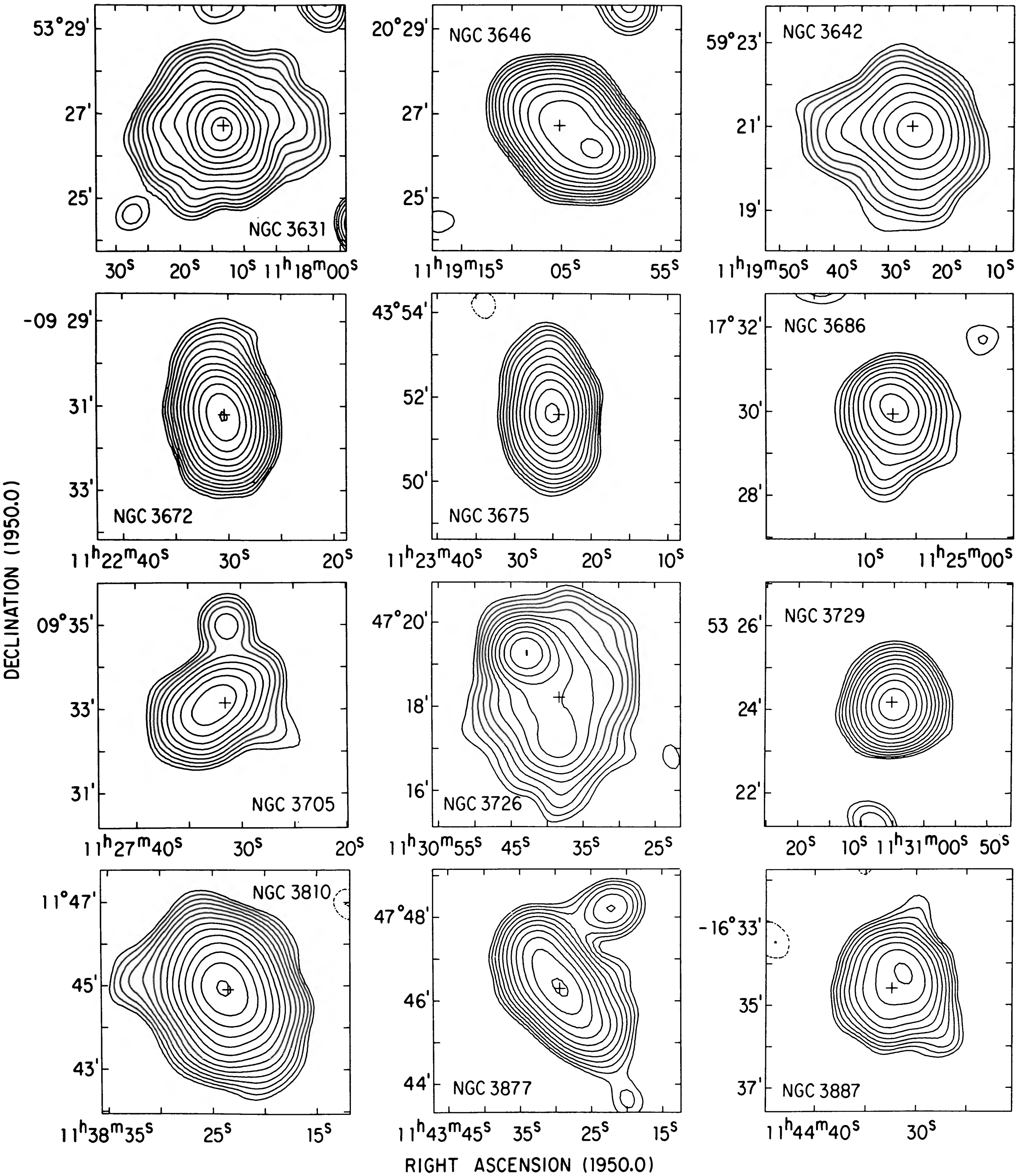

FIG. 7—*Continued*

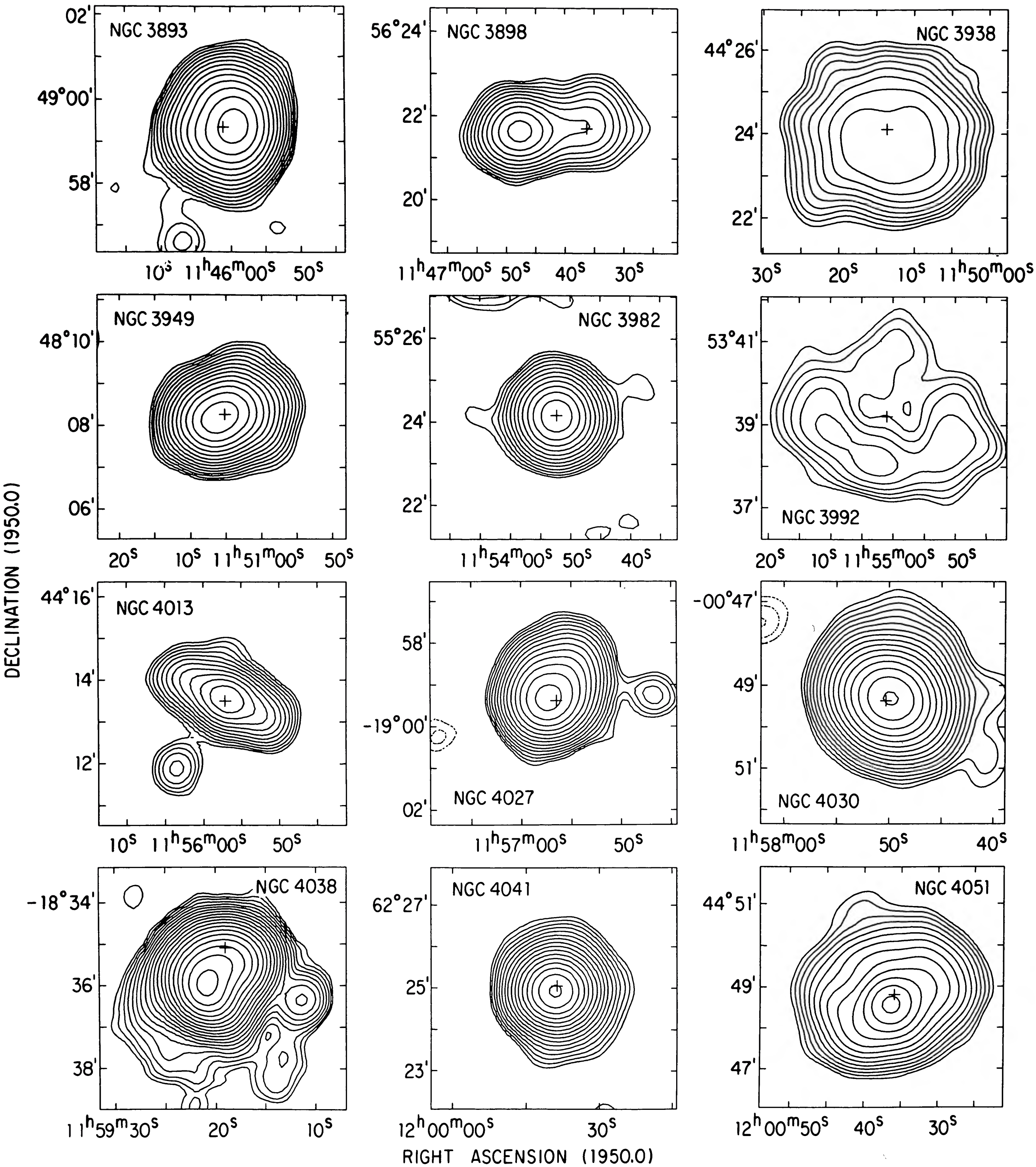

FIG. 7—*Continued*

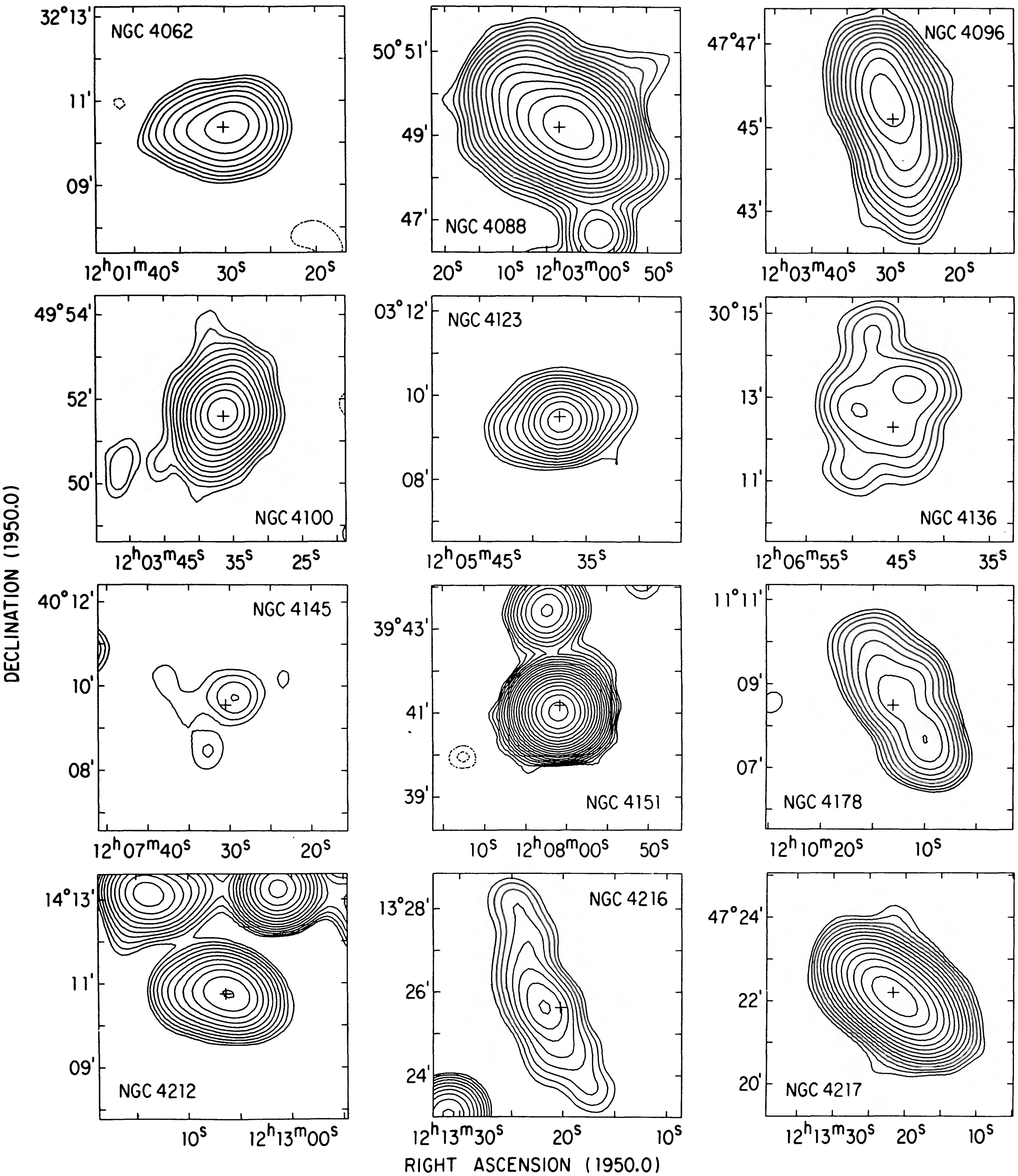

FIG. 7—*Continued*

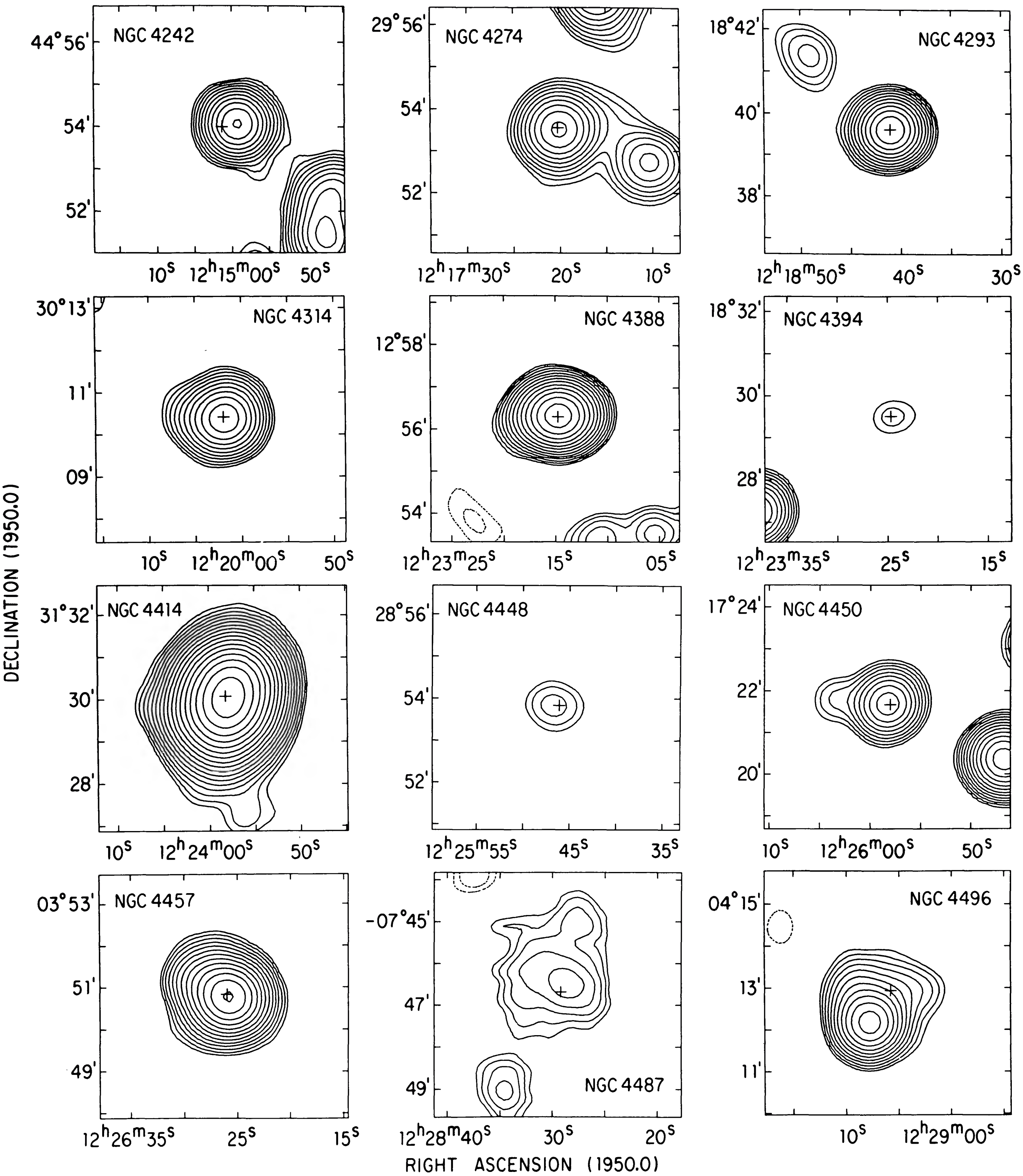

FIG. 7—*Continued*

1987ApJS...65..485C

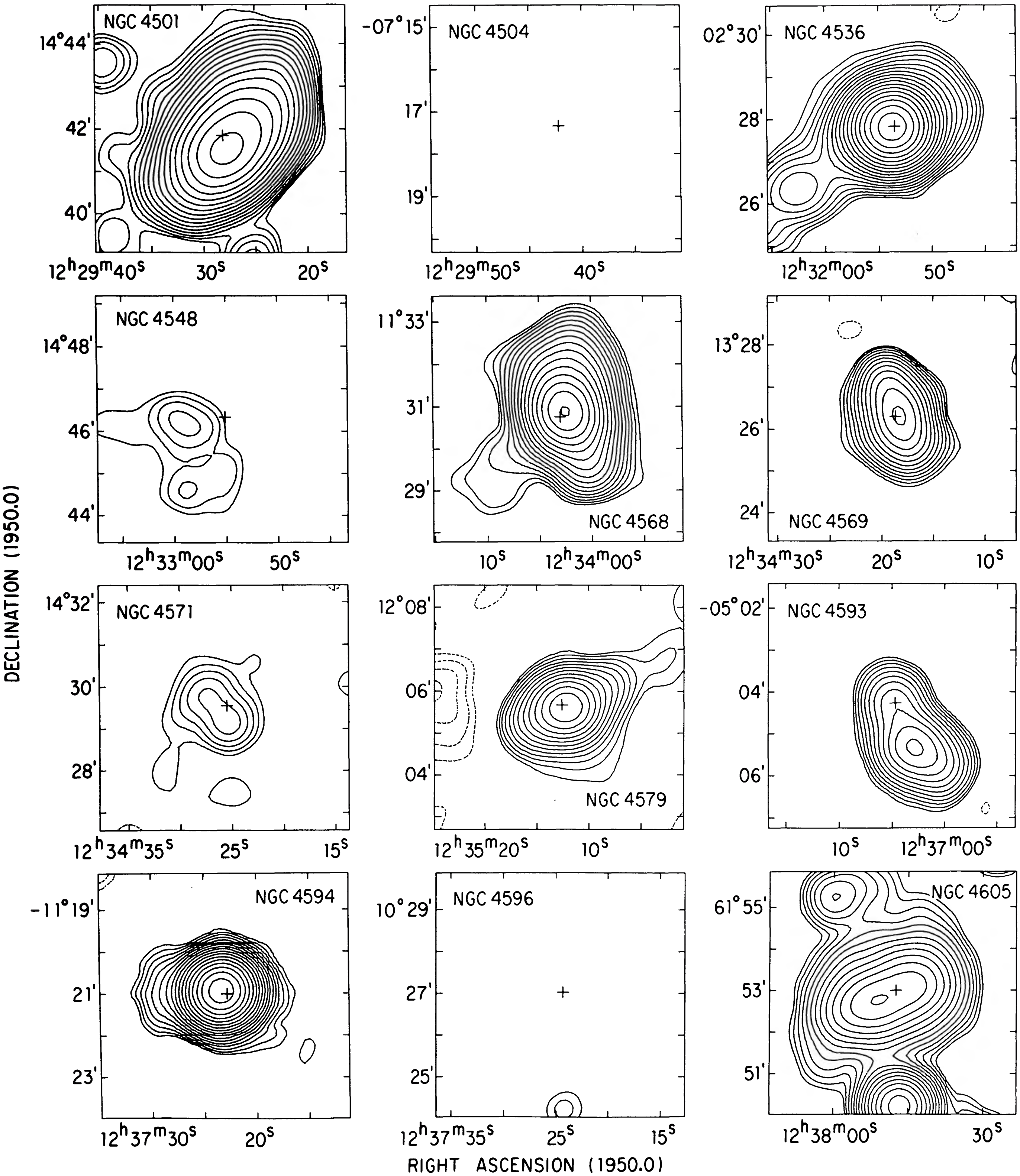

FIG. 7—*Continued*

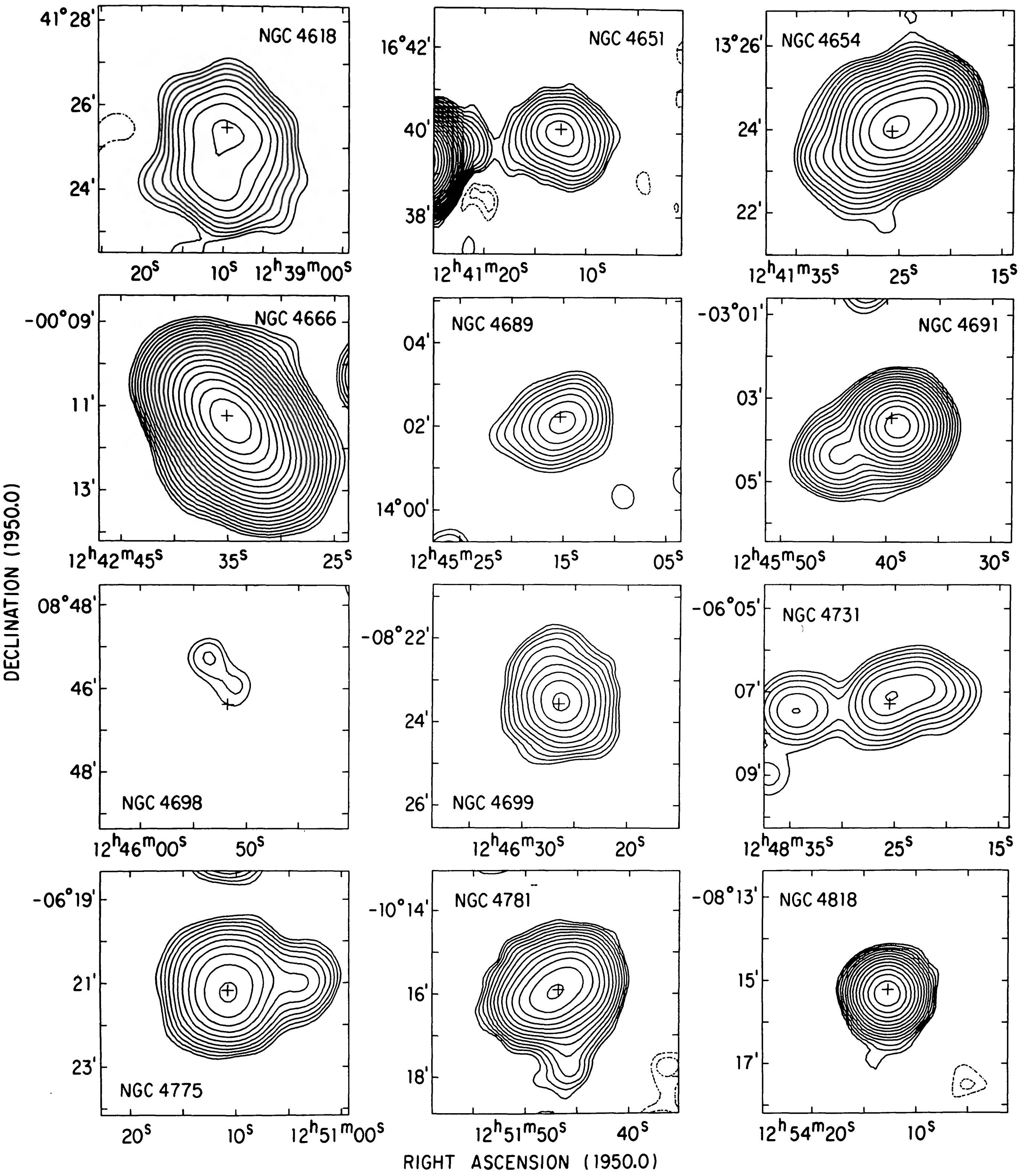

FIG. 7—*Continued*

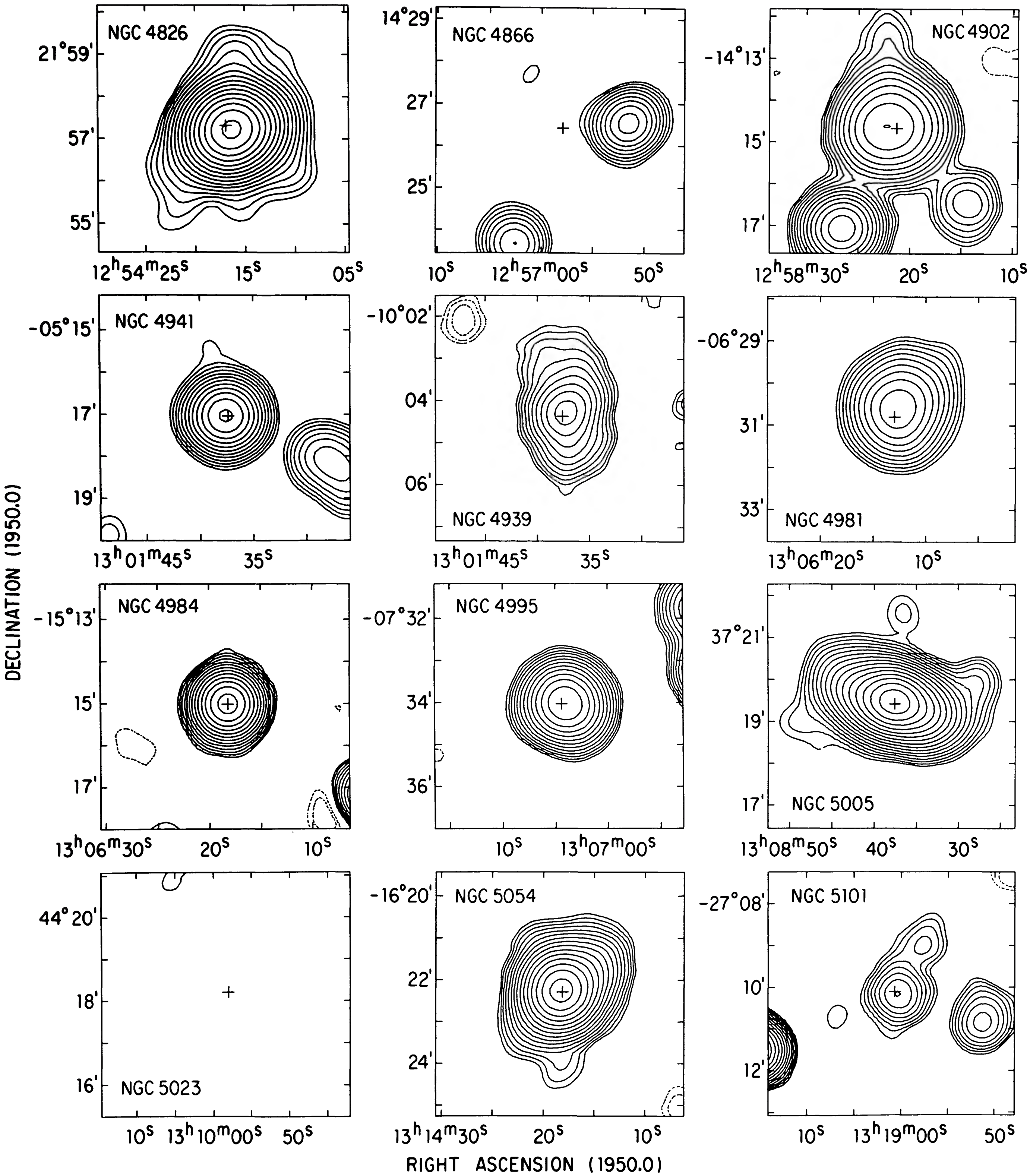

FIG. 7—*Continued*

1987ApJS...65..485C

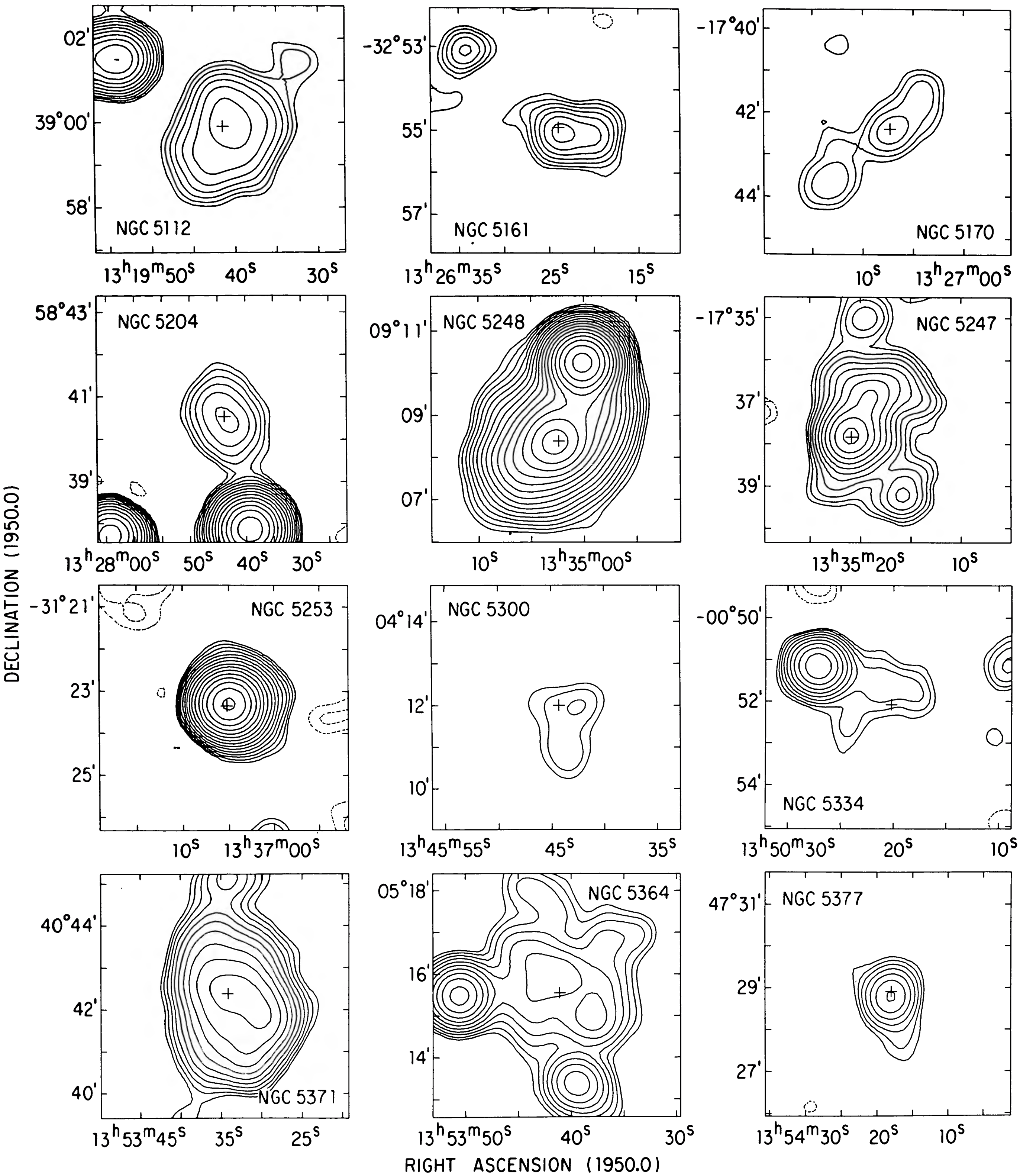

FIG. 7—*Continued*

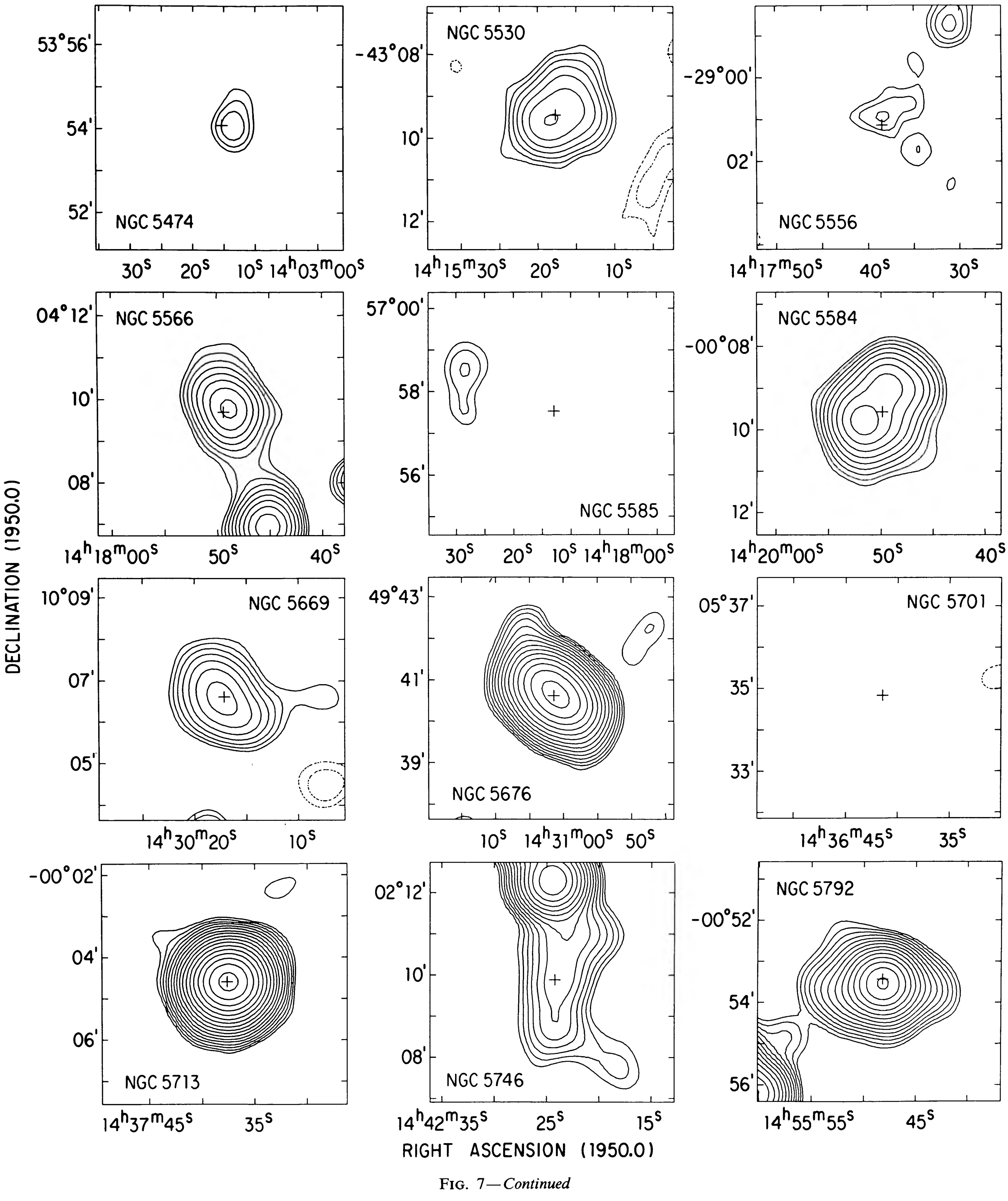

FIG. 7—*Continued*

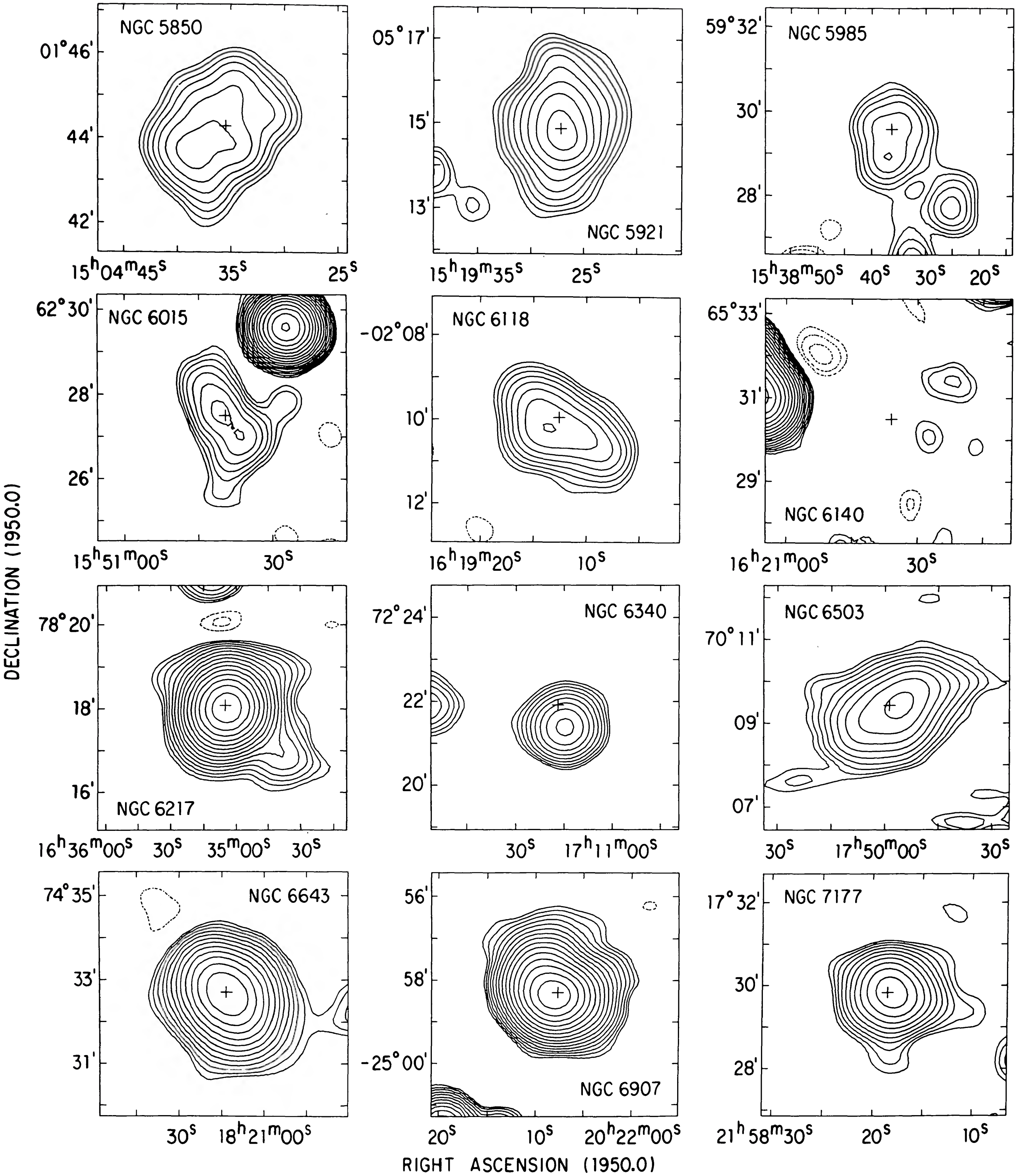

FIG. 7—*Continued*

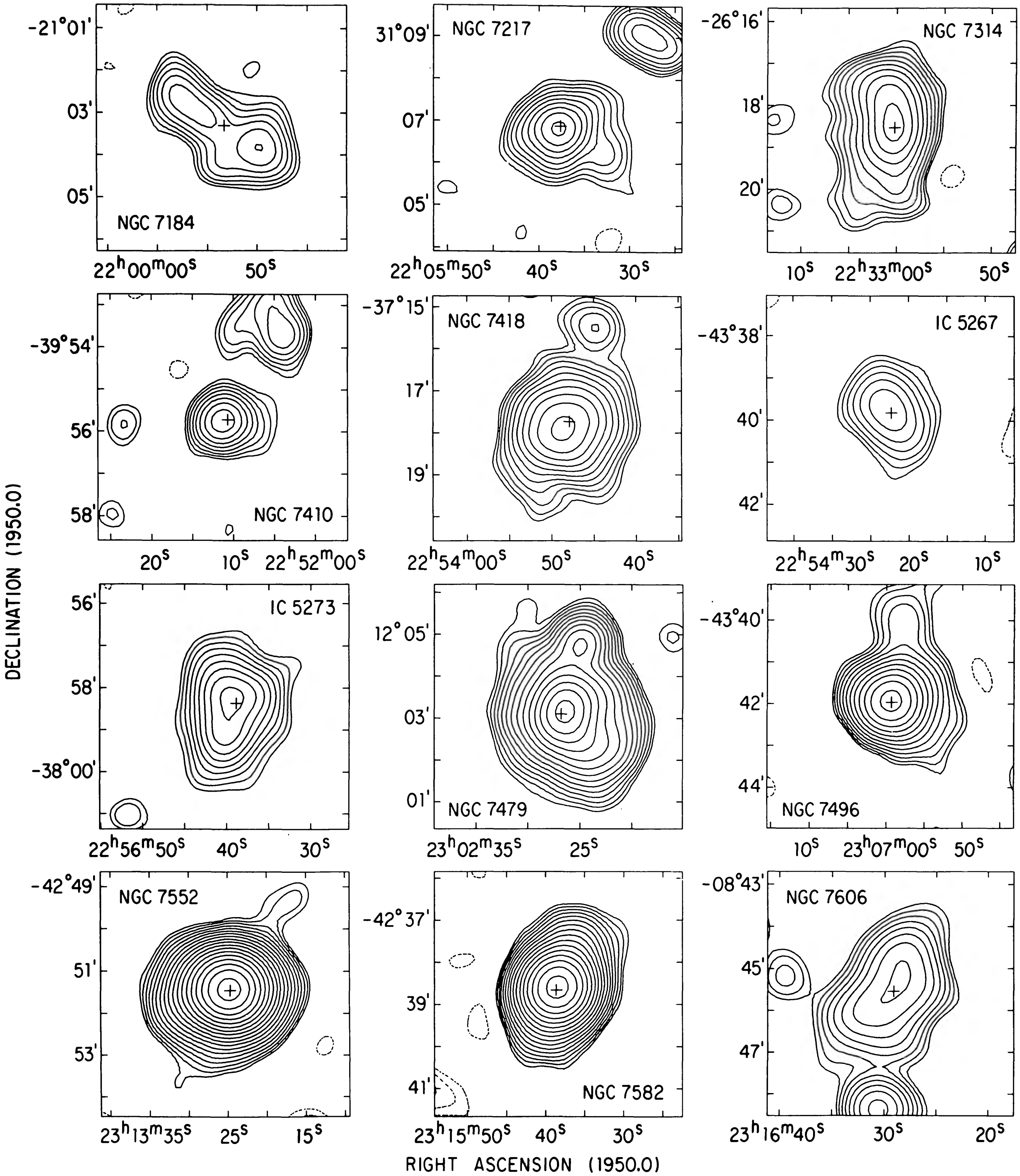

FIG. 7—*Continued*

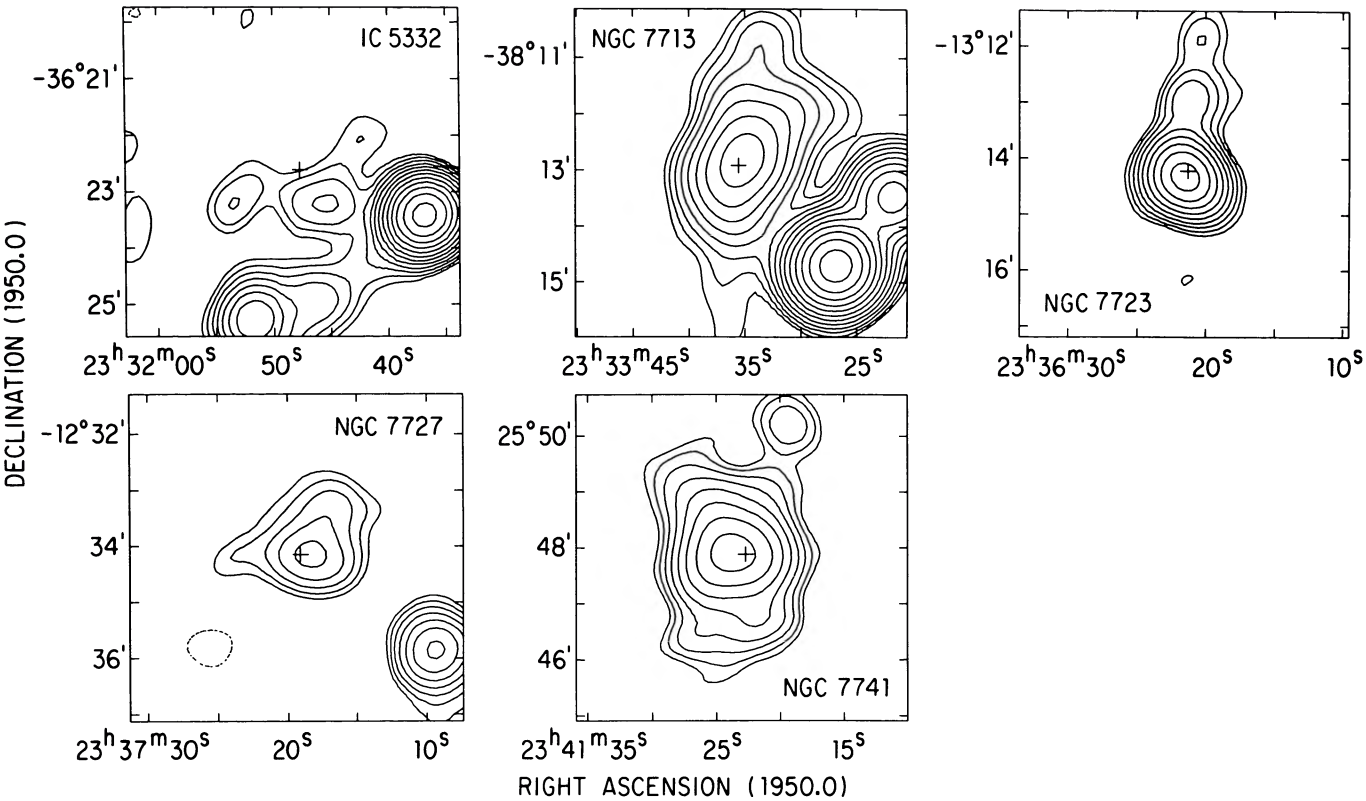

FIG. 7—*Continued*

TABLE 2

RADIO DATA

Galaxy Name	Beam	Plot n	S (mJy)	log(L) (W Hz^{-1})	Component Parameters: R.A. (1950.0)	Decl. (1950.0)	S_P (mJy)	S_I (mJy)	$\theta_M \times \theta_m$	$P.A.$	Notes
NGC 7814	0'.8	−3	1.1	19.95	00^{h}00^{m}40^s.8	+15°51′52″	1.1				*
NGC 0045	0.8	−3	(1.9)	(19.41)							*
NGC 0055	1.0	−1	381.0	20.66	00 12 28.1	−39 29 09	60.4				*
IC 0010	0.8	−1	298.0	19.79	00 17 34.3	+59 02 03	27.6				*
					00 17 45.0	+59 00 26	62.3				
NGC 0134	0.8	−2	191.0	22.37	00 27 57.0	−33 30 40	21.2	44.2	1'.1 × 0'.6	30°	*
					00 27 53.0	−33 31 13	30.7	145.0	2.5 × 0.8	47	
NGC 0150	0.8	−3	51.9	21.82	00 31 46.8	−28 04 46	29.2	48.8	0.8 × 0.5	111	*
NGC 0157	1.0	−3	171.0	22.43	00 32 14.0	−08 40 18	53.4	173.0	1.8 × 1.3	24	*
NGC 0210	0.8	−3	(7.2)	(21.09)	00 38 04.0	−14 08 53	3.6				*
NGC 0224	0.8	−2	[8400.0]	[20.73]	00 40 01.1	+40 59 50	14.5				*
NGC 0247	0.9	−3	(24.0)	(19.46)	00 44 36.4	−21 02 27	1.9	10.9	2.2 × 1.7	84	*
NGC 0253	1.0	+3	5594.0	22.07	00 45 05.7	−25 33 40	2560.0				*
NGC 0278	0.8	−3	138.0	21.76	00 49 14.9	+47 16 46	71.0	134.0	0.8 × 0.7		*
NGC 0289	0.8	−3	47.0	21.88	00 50 17.5	−31 28 39	17.6	43.5	1.2 × 0.8	153	*
NGC 0300	0.8	−2	(3.8)	(18.42)							*
IC 1613	1.0	−3	(3.3)	(17.46)							*
NGC 0428	1.0	−3	18.9	21.20	01 10 20.0	+00 43 17	5.2				
NGC 0488	1.0	−3	7.6	21.34							*
NGC 0578	1.0	−3	35.0	21.68	01 28 05.4	−22 55 22	10.7	35.4	2.1 × 1.0	123	
NGC 0598	0.8	0	[3300.0]	[20.50]							*
NGC 0613	1.0	−2	220.0	22.40	01 31 59.4	−29 40 27	80.0	70.7	< 0.3		*
					01 31 59.7	−29 40 33	39.1	149.0	2.4 × 1.1	116	
NGC 0628	1.0	−3	[180.0]	[21.81]							*
NGC 0660	1.0	−1	387.0	22.25	01 40 21.7	+13 23 40	310.0	374.0	0.6 × 0.3	45	*
IC 1727	0.8	−3	(1.1)	(19.17)	01 44 40.5	+27 05 24	0.7	1.3	1.0 × 0.5	12	*
NGC 0672	0.8	−3	13.9	20.45							*
NGC 0772	1.0	−3	71.4	22.39	01 56 35.0	+18 45 56	27.2	60.9	1.2 × 1.1	140	*

Galaxy Name	Beam	Plot n	S (mJy)	log(L) (W Hz^{-1})	Component Parameters: R.A. (1950.0)	Decl. (1950.0)	S_P (mJy)	S_I (mJy)	$\theta_M \times \theta_m$	$P.A.$	Notes
NGC 0779	1.0	−3	11.8	21.10	01 57 12.7	−06 12 22	6.3	11.2	1.4 × 0.3	160	*
NGC 0784	0.8	−3	(1.0)	(18.95)	01 58 24.3	+28 35 38	0.8				*
NGC 0864	1.0	−3	28.9	21.61	02 12 50.1	+05 46 02	8.1	27.8	1.7 × 1.4	24	
NGC 0891	0.8	−2	701.0	22.31	02 19 24.3	+42 07 15	17.3				*
					02 19 24.8	+42 07 32	84.8	654.0	4.2 × 0.9	23	
NGC 0908	0.8	−2	178.0	22.32	02 20 44.4	−21 27 37	35.8	132.0	1.5 × 1.1	83	*
					02 20 52.1	−21 27 23	17.6	48.3	1.4 × 0.8	48	
NGC 0925	0.8	−2	(46.0)	(21.14)	02 24 16.8	+33 21 18	4.9				*
NGC 0986	1.0	−3	110.0	22.33	02 31 34.2	−39 15 45	78.4	105.0	0.7 × 0.4	40	
IC 0239	0.8	−3	5.7	20.49	02 33 19.6	+38 44 52	1.0				
NGC 1042	1.0	−3	4.3	20.63							*
NGC 1055	1.0	−2	213.0	22.09	02 39 11.1	+00 13 51	99.7	203.0	1.5 × 0.5	103	*
NGC 1068	1.0	0	4991.0	23.56	02 40 07.0	−00 13 31	3860.0				*
					02 40 07.0	−00 13 33	700.0	1100.0	0.9 × 0.7	61	
NGC 1073	1.0	−3	(30.0)	(21.40)							*
NGC 1084	1.0	−3	281.0	22.47	02 43 32.1	−07 47 17	135.0	280.0	1.3 × 0.8	28	*
NGC 1087	1.0	−3	133.0	22.23	02 43 52.6	−00 42 25	57.2	133.0	1.3 × 1.0	81	
NGC 1097	1.0	−2	415.0	22.52	02 44 11.1	−30 29 00	199.0	219.0	0.4 × 0.2	125	*
					02 44 11.8	−30 28 57	19.9	188.0	3.6 × 2.3	156	
NGC 1187	0.8	−3	69.0	21.83	03 00 24.1	−23 03 45	20.5	21.9	< 0.4		
					03 00 23.9	−23 03 44	8.7	47.2	2.0 × 1.4	156	
NGC 1232	0.8	−3	58.5	21.95							
NGC 1255	1.0	−3	32.5	21.63	03 11 22.6	−25 54 38	7.6	34.6	2.2 × 1.6	123	*
NGC 1291	1.0	−3	4.4	20.06	03 15 29.2	−41 17 19	3.7	3.9	< 0.5		*
NGC 1300	0.8	−3	35.2	21.60	03 17 25.2	−19 35 30	9.3				*
NGC 1302	0.8	−3	(3.7)	(20.70)	03 17 38.9	−26 14 37	1.2				*
NGC 1309	0.8	−3	67.1	22.17	03 19 47.0	−15 34 33	25.4	67.5	1.1 × 1.0	20	*
NGC 1326	1.0	−2	30.6	21.53	03 22 01.2	−36 38 26	29.4	29.4	< 0.2		
NGC 1337	1.0	−3	6.2	20.68	03 25 38.7	−08 33 32	1.7	6.9	2.5 × 1.0	143	
NGC 1350	0.8	−3	1.1	20.08	03 29 10.1	−33 47 33	0.8				
NGC 1365	0.8	−2	530.0	22.77	03 31 41.9	−36 18 23	316.0	347.0	0.3 × 0.1	49	*
					03 31 41.9	−36 18 15	13.3	194.0	3.5 × 2.5	131	
NGC 1371	0.8	−3	14.8	21.16	03 32 52.7	−25 05 57	9.2	13.5	0.8 × 0.2	120	
NGC 1386	0.8	−1	35.1	21.59	03 34 51.9	−36 09 44	32.8	35.0	< 0.3		
NGC 1385	0.8	−3	172.0	22.51	03 35 19.7	−24 39 49	77.3	163.0	0.9 × 0.8	30	*
NGC 1398	0.8	−3	(6.2)	(20.81)							
NGC 1421	0.8	−2	102.0	22.33	03 40 08.9	−13 38 51	33.8	101.0	1.9 × 0.5	1	*
NGC 1425	0.8	−3	12.7	21.10	03 40 10.1	−30 03 08	1.7	15.7	3.6 × 1.4	130	
IC 0342	0.9	+1	[2250.0]	[21.77]	03 41 56.1	+67 56 26	157.0	209.0	0.6 × 0.3	14	*
NGC 1448	1.0	−2	95.5	21.70	03 42 52.7	−44 48 04	31.8	93.2	2.2 × 0.7	41	*
NGC 1512	1.0	−3	7.0	20.29	04 02 15.6	−43 29 11	6.6	6.4	< 0.3		
IC 0356	0.8	−3	29.5	21.17							*
NGC 1532	1.0	−2	95.8	21.75	04 10 09.1	−33 00 07	17.0				*
NGC 1569	1.0	−3	411.0	20.61	04 26 04.2	+64 44 31	88.3				*
					04 26 05.3	+64 44 20	106.0	298.0	1.6 × 1.1	113	
NGC 1560	1.0	−3	9.4	19.39	04 27 04.5	+71 46 40	2.6	9.8	2.0 × 1.3	170	
NGC 1637	1.0	−3	16.5	20.61	04 38 57.5	−02 57 10	11.3	15.6	0.6 × 0.6		
NGC 1744	0.8	−3	6.4	20.10							*
NGC 1792	1.0	−3	276.0	22.17	05 03 30.6	−38 02 48	89.6	276.0	1.9 × 1.1	136	*
NGC 1808	1.0	−2	519.0	22.22	05 05 58.5	−37 34 39	425.0	497.0	0.5 × 0.3	147	*
NGC 1964	0.8	−3	47.8	21.76	05 31 14.4	−21 58 49	31.0	42.7	0.6 × 0.3	17	*
NGC 1961	1.0	−3	182.0	23.19	05 36 34.0	+69 21 04	74.0	180.0	1.5 × 0.9	100	*
NGC 2090	1.0	−2	8.6	20.37	05 45 13.3	−34 16 05	5.9	6.8	< 0.5		
NGC 2146	1.0	−1	1087.0	22.81	06 10 40.3	+78 22 28	912.0	1075.0	0.5 × 0.3	132	*
NGC 2207	0.8	−2	310.0	23.00							*
NGC 2217	1.0	−2	29.7	21.47	06 19 39.9	−27 12 25	18.3				
NGC 2280	1.0	−3	59.7	21.93	06 42 49.7	−27 35 12	20.0	52.8	1.6 × 1.0	159	*
NGC 2276	1.0	−3	283.0	22.98	07 10 22.0	+85 50 56	118.0	275.0	1.3 × 1.0	133	*
NGC 2336	1.0	−3	17.7	21.70							*
NGC 2366	0.8	−2	25.0	19.58							*
NGC 2403	0.8	−2	[330.0]	[20.70]							*
NGC 2541	0.8	−1	(3.2)	(19.81)	08 11 00.6	+49 12 34	1.5				
Ho II	0.8	−3	22.1	19.51							*
NGC 2613	0.8	−3	50.6	21.71	08 31 11.3	−22 48 09	10.7	51.7	2.9 × 0.7	113	*
IC 0520	0.8	−3	3.0	21.29	08 48 21.5	+73 40 47	2.5	3.1	0.4 × 0.3		
NGC 2655	0.8	−3	121.0	22.17	08 49 08.6	+78 24 48	112.0	121.0	0.3 × 0.2	13	*
NGC 2683	0.8	−3	65.9	20.70	08 49 35.0	+33 36 41	14.6	65.0	2.4 × 0.8	40	*
NGC 2681	0.8	−3	12.0	20.57	08 49 57.6	+51 30 13	7.7	10.9	0.6 × 0.5		
NGC 2715	0.8	−3	23.7	21.43	09 01 51.9	+78 17 01	4.7	22.9	2.5 × 0.9	14	
NGC 2770	0.8	−2	14.7	21.41	09 06 29.9	+33 19 38	5.2	14.8	1.8 × 0.5	147	
NGC 2775	1.0	−3	(8.1)	(20.75)	09 07 41.2	+07 14 32	2.8	8.4	1.5 × 1.3	178	*
NGC 2835	0.9	−2	(18.2)	(20.53)							*

1987ApJS...65..485C

TABLE 2—*Continued*

Galaxy Name	Beam	Plot n	S (mJy)	log(L) (W Hz^{-1})	R.A. (1950.0)	Decl. (1950.0)	S_P (mJy)	S_I (mJy)	$\theta_M \times \theta_m$	$P.A.$	Notes
					Component Parameters						
NGC 2805	1.0	−3	14.7	21.38							
NGC 2841	0.8	−2	83.8	21.31	09 18 36.0	+51 11 23	7.5	9.3	3.9 × 1.8	151	*
NGC 2903	1.0	−2	407.0	21.64	09 29 20.3	+21 43 21	51.7	44.2	< 0.6		*
					09 29 20.3	+21 43 29	73.7	354.0	2.5 × 1.5	12	
NGC 2935	0.8	−3	40.0	21.89	09 34 26.4	−20 54 11	8.6	9.1	< 0.4		
					09 34 26.2	−20 54 16	6.8	31.4	1.6 × 1.4	0	
NGC 2976	1.0	−3	50.8	19.89							*
NGC 2997	0.8	−3	290.0	21.95	09 43 27.5	−30 57 34	41.3				*
NGC 2985	1.0	−2	61.9	21.80	09 45 53.7	+72 30 44	28.1				*
NGC 3031	1.0	0	(380.0)	(20.76)	09 51 27.5	+69 18 09	85.0	92.8	0.3 × 0.3		*
NGC 3034	1.0	+2	7657.0	22.07	09 51 43.3	+69 55 01	6024.0	7381.0	0.6 × 0.3	70	*
DDO 70	1.0	−3	(0.1)	(16.92)							*
NGC 3079	1.0	−1	849.0	22.79	09 58 35.2	+55 55 16	428.0	458.0	0.3 × 0.2		*
					09 58 34.7	+55 55 18	156.0	384.0	1.9 × 0.6	168	
NGC 3077	1.0	−3	33.2	19.70	09 59 19.4	+68 58 31	26.2	31.1	0.4 × 0.4		
NGC 3109	0.8	−3	(5.9)	(18.67)	10 00 44.5	−25 54 52	1.4				*
DDO 75	1.0	−3	(0.8)	(17.72)							*
NGC 3166	1.0	−3	54.2	21.55	10 11 08.9	+03 40 19	24.2	54.6	1.7 × 0.5	69	
NGC 3169	1.0	−3	92.6	21.71	10 11 39.5	+03 42 52	45.1	86.4	1.2 × 0.7	53	*
NGC 3147	1.0	−3	100.0	22.61	10 12 39.9	+73 39 01	49.8	96.6	1.0 × 0.9	158	*
NGC 3184	0.8	−2	55.9	21.00							*
NGC 3190	1.0	−3	(43.0)	(21.60)							*
NGC 3198	0.8	−2	27.6	20.82	10 16 51.9	+45 48 09	5.4				*
NGC 3223	0.9	−2	32.2	22.03	10 19 19.8	−34 00 51	11.1	32.5	1.5 × 1.0	128	
NGC 3227	0.8	−3	126.0	21.87	10 20 46.7	+20 07 06	79.5	81.0	< 0.2		*
					10 20 45.9	+20 07 16	13.3	44.7	1.5 × 0.9	126	
IC 2574	1.0	−3	(10.7)	(19.20)							*
NGC 3256	1.0	0	659.0	23.31	10 25 42.8	−43 38 53	623.0	661.0	< 0.3		
NGC 3310	1.0	−3	383.0	22.33	10 35 40.0	+53 45 48	254.0	373.0	0.8 × 0.6	164	*
NGC 3319	0.8	−3	(11.5)	(20.52)	10 36 14.9	+41 56 47	1.4				*
NGC 3338	1.0	−3	28.1	21.27							*
NGC 3344	1.0	−3	85.5	21.21	10 40 47.1	+25 11 03	11.5				*
NGC 3351	0.9	−3	(47.8)	(20.97)	10 41 19.3	+11 57 56	34.8	45.3	0.6 × 0.3	37	*
NGC 3359	1.0	−3	50.1	21.50	10 43 19.7	+63 29 08	11.5				
NGC 3368	0.9	−3	30.0	20.92	10 44 07.2	+12 05 00	10.5				*
NGC 3423	1.0	−3	28.4	20.99	10 48 38.2	+06 06 32	5.9				*
NGC 3432	0.9	−3	86.1	21.18	10 49 43.7	+36 53 21	22.6	82.7	2.3 × 0.8	40	*
NGC 3486	1.0	−3	59.4	21.06	10 57 40.5	+29 14 57	4.2	7.7	1.0 × 0.8	75	
					10 57 40.2	+29 14 35	8.3	50.8	2.5 × 2.1	98	
NGC 3504	0.9	−2	265.0	22.45	11 00 28.5	+28 14 31	234.0	263.0	0.4 × 0.2	128	*
NGC 3507	0.9	−3	16.0	20.78	11 00 46.0	+18 24 25	6.2				
NGC 3511	0.9	−3	68.3	21.47	11 00 57.4	−22 49 02	19.7	68.0	2.1 × 0.9	75	
NGC 3513	0.9	−3	16.1	20.74	11 01 19.0	−22 58 22	5.5				*
NGC 3521	1.0	−3	(357.0)	(21.83)	11 03 14.8	+00 14 07	71.8	353.0	2.8 × 1.3	164	*
NGC 3556	1.0	−2	306.0	21.96	11 08 35.4	+55 56 46	24.1	18.9	< 0.6		*
					11 08 35.4	+55 56 43	51.3	281.0	3.5 × 1.1	81	
NGC 3593	0.9	−3	84.7	20.99	11 12 00.0	+13 05 27	68.3	82.8	0.5 × 0.3	96	
NGC 3596	0.9	−3	17.6	20.99	11 12 29.2	+15 03 25	7.1				
NGC 3621	0.9	−3	198.0	21.25	11 15 51.6	−32 32 26	27.5	195.0	3.0 × 1.6	157	*
NGC 3623	0.9	−3	(9.2)	(20.30)	11 16 19.2	+13 21 46	2.6	9.2	2.7 × 0.5	172	*
NGC 3626	0.9	−3	10.0	20.98	11 17 26.2	+18 37 50	8.3	10.0	0.5 × 0.3	2	
NGC 3627	0.9	−2	458.0	21.89	11 17 38.6	+13 15 54	80.0	475.0	2.7 × 1.5	167	*
NGC 3628	0.9	−2	525.0	22.12	11 17 40.3	+13 51 47	257.0	290.0	< 0.5		*
					11 17 40.6	+13 51 46	33.6	229.0	4.1 × 1.0	105	
NGC 3631	0.8	−3	80.8	21.78	11 18 13.4	+53 26 38	27.7				
NGC 3646	0.9	−3	62.6	22.71	11 19 04.7	+20 26 48	15.4				*
NGC 3642	1.0	−3	26.9	21.59	11 19 25.1	+59 20 56	10.1				*
NGC 3672	0.8	−3	64.5	21.92	11 22 30.5	−09 31 16	23.3	63.3	1.4 × 0.7	12	
NGC 3675	0.8	−3	43.7	21.12	11 23 25.2	+43 51 38	17.2	42.5	1.4 × 0.6	3	*
NGC 3686	0.9	−3	15.4	20.90	11 25 07.0	+17 29 59	7.1	14.9	1.0 × 0.8	28	*
NGC 3705	0.9	−3	20.4	20.87	11 27 32.5	+09 33 06	7.6	20.8	1.6 × 0.8	128	*
NGC 3718	1.0	−3	27.3	21.19	11 29 49.8	+53 20 38	16.8	18.3	0.3 × 0.3		*
NGC 3726	0.9	−3	(27.4)	(21.04)							*
NGC 3729	1.0	−3	20.6	21.09	11 31 04.9	+53 24 08	15.6	20.5	0.6 × 0.5	177	
NGC 3810	0.9	−3	115.0	21.61	11 38 23.7	+11 44 54	32.4	112.0	1.7 × 1.1	23	
NGC 3877	0.9	−3	37.0	21.20	11 43 29.6	+47 46 23	12.2	37.1	2.1 × 0.6	35	*
NGC 3887	0.8	−3	33.9	21.14	11 44 31.8	−16 34 26	8.7	35.4	1.5 × 1.3	9	*
NGC 3893	0.8	−3	134.0	21.83	11 46 00.0	+48 59 22	39.5	135.0	1.4 × 1.1	169	*
NGC 3898	1.0	−3	(6.3)	(20.68)	11 46 36.2	+56 21 47	4.3	6.3	0.7 × 0.7		*
NGC 3938	0.9	−3	61.7	21.33	11 50 13.4	+44 23 50	8.5	65.9	2.5 × 2.1	84	
NGC 3949	0.8	−3	112.0	21.60	11 51 05.7	+48 08 13	42.8	111.0	1.2 × 0.8	114	*
NGC 3953	1.0	−2	41.1	21.33	11 51 11.6	+52 36 05	7.2	44.5	3.5 × 1.4	11	*

TABLE 2—*Continued*

Galaxy Name	Beam	Plot n	S (mJy)	$\log(L)$ (W Hz^{-1})	Component Parameters R.A. (1950.0)	Decl. (1950.0)	S_P (mJy)	S_I (mJy)	$\theta_M \times \theta_m$	P.A.	Notes
NGC 3982	1.0	−1	61.0	21.62	11 53 52.3	+55 24 09	44.0	60.0	0.6 × 0.6		*
NGC 3992	0.9	−3	21.3	21.12							
NGC 4013	0.8	−3	34.6	21.10	11 55 58.1	+44 13 18	2.4				*
					11 55 56.6	+44 13 34	13.9	31.2	1.5 × 0.2	63	
NGC 4027	0.8	−3	101.0	21.99	11 56 57.1	−18 59 14	38.4	101.0	1.2 × 0.9	145	*
NGC 4030	1.0	−3	151.0	22.10	11 57 49.8	−00 49 19	66.5	147.0	1.2 × 1.0	57	
NGC 4038	0.8	−3	572.0	22.73							*
NGC 4041	0.9	−3	103.0	21.96	11 59 39.0	+62 24 56	69.7	98.7	0.6 × 0.6		*
NGC 4051	0.9	−3	77.0	21.31	12 00 36.3	+44 48 30	13.7	13.7	< 0.2		*
					12 00 35.9	+44 48 42	11.7	65.7	2.4 × 1.5	118	
NGC 4062	1.0	−3	11.6	20.49	12 01 30.1	+32 10 21	5.2	11.9	1.5 × 0.8	98	
NGC 4088	0.9	−3	212.0	21.84	12 03 02.2	+50 49 14	61.8	209.0	1.8 × 1.0	57	*
NGC 4096	0.9	−3	52.2	20.98	12 03 29.1	+47 45 30	14.1	50.3	2.3 × 0.7	18	
NGC 4100	0.9	−2	52.7	21.51	12 03 36.5	+49 51 40	31.3	49.4	0.9 × 0.5	158	
NGC 4123	0.9	−3	22.0	21.15	12 05 37.4	+03 09 24	11.6	11.3	< 0.2		
					12 05 37.6	+03 09 25	3.6	10.7	1.8 × 0.8	103	
NGC 4136	1.0	−3	9.0	19.86							*
NGC 4145	0.9	−3	(2.8)	(20.16)	12 07 29.4	+40 09 44	1.1				*
NGC 4151	0.9	−2	332.0	22.18	12 08 01.0	+39 41 02	323.0	330.0	< 0.2		*
NGC 4157	0.9	−3	180.0	21.80	12 08 33.2	+50 45 44	55.8	180.0	2.2 × 0.6	64	*
NGC 4178	0.9	−3	23.3	21.13	12 10 13.6	+11 08 36	5.5				*
NGC 4192	0.9	−3	73.9	21.63	12 11 15.8	+15 10 32	22.4				
NGC 4212	0.9	−3	23.7	21.13	12 13 06.5	+14 10 45	11.9	23.7	1.2 × 0.6	76	
NGC 4214	0.9	−3	51.9	20.32	12 13 09.3	+36 36 08	23.4				*
NGC 4216	0.9	−3	13.4	20.89	12 13 21.8	+13 25 38	4.3				*
NGC 4217	0.9	−3	109.0	21.79	12 13 21.4	+47 22 06	43.9	108.0	1.8 × 0.5	50	
NGC 4236	0.9	−3	(28.1)	(19.63)							*
NGC 4244	0.9	−3	(8.8)	(19.42)	12 14 58.8	+38 04 59	1.2				*
NGC 4242	0.9	−3	13.8	20.32	12 14 59.2	+45 54 04	12.8	13.0	< 0.2		*
NGC 4254	0.9	−3	422.0	22.39	12 16 17.6	+14 41 32	72.1				*
NGC 4258	0.0		[790.0]	[22.01]							*
NGC 4274	1.0	−3	11.2	20.62	12 17 20.0	+29 53 31	9.5	10.0	< 0.3		*
NGC 4293	0.9	−3	17.6	21.01	12 18 41.1	+18 39 36	16.9	17.5	< 0.2		
NGC 4303	0.9	−2	416.0	22.38	12 19 21.7	+04 45 02	67.4	427.0	2.3 × 1.9	30	*
NGC 4314	1.0	−3	12.5	20.64	12 20 02.0	+30 10 23	11.0	12.6	0.5 × 0.3	86	*
NGC 4321	0.9	−2	[340.0]	[22.29]	12 20 22.9	+16 06 00	51.2	53.1	< 0.4		*
					12 20 23.0	+16 06 00	23.8	180.0	2.8 × 1.9	134	
NGC 4388	0.9	+1	146.0	21.93	12 23 14.8	+12 56 19	121.0	148.0	0.6 × 0.2	94	*
NGC 4395	1.0	−3	(21.5)	(19.98)							*
NGC 4394	0.9	−3	0.7	19.61	12 23 24.6	+18 29 30	0.6				
NGC 4414	1.0	−3	231.0	21.74	12 23 57.9	+31 30 02	121.0	229.0	1.2 × 0.7	161	
NGC 4438	0.9	+2	(116.0)	(21.82)	12 25 13.6	+13 17 10	82.8				*
NGC 4449	0.9	−3	266.0	20.90	12 25 45.4	+44 22 14	46.6				*
NGC 4448	1.0	−3	1.0	19.31	12 25 46.7	+28 53 50	0.9				*
NGC 4450	0.9	−3	8.3	20.68	12 25 58.3	+17 21 42	7.5	8.3	0.3 × 0.3		*
NGC 4457	0.9	−3	37.4	21.33	12 26 26.0	+03 50 48	23.9	36.3	0.8 × 0.5	55	
NGC 4490	0.9	−3	774.0	22.13							*
NGC 4487	1.0	−3	4.5	20.17	12 28 28.7	−07 46 29	1.9				
NGC 4496	0.9	−3	21.1	21.09							*
NGC 4501	0.9	−3	278.0	22.21	12 29 27.4	+14 41 41	73.7	279.0	2.0 × 1.1	140	*
NGC 4504	0.8	−3	(0.5)	(19.18)							*
NGC 4517	0.9	−3	32.0	21.15	12 30 12.3	+00 23 29	6.1	33.6	3.8 × 0.7	82	*
NGC 4527	0.9	−3	214.0	22.41	12 31 35.1	+02 55 46	61.0	55.5	< 0.3		*
					12 31 35.4	+02 55 47	49.7	156.0	2.1 × 0.7	68	
NGC 4535	0.9	−3	(64.5)	(21.57)	12 31 47.7	+08 28 25	13.8				
NGC 4536	1.0	−3	203.0	22.42	12 31 53.7	+02 27 49	172.0	196.0	0.4 × 0.3	105	*
NGC 4548	0.9	−3	(4.6)	(20.42)							*
NGC 4559	1.0	−3	65.4	21.27	12 33 28.7	+28 13 59	11.6				*
NGC 4565	1.0	−2	131.0	21.94	12 33 52.1	+26 15 46	18.0	133.0	6.0 × 0.7	136	*
NGC 4568	0.9	−3	136.0	21.90							*
NGC 4569	0.8	−1	83.4	21.68	12 34 18.4	+13 26 20	35.6	84.1	1.4 × 0.5	19	*
NGC 4571	0.9	−3	4.2	20.38	12 34 26.5	+14 29 29	1.6	5.3	1.6 × 1.1	43	
NGC 4579	0.9	0	103.0	21.78	12 35 12.3	+12 05 36	62.9	96.2	0.9 × 0.4	113	*
NGC 4593	1.0	−3	(5.0)	(21.18)	12 37 04.7	−05 04 09	4.4				*
NGC 4594	0.9	−3	137.0	21.70	12 37 23.4	−11 20 56	125.0	134.0	< 0.3		
NGC 4596	0.9	−3	(0.4)	(19.36)							*
NGC 4605	0.9	−3	85.5	20.49	12 37 49.0	+61 52 53	24.0	85.5	2.0 × 0.9	113	*
NGC 4618	0.9	−3	31.9	20.69	12 39 09.5	+41 25 21	6.1				*
NGC 4631	1.0	0	1200.0	22.33	12 39 41.9	+32 48 57	196.0				*
NGC 4651	0.9	−1	24.0	21.14	12 41 12.5	+16 39 56	14.1	24.4	0.8 × 0.8		*

TABLE 2—*Continued*

Galaxy Name	Beam	Plot n	S (mJy)	$\log(L)$ (W Hz^{-1})	Component Parameters R.A. (1950.0)	Decl. (1950.0)	S_P (mJy)	S_I (mJy)	$\theta_M \times \theta_m$	*P.A.*	Notes
NGC 4654	0.9	−3	117.0	21.83	12 41 24.9	+13 24 09	35.9	117.0	1.8 × 0.9	121	*
NGC 4656	1.0	−3	62.6	21.07	12 41 32.1	+32 26 46	11.3	21.3	1.2 × 0.7	31	*
NGC 4666	1.0	−3	417.0	22.64	12 42 34.7	−00 11 22	172.0	407.0	1.7 × 0.6	39	*
NGC 4689	0.9	−3	9.6	20.74	12 45 15.1	+14 02 06	4.9	8.7	0.8 × 0.8		*
NGC 4691	1.0	−3	47.5	21.31	12 45 38.9	−03 03 39	40.8	47.2	0.4 × 0.4		*
NGC 4698	0.9	−3	(0.6)	(19.54)							*
NGC 4699	1.0	−3	15.9	21.12	12 46 26.3	−08 23 30	8.5	15.7	1.0 × 0.8	22	
NGC 4725	1.0	−3	(28.2)	(21.27)							*
NGC 4731	1.0	−3	9.2	20.88	12 48 25.6	−06 07 11	3.7				*
NGC 4736	0.9	−3	254.0	21.16	12 48 32.4	+41 23 27	61.4	250.0	1.7 × 1.4	98	*
NGC 4775	1.0	−3	28.5	21.41	12 51 10.7	−06 21 09	12.3	29.4	1.3 × 1.1	168	*
NGC 4781	0.8	−3	75.9	21.24	12 51 47.0	−10 15 54	24.5	78.0	1.5 × 0.9	122	*
NGC 4818	0.9	−2	48.3	21.22	12 54 12.7	−08 15 19	45.4	48.0	< 0.3		
NGC 4826	1.0	−3	103.0	20.78	12 54 16.3	+21 57 13	72.3	99.5	0.6 × 0.6		*
NGC 4866	0.9	−3	(0.2)	(19.06)							*
NGC 4902	1.0	−2	52.0	22.17	12 58 22.1	−14 14 37	24.0	53.8	1.2 × 1.0	98	*
NGC 4941	1.0	−3	19.0	20.85	13 01 37.7	−05 17 02	18.8	17.9	< 0.3		
NGC 4939	0.8	−3	24.2	22.00	13 01 37.3	−10 04 17	10.0				*
NGC 4981	1.0	−3	21.0	21.35	13 06 12.6	−06 30 35	10.7	21.0	1.0 × 1.0		*
NGC 4984	0.9	−3	29.7	21.19	13 06 18.2	−15 15 00	28.8	29.9	< 0.3		
NGC 4995	1.0	−3	28.4	21.57	13 07 04.0	−07 34 02	23.6	28.8	0.5 × 0.4		
NGC 5005	0.8	−3	176.0	21.96	13 08 37.6	+37 19 28	39.4	38.5	< 0.3		*
					13 08 37.6	+37 19 27	49.5	136.0	1.6 × 0.6	72	
NGC 5023	0.9	−3	(0.5)	(18.53)							*
NGC 5033	0.9	−3	178.0	21.84	13 11 09.1	+36 51 32	86.3				*
NGC 5055	0.9	−3	[390.0]	[21.75]	13 13 34.8	+42 17 34	56.9				*
NGC 5054	0.9	−3	87.2	21.99	13 14 18.3	−16 22 16	38.8	43.2	< 0.4		*
					13 14 17.7	−16 22 10	18.7	44.4	1.4 × 0.8	135	
NGC 5068	0.9	−3	39.0	20.35							*
NGC 5101	0.8	−3	5.7	20.85	13 19 00.3	−27 10 09	4.3	5.4	0.5 × 0.3		*
NGC 5112	0.9	−3	14.6	20.85	13 19 40.8	+38 59 46	3.7	15.5	1.7 × 1.5	153	*
NGC 5161	0.8	−3	7.5	21.21	13 26 23.6	−32 55 04	3.5				
NGC 5170	0.9	−3	4.8	20.58	13 27 07.1	−17 42 25	1.4				*
NGC 5204	0.9	−3	5.0	19.54	13 27 43.4	+58 40 27	2.3	5.2	1.3 × 0.7	24	
NGC 5194	0.9	−1	[1490.0]	[22.32]	13 27 46.3	+47 27 14	139.0				*
NGC 5236	0.9	+1	2445.0	22.15	13 34 11.2	−29 36 40	370.0				*
NGC 5248	0.9	−3	140.0	21.87	13 35 02.7	+09 08 24	48.9	134.0	1.5 × 0.9	130	*
NGC 5247	0.8	−2	52.9	21.52	13 35 20.9	−17 37 49	18.9				*
NGC 5253	0.9	−2	83.8	20.68	13 37 04.9	−31 23 18	71.9	83.3	0.4 × 0.3		
NGC 5300	0.9	−3	2.5	20.12							
NGC 5334	0.9	−3	(2.1)	(20.19)							*
NGC 5371	0.9	−3	50.3	22.22	13 53 32.7	+40 42 10	10.3	52.5	2.0 × 1.6	23	*
NGC 5364	0.9	−3	(13.9)	(20.94)							*
NGC 5377	0.9	−3	3.5	20.78	13 54 18.1	+47 28 48	3.1	3.7	< 0.6		
NGC 5457	0.8	−2	[750.0]	[21.71]							*
NGC 5474	0.8	−3	1.3	18.95	14 03 13.5	+53 54 04	1.0				*
NGC 5530	1.0	−1	14.1	20.78	14 15 17.3	−43 09 25	6.0	14.7	1.4 × 1.0	138	
NGC 5556	0.8	−3	2.6	20.23							
NGC 5566	0.9	−3	8.5	20.95	14 17 49.0	+04 09 48	4.6	7.7	1.0 × 0.4	33	*
NGC 5585	0.9	−3	(1.0)	(18.84)							*
NGC 5584	0.9	−3	21.3	21.37	14 19 50.6	−00 09 32	6.5	22.1	1.8 × 1.0	146	*
NGC 5643	1.0	−2	203.0	21.94	14 29 26.7	−43 57 17	29.8	26.2	< 0.6		*
					14 29 27.3	−43 57 18	41.3	179.0	2.0 × 1.7	70	
NGC 5669	1.0	−2	10.7	20.94	14 30 17.2	+10 06 36	4.7	11.1	1.4 × 0.9	43	*
NGC 5676	0.8	−3	96.7	22.37	14 31 01.2	+49 40 39	39.3	96.6	1.3 × 0.6	46	*
NGC 5701	0.9	−3	(−0.1)	< 19.69							*
NGC 5713	0.9	−3	154.0	22.37	14 37 37.5	−00 04 35	106.0	150.0	0.6 × 0.6		*
NGC 5746	0.9	−3	(10.9)	(21.15)							*
NGC 5792	0.9	−3	51.8	21.95	14 55 48.1	−00 53 31	28.3	29.4	< 0.3		
					14 55 48.7	−00 53 40	8.0	22.6	1.6 × 0.8	90	
NGC 5850	0.9	−3	17.9	21.71	15 04 36.6	+01 44 04	3.5	19.0	2.3 × 1.5	142	
NGC 5907	0.8	−3	89.5	21.42	15 14 34.7	+56 30 52	16.2	89.9	3.6 × 0.6	155	*
NGC 5921	0.9	−3	23.1	21.36	15 19 27.0	+05 14 43	2.4	2.8	< 0.8		*
					15 19 27.2	+05 15 00	5.1	20.8	2.0 × 1.2	175	
NGC 5985	0.8	−3	6.5	21.36	15 38 36.3	+59 29 18	2.0	7.3	1.6 × 1.0	176	*
NGC 6015	0.8	−2	14.4	20.86							*
NGC 6118	0.9	−3	14.2	21.21	16 19 12.5	−02 10 13	4.3	15.0	2.0 × 0.9	60	*
NGC 6140	0.9	−3	(0.5)	(19.50)							*
NGC 6217	1.0	−3	78.4	21.99	16 35 04.2	+78 18 02	61.4	76.2	0.6 × 0.4	157	*
NGC 6340	1.0	−3	< 1.5	< 20.19							*

TABLE 2—*Continued*

Galaxy Name	Beam	Plot n	S (mJy)	log(L) (W Hz^{-1})	Component Parameters: R.A. (1950.0)	Decl. (1950.0)	S_P (mJy)	S_I (mJy)	$\theta_M \times \theta_m$	$P.A.$	Notes
NGC 6384	1.2	−3	34.9	21.71	17 29 59.0	+07 05 32	6.8	36.8	3.1 × 2.0	41	*
NGC 6503	1.0	−1	36.5	20.21	17 49 57.4	+70 09 21	12.7	37.3	2.0 × 0.9	120	*
NGC 6643	1.0	−1	92.2	22.13	18 21 12.9	+74 32 40	45.7	91.5	1.2 × 0.8	39	*
NGC 6822	0.8	−1	(47.6)	(18.42)							*
NGC 6907	0.8	−3	136.0	22.83	20 22 08.1	−24 58 19	60.6	131.0	1.0 × 0.7	59	*
NGC 6946	0.8	0	1395.0	21.88	20 33 49.1	+59 58 50	149.0				*
NGC 7177	0.8	−3	26.2	21.41	21 58 18.1	+17 29 49	10.4	26.0	1.0 × 0.9	95	
NGC 7184	0.8	−3	13.4	21.68							*
NGC 7217	0.8	−3	16.2	21.08	22 05 38.0	+31 06 47	10.5	11.7	< 0.4		*
NGC 7314	0.8	−3	33.8	21.56	22 33 00.6	−26 18 23	9.0	33.0	1.6 × 1.0	179	*
NGC 7331	0.8	−2	373.0	22.35	22 34 46.5	+34 09 18	71.8	357.0	2.4 × 0.9	166	*
NGC 7410	0.8	−3	7.3	21.02	22 52 11.1	−39 55 45	6.0	6.2	< 0.3		
NGC 7418	0.8	−3	45.6	21.67	22 53 48.5	−37 17 52	12.6	45.2	1.3 × 1.3		*
IC 5267	1.0	−2	7.7	21.03	22 54 22.4	−43 39 50	4.1	7.0	0.9 × 0.7	40	
NGC 7424	1.0	−2	(2.2)	(19.96)							*
IC 5273	0.8	−2	33.4	21.43	22 56 39.6	−37 58 28	9.2	32.9	1.7 × 0.9	172	
NGC 7479	0.8	−3	109.0	22.56	23 02 26.2	+12 03 07	32.7	100.0	1.3 × 1.0	17	*
NGC 7496	1.0	−2	36.3	21.56	23 06 59.3	−43 41 56	26.4	35.0	0.6 × 0.6		*
NGC 7552	1.0	−2	276.0	22.51	23 13 24.9	−42 51 26	221.0	267.0	0.5 × 0.4	92	*
NGC 7582	1.0	0	270.0	22.45	23 15 38.5	−42 38 36	220.0	262.0	0.6 × 0.2	154	*
NGC 7606	1.0	−3	15.5	21.61	23 16 29.5	−08 45 30	4.7	16.0	2.3 × 0.9	147	*
NGC 7640	0.8	−3	29.3	20.80	23 19 42.3	+40 34 30	4.9				
IC 5332	0.8	−3	(0.9)	(19.34)							*
NGC 7713	1.0	−2	16.8	20.58	23 33 35.2	−38 12 49	7.0	17.9	1.7 × 0.9	158	*
NGC 7723	0.8	−3	10.4	21.29	23 36 21.5	−13 14 19	7.2	10.6	0.7 × 0.4	44	*
NGC 7727	1.0	−3	3.4	20.81	23 37 18.3	−12 34 09	1.7				
NGC 7741	1.0	−3	13.3	20.83	23 41 23.7	+25 47 54	4.9	12.2	1.4 × 1.1	22	*
NGC 7793	1.0	−2	103.0	20.33	23 55 14.5	−32 52 13	9.6				*
DDO 221	0.9	−3	(1.6)	(17.69)	23 59 23.3	−15 45 01	0.8				*

source at $\alpha = 00^h45^m31\overset{s}{.}4$, $\delta = -25°34'52''$. [1.465 GHz VLA C-array map in Condon (1983); VLA D-array maps at 1.46 and 4.9 GHz in Hummel, Smith, and van der Hulst (1984); 843 MHz MOST map in Reynolds and Harnett (1983); 1413 and 4885 MHz VLA A-array maps of the central region in Condon *et al.* (1982); VLA maps with 1″ resolution at 6 and 2 cm in Turner and Ho (1983); VLA A-array map at 2 cm of nucleus in Turner and Ho (1985); 8.7 GHz 100 m telescope map in Beck *et al.* (1979); 10.7 GHz map in Klein *et al.* (1983).]

NGC 0278.—[1.465 GHz VLA C-array and B-array maps in Condon (1983); 4.86 GHz VLA D-array map in Gioia and Fabbiano (1987).]

NGC 0289.—S does not include the $S_P = 16.0$ mJy source at $\alpha = 00^h50^m20\overset{s}{.}8$, $\delta = -31°31'18''$.

NGC 0300.—Detected? Low T_B, very uncertain S. The $S_I = 130$ mJy source at $\alpha = 00^h51^m31\overset{s}{.}7$, $\delta = -37°56'37''$; the $S_I = 136$ mJy source at $\alpha = 00^h51^m41\overset{s}{.}8$, $\delta = -38°02'50''$; the $S_I = 14.3$ mJy source at $\alpha = 00^h52^m33\overset{s}{.}7$, $\delta = -37°52'14''$; the $S_I = 4.5$ mJy source at $\alpha = 00^h52^m26\overset{s}{.}3$, $\delta = -38°10'03''$; and the $S_I = 2.6$ mJy source at $\alpha = 00^h53^m02\overset{s}{.}2$, $\delta = -38°02'45''$ do not coincide with bright H II regions in NGC 0300 and are probably confusion.

IC 1613.—Low T_B, very uncertain S. The $S_I = 2.8$ mJy extended source centered on $\alpha = 01^h02^m28\overset{s}{.}2$, $\delta = +01°52'58''$ overlaps the H II complex in the northeastern quadrant (cf. Sandage 1971) and the radio supernova remnant detected by Dickel, D'Odorico, and Silverman (1985). S does not include any of the remaining discrete sources visible in the contour map, since none of them coincide with prominent optical objects in IC 1613. [4.75 GHz 100 m telescope map in Klein and Gräve (1986).]

NGC 0488.—S does not include the $S_P = 6.6$ mJy source at $\alpha = 01^h19^m11\overset{s}{.}3$, $\delta = +05°02'49''$ or the $S_I = 2.3$ mJy confusing (?) source at $\alpha = 01^h19^m16\overset{s}{.}6$, $\delta = +04°58'45''$.

NGC 0598.—Contour plot of the central region only. The total flux density $S = [3300]$ mJy for the entire galaxy was estimated from the $S = 3.3 \pm 0.5$ Jy at 1410 MHz and $\alpha \approx +0.2$ measured with the NRAO 91 m telescope (Dennison *et al.* 1975). [1.4 GHz WSRT maps in van der Kruit (1973*a*) and Viallefond *et al.* (1986); 4.85 GHz 100 m telescope map in von Kap-herr, Berkhuijsen, and Wielebinski (1978).]

NGC 0613.—[1.465 GHz VLA C-array maps in Condon (1983) and Hummel *et al.* (1985); A-array map of the core in Hummel, van der Hulst, and Dickey (1984).]

NGC 0628.—The total flux density $S = [180]$ mJy was estimated using $S = 0.18$ Jy at 1400 MHz from the NRAO 91 m telescope survey maps (Condon and Broderick 1986), converted to 1.49 GHz assuming $\alpha \approx +0.75$. $S = 120$ mJy appears in the VLA map. S does not include the $S_P = 2.2$ mJy source at $\alpha = 01^h33^m50\overset{s}{.}9$, $\delta = +15°36'16''$ or the $S_P = 8.5$ mJy source at $\alpha = 01^h34^m16\overset{s}{.}1$, $\delta = +15°29'06''$. [1415 MHz WSRT map in van der Kruit (1973*b*).]

NGC 0660.—Slightly resolved parallel to the $2\overset{'}{.}8 \times 0\overset{'}{.}9$ optical bar in P.A. 217° (Nilson 1973). [1413 and 4885 MHz VLA A-array maps of the central region in Condon *et al.* (1982).]

IC 1727.—Detected?

NGC 0672.—[1.49 GHz VLA D-array map in Gioia and Fabbiano (1987).]

NGC 0772.—S does not include the $S_P = 2.5$ mJy source at $\alpha = 01^h56^m29\overset{s}{.}3$, $\delta = +18°49'11''$. Gaussian fit to the core component only. The northwestern radio extension coincides with an optically bright arm (cf. Arp 1970).

NGC 0779.—Eastern extension is probably confusion, not included in S.

NGC 0784.—S does not include the $S_P = 5.7$ mJy source at $\alpha = 01^h58^m28\overset{s}{.}9$, $\delta = +28°36'35''$.

NGC 0891.—[VLA D-array maps at 1.49 and 4.86 GHz in Gioia and Fabbiano (1987); 1.465 GHz VLA C-array map in Condon (1983); WSRT maps at 610, 1412, and 4995 MHz in Allen, Baldwin, and Sancisi (1978); NRAO interferometer maps at 2.7 and 8.1 GHz in Seaquist and Bignell (1976); 8.7 GHz 100 m telescope map in Beck *et al.* (1979); 10.7 GHz map in Klein, Wielebinski, and Beck (1984*a*).]

NGC 0908.—The eastern radio extension coincides with the large bifurcated optical arm (see Fig. 10 of Arp 1968). S does not include the $S_P = 31.1$ mJy source at $\alpha = 02^h20^m32\overset{s}{.}2$, $\delta = -21°26'50''$.

NGC 0925.—Low T_B, very uncertain S. S includes all features visible in the contour plot. [1.49 GHz VLA D-array map in Gioia and Fabbiano (1987).]

NGC 1042.—S does not include the faint double-peaked southern component.

NGC 1055.—S does not include the small northern extension.

NGC 1068.—[VLA maps of the inner disk at 2, 6, and 20 cm with 6".5 resolution in Wynn-Williams, Becklin, and Scoville (1985); 1.465 and 14.985 GHz VLA C-array maps in Wilson and Ulvestad (1982); 1.465 GHz VLA C-array map in Condon (1983); 4.9 and 15.0 GHz VLA A-array maps of the central region in Wilson and Ulvestad (1983); 15.04 GHz VLA A-array maps of the central region in van der Hulst, Hummel, and Dickey (1982) and Hummel, van der Hulst, and Dickey (1984); 1413 and 4885 MHz VLA A-array maps of the central region in Condon *et al.* (1982); 408 and 1666 MHz MERLIN maps of the central region in Pedlar *et al.* (1983).]

NGC 1073.—Badly confused by the $S_P = 78.7$ mJy quasar (Condon and Dressel 1978; Arp and Sulentic 1979) at $\alpha = 02^h41^m04\overset{s}{.}8$, $\delta = +01°08'29''$ and the $S_P = 73.3$ mJy source at $\alpha = 02^h40^m57\overset{s}{.}0$, $\delta = +01°07'18''$.

NGC 1084.—S does not include the southwestern extensions to the main radio component. [1.465 GHz VLA C-array and B-array maps in Condon (1983).]

NGC 1097.—[1465 MHz VLA B-array map of the bar in Ondrechen and van der Hulst (1983); 4.885 GHz VLA A-array map of the core in Hummel, van der Hulst, and Dickey (1984); partial–VLA 1446 MHz maps of the central region in Wolstencroft, Tully, and Perley (1984).]

NGC 1255.—S does not include the $S_P = 6.1$ mJy source at $\alpha = 03^h11^m15\overset{s}{.}3$, $\delta = -25°51'19''$; the $S_P = 4.2$ mJy source at $\alpha = 03^h11^m20\overset{s}{.}8$, $\delta = -25°50'46''$; or the $S_P = 2.3$ mJy source at $\alpha = 03^h11^m27\overset{s}{.}7$, $\delta = -25°57'15''$. [1.465 GHz VLA C-array map in Hummel *et al.* (1985).]

NGC 1291.—S is of central source only; disk not detected.

NGC 1300.—The $S_P = 4.0$ mJy peak at $\alpha = 03^h17^m19\overset{s}{.}7$, $\delta = -19°34'53''$ coincides with a chain of bright H II regions (Nos. 14–17 and 19 in Hodge 1969) at the end of the bar. [1.465 GHz VLA C-array in Hummel *et al.* (1985).]

NGC 1302.—Detected? Confusion?

NGC 1309.—Asymmetric; peak position is $\alpha = 03^h19^m47\overset{s}{.}1$, $\delta = -15°34'27''$. S does not include the $S_P = 4.6$ mJy source at $\alpha = 03^h19^m54\overset{s}{.}3$, $\delta = -15°33'10''$.

NGC 1365.—[Partial–VLA 1.465 and 4.885 GHz maps of the nuclear region in Sandqvist, Jörsäter, and Lindblad (1982).]

NGC 1385.—S does not include the $S_P = 5.2$ mJy source at $\alpha = 03^h35^m20\overset{s}{.}4$, $\delta = -24°36'52''$. [1.465 GHz VLA C-array map in Condon (1983).]

NGC 1421.—S does not include the $S_P = 9.5$ mJy source at $\alpha = 03^h40^m18\overset{s}{.}2$, $\delta = -13°40'19''$. [1.465 GHz VLA C-array map in Hummel *et al.* (1985).]

IC 0342.—Gaussian fit to core source only. The total flux density $S = [2250]$ mJy was estimated using $S = 2.40$ Jy at 1400 MHz measured from the NRAO 91 m telescope survey maps (Condon and Broderick 1986), after converting to 1.49 GHz assuming $\alpha \approx +0.75$ and subtracting the $S_P = 51.4$ mJy source at $\alpha = 03^h42^m37\overset{s}{.}0$, $\delta = +67°59'08''$. $S = 982$ mJy appears in the VLA map. [1415 MHz WSRT map in van der Kruit (1973*b*); 1413 MHz VLA A-array map of the central region in Condon *et al.* (1982); VLA maps with 1" resolution at 6 and 2 cm of core in Turner and Ho (1985); 4800 MHz 100 m telescope map in Baker *et al.* (1977).]

NGC 1448.—S does not include the $S_P = 3.2$ mJy source at $\alpha = 03^h42^m36\overset{s}{.}3$, $\delta = -44°49'17''$.

IC 0356.—S does not include the $S_P = 41.5$ mJy source at $\alpha = 04^h02^m49\overset{s}{.}6$, $\delta = +69°43'41''$ or the $S_P = 66.5$ mJy source at $\alpha = 04^h03^m07\overset{s}{.}6$, $\delta = +69°42'08''$.

NGC 1532.—The southwestern extension and off-nuclear peak ($S_P = 23.8$ mJy at $\alpha = 04^h10^m06\overset{s}{.}1$, $\delta = -33°01'18''$) coincide with bright optical "tails." S does not include the northwestern radio extension produced by (?) the interacting companion galaxy NGC 1531 (optical position $\alpha = 04^h10^m04\overset{s}{.}0$, $\delta = -32°58'40''$).

NGC 1569.—[1.465 GHz VLA C-array and B-array maps in Condon (1983); NRAO interferometer maps at 2.7 and 8.1 GHz in Seaquist and Bignell (1976); 24.5 GHz 100 m telescope map in Klein and Gräve (1986).]

NGC 1744.—The two radio peaks at $\alpha = 04^h57^m53\overset{s}{.}5$, $\delta = -26°04'45''$ and $\alpha = 04^h57^m56\overset{s}{.}5$, $\delta = -26°07'03''$ coincide with the ends of the optical bar.

NGC 1792.—S does not include the southwest or northeast extensions of the main radio component.

NGC 1808.—S does not include the $S_P = 4.1$ mJy source at $\alpha = 05^h05^m49\overset{s}{.}7$, $\delta = -37°35'35''$.

NGC 1964.—Gaussian fit to core component only. S does not include the $S_P = 3.5$ mJy source at $\alpha = 05^h31^m19\overset{s}{.}3$, $\delta = -22°00'32''$ or the $S_P = 17.0$ mJy source at $\alpha = 05^h31^m24\overset{s}{.}6$, $\delta = -21°57'39''$.

NGC 1961.—[1.465 GHz VLA C-array and B-array maps in Condon (1983).]

NGC 2146.—[1.465 GHz VLA C-array map in Condon (1983); WSRT maps at 1410 and 4995 MHz in de Bruyn (1977*b*); 1413 MHz VLA A-array map of the central region in Condon *et al.* (1982); high-resolution maps on the central region (VLA at 1465 and 4885 MHz and NRAO interferometer at 8085 MHz) in Kronberg and Biermann (1981).]

NGC 2207.—S includes IC 2163 (optical position $\alpha = 06^h14^m20^s.5$, $\delta = -21°21'27''$) but not the $S_P = 1.9$ mJy source at $\alpha = 06^h14^m13^s.7$, $\delta = -21°24'03''$. [1.465 GHz VLA C-array and B-array maps in Condon (1983); 1.465 GHz VLA C-array map in Hummel *et al.* (1985).]

NGC 2280.—Gaussian fit to the central component only. S does not include the $S_P = 4.6$ mJy source at $\alpha = 06^h42^m54^s.7$, $\delta = -27°40'04''$.

NGC 2276.—Asymmetric source cuts off sharply on western edge. S does not include the three faint western peaks, which are background sources. [1.465 GHz VLA C-array and B-array maps in Condon (1983).]

NGC 2336.—S does not include the $S_P = 1.2$ mJy source at $\alpha = 07\ 18\ 00.5$, $\delta = +80\ 14\ 20$. [1.465 GHz VLA C-array map in Hummel *et al.* (1985).]

NGC 2366.—The $S_P = 13.0$ mJy southern radio peak at $\alpha = 07^h23^m25^s.9$, $\delta = +69°17'31''$ coincides with the bright H II complex NGC 2363 = Mrk 71 = H II regions I and II of Sandage and Tammann (1974). [10.7 GHz 100 m telescope map in Klein, Gräve, and Wielebinski (1983).]

NGC 2403.—$S = [330]$ mJy estimated from $S = 0.35$ Jy at 1400 MHz from the NRAO 91 m telescope sky maps (Condon and Broderick 1985), converted to 1.49 GHz assuming $\alpha \approx +0.75$. $S = 218$ mJy in VLA map. [1415 MHz WSRT map in van der Kruit (1973*a*); 10.7 GHz 100 m telescope map in Klein and Emerson (1981).]

Ho II.—The $S_I = 6.7$ mJy radio peak at $\alpha = 08^h14^m06^s.1$, $\delta = +70°52'55''$ and the $S_I = 13.3$ mJy radio peak at $\alpha = 08^h14^m16^s.2$, $\delta = 70°52'04''$ lie near optically bright H II regions (cf. Hodge 1969).

NGC 2613.—Two peaks, $S_P = 11.0$ mJy at $\alpha = 08^h31^m08^s.6$, $\delta = -22°47'54''$ and $S_P = 10.3$ mJy at $\alpha = 08^h31^m14^s.6$, $\delta = -22°48'30''$.

NGC 2655.—[1.465 and 4.885 GHz VLA A-array maps of the core in Hummel, van der Hulst, and Dickey (1984).]

NGC 2683.—S does not include extensions from the main Gaussian body of the radio source. [VLA D-array maps at 1.49 and 4.86 GHz in Gioia and Fabbiano (1987).]

NGC 2775.—S does not include the $S_I = 2.4$ mJy confusing (?) source at $\alpha = 09^h07^m42^s.8$, $\delta = 07°16'19''$.

NGC 2835.—Confused? Uncertain S does not include the $S_P = 8.7$ mJy source at $\alpha = 09^h15^m33^s.9$, $\delta = -22°07'14''$ or the $S_P = 1.6$ mJy source at $\alpha = 09^h15^m35^s.5$, $\delta = -22°05'00''$.

NGC 2841.—[VLA D-array maps at 1.49 and 4.86 GHz in Gioia and Fabbiano (1987); WSRT maps at 610 and 1410 MHz in Hummel and Bosma (1982); 10.7 GHz 100 m telescope map in Klein and Emerson (1981).]

NGC 2903.—[1.465 GHz VLA C-array map in Hummel *et al.* (1985); 1415 MHz WSRT map in van der Kruit (1973*a*); VLA maps with 2″ resolution at $\lambda = 20$, 6, and 2 cm in Wynn-Williams and Becklin (1985); partial-VLA map at 4885 MHz in van der Hulst, Crane, and Keel (1981); 10.7 GHz 100 m telescope map in Klein and Emerson (1981).]

NGC 2976.—Asymmetric radio structure, $S_P = 11.8$ mJy off-nuclear peak at $09^h43^m02^s.6$, $\delta = +68°09'36''$. S does not include the $S_P = 1.3$ mJy source at $\alpha = 09^h43^m31^s.3$, $\delta = +68°10'55''$.

NGC 2997.—S does not include the $S_P = 1.1$ mJy source at $\alpha = 09^h43^m16^s.9$, $\delta = -31°01'36''$.

NGC 2985.—S does not include the small northeastern extension to the radio source.

NGC 3031.—Gaussian fit to the compact nuclear source only. [1415 MHz WSRT map in Segalovitz (1977*b*); multi-configuration VLA maps at 6 and 20 cm in Bash and Kaufman (1986).]

NGC 3034.—Gaussian fit to the central source only. [1.465 GHz VLA C-array map in Condon (1983); VLA A-array maps at 1413 and 4873 MHz in Kronberg, Biermann, and Schwab (1985); partial-VLA maps at 1465, 1667, and 4885 MHz in Kronberg, Biermann, and Schwab (1981); 1413 MHz VLA A-array map of the central region in Condon *et al.* (1982); VLA maps at 1.48 GHz (B-array) and 4.87 GHz (C-array) in Seaquist, Bell, and Bignell (1985).]

DDO 70.—Not detected.

NGC 3079.—S does not include the $S_P = 1.7$ mJy source at $\alpha = 09^h58^m31^s.6$, $\delta = +55°51'55''$. [1.465 GHz VLA C-array map in Condon (1983); WSRT maps at 1410 and 4995 MHz in de Bruyn (1977*b*); VLA maps at 1.4 and 4.9 GHz of the central region in Duric *et al.* (1983) and Duric and Seaquist (1986); 1413 MHz VLA A-array map of the central region in Condon *et al.* (1982); VLA 6 cm map of the central region in Hummel, van Gorkom, and Kotanyi (1983); 2.7 and 8.1 GHz NRAO interferometer maps in Seaquist, Davis, and Bignell (1978); 10.7 GHz 100 m telescope map in Klein, Wielebinski, and Beck (1984*a*).]

NGC 3109.—Low T_B, very uncertain S. S does not include the $S_P = 1.5$ mJy source at $\alpha = 10^h00^m33^s.5$, $\delta = -25°52'42''$ or the $S_P = 11.0$ mJy source at $\alpha = 10^h00^m41^s.7$, $\delta = -25°57'19''$.

DDO 75.—Not detected? Confusion? The $S_P = 0.6$ mJy peak at $\alpha = 10^h08^m33^s.7$, $\delta = -04°26'43''$ may be a background source.

NGC 3169.—S does not include the $S_P = 1.0$ mJy source at $\alpha = 10^h11^m47^s.2$, $\delta = +03°40'40''$.

NGC 3147.—S does not include the $S_P = 0.8$ mJy source at $\alpha = 10^h12^m01^s.6$, $\delta = +73°38'05''$. [1.465 GHz VLA C-array map in Hummel *et al.* (1985).]

NGC 3184.—VLA D-array maps at 1.49 and 4.86 GHz in Gioia and Fabbiano (1987).

NGC 3190.—Confused? The double-peaked source ($S_P = 15.8$ mJy at $\alpha = 10^h15^m16^s.4$, $\delta = +22°04'47''$ and $S_P = 20.2$ mJy at $\alpha = 10^h15^m20^s.9$, $\delta = +22°04'30''$) is not well centered on the galaxy. S does not include the $S_P = 2.0$ mJy source at $\alpha = 10^h15^m07^s.3$, $\delta = +22°02'38''$. [1.49 GHz VLA D-array map in Gioia and Fabbiano (1987).]

NGC 3198.—S does not include the two northern peaks.

NGC 3227.—S does not include the $S_I = 6.4$ mJy source at $\alpha = 10^h20^m43^s.6$, $\delta = +20°09'03''$ produced by NGC 3226 (optical position: $\alpha = 10^h20^m43^s.5$, $\delta = +20°09'07''$). [4.885 GHz partial-VLA map of the nucleus in Ulvestad, Wilson, and Sramek (1981).]

IC 2574.—Low T_B, uncertain S. The $S_P = 4.1$ mJy component at $\alpha = 10^h25^m03^s.0$, $\delta = +68°43'31''$ coincides with the bright complex containing H II regions I and II of Sandage and Tammann (1974). The $S_P = 0.7$ mJy source at $\alpha = 10^h25^m07^s.7$, $\delta = +68°40'39''$ coincides with their H II region III.

NGC 3310.—The low-brightness western extension of the radio source covers the optical "bow and arrow." [1.465 GHz VLA C-array maps in Condon (1983) and Hummel *et al.* (1985); high-resolution VLA maps at 2, 6, and 20 cm in Duric *et al.* (1986); 610 and 4995 MHz WSRT maps in van der Kruit and de Bruyn (1976); partial–VLA $\lambda = 6$ cm maps of the core in Balick and Heckman (1981); 2.7 and 8.1 GHz NRAO interferometer maps in Seaquist and Bignell (1977).]

NGC 3319.—The $S_P = 2.4$ mJy component at $\alpha = 10^h36^m08^s.3$, $\delta = +41°56'32''$ may be a background source. S does not include the $S_P = 19.4$ mJy source at $\alpha = 10^h36^m27^s.2$, $\delta = +42°00'06''$. [1.49 GHz VLA D-array map in Gioia and Fabbiano (1987).]

NGC 3338.—The $S_P = 7.7$ mJy peak at $\alpha = 10^h39^m23^s.2$, $\delta = +14°00'15''$ may indicate confusion.

NGC 3344.—S does not include the $S_P = 13.3$ mJy source at $\alpha = 10^h40^m51^s.1$, $\delta = +25°06'49''$ or the $S_P = 47.2$ mJy source at $\alpha = 10^h40^m57^s.6$, $\delta = +25°08'08''$.

NGC 3351.—Confused by the $S_I = 46.7$ mJy source at $\alpha = 10^h41^m22^s.1$, $\delta = +11°59'14''$. S does not include the $S_P = 16.4$ mJy source at $\alpha = 10^h41^m23^s.9$, $\delta = +11°55'49''$.

NGC 3368.—S includes only the component centered on the galaxy.

NGC 3423.—S does not include the $S_P = 1.5$ mJy source at $\alpha = 10^h48^m47^s.5$, $\delta = +06°08'26''$.

NGC 3432.—S does not include the $S_P = 28.0$ mJy source at $\alpha = 10^h49^m48^s.7$, $\delta = +36°56'58''$. [1.49 GHz VLA D-array map in Gioia and Fabbiano (1987); 1415 MHz WSRT map in van der Kruit (1973*b*).]

NGC 3504.—S does not include the $S_I = 4.9$ mJy source at $\alpha = 11^h00^m32^s.6$, $\delta = +28°12'46''$. [4.86 GHz VLA D-array map in Gioia and Fabbiano (1987); 1.465 and 4.885 GHz partial–VLA maps of the nucleus in Ulvestad, Wilson, and Sramek (1981).]

NGC 3513.—S does not include the $S_P = 19.4$ mJy source at $\alpha = 11^h01^m27^s.3$, $\delta = -22°56'20''$.

NGC 3521.—S does not include the double confusing source with $S_I = 106$ mJy at $\alpha = 11^h03^m19^s.4$, $\delta = +00°12'55''$ and $S_I = 115$ mJy at $\alpha = 11^h03^m22^s.7$, $\delta = +00°12'22''$.

NGC 3556.—[VLA D-array maps at 1.49 and 4.86 GHz in Gioia and Fabbiano (1987); WSRT maps at 610, 1410, and 4995 MHz in de Bruyn and Hummel (1979); 10.7 GHz 100 m telescope map in Klein, Wielebinski, and Beck (1984*a*).]

NGC 3621.—S does not include the $S_P = 1.5$ mJy source at $\alpha = 11^h16^m04^s.5$, $\delta = -32°31'14''$.

NGC 3623.—Badly confused by the $S_I = 14.7$ mJy source at $\alpha = 11^h16^m20^s.0$, $\delta = +13°20'31''$.

NGC 3627.—The double-peaked radio "bar" with major-axis P.A. approximately 165° is also visible in the 10.7 GHz 100 m telescope map (Urbanik, Gräve, and Klein 1985).

NGC 3628.—[2.68 and 4.75 GHz 100 m telescope maps in Schlickeiser, Werner, and Wielebinski (1984); 4885 MHz VLA A-array map of the central region in Condon *et al.* (1982).]

NGC 3646.—The $S_P = 17.9$ mJy radio peak at $\alpha = 11^h19^m01^s.9$, $\delta = +20°26'10''$ coincides with the edge of the optical ring. [1.465 GHz VLA C-array map in Hummel *et al.* (1985).]

NGC 3642.—S does not include the faint southern extension. 1.465 GHz VLA C-array map in Hummel *et al.* (1985).

NGC 3675.—[1.49 GHz VLA D-array map in Gioia and Fabbiano (1987).]

NGC 3686.—[1.465 GHz VLA C-array map in Hummel *et al.* (1985).]

NGC 3705.—S does not include the $S_P = 1.9$ mJy source at $\alpha = 11^h27^m31^s.3$, $\delta = +09°34'59''$ or the faint southwest extension.

NGC 3718.—S includes the entire source enclosed by the lowest contour in the contour map. [1.49 GHz VLA D-array map in Gioia and Fabbiano (1987).]

NGC 3726.—S does not include the $S_I = 23.3$ mJy confusing (?) source at $\alpha = 11^h30^m42^s.7$, $\delta = +47°19'15''$.

NGC 3877.—S does not include the $S_P = 2.1$ mJy source at $\alpha = 11^h43^m22^s.2$, $\delta = +47°48'13''$.

NGC 3887.—Asymmetric radio source. The $S_P = 9.5$ mJy peak at $\alpha = 11^h44^m31^s.1$, $\delta = -16°34'15''$ lies on an optically bright H II region. [1.465 GHz VLA C-array map in Hummel *et al.* (1985).]

NGC 3893.—S does not include the $S_P = 0.9$ mJy source at $\alpha = 11^h46^m06^s.9$, $\delta = +48°56'36''$.

NGC 3898.—Badly confused. S does not include the $S_I = 17.1$ mJy source at $\alpha = 11^h46^m47^s.7$, $\delta = +56°21'38''$. [1.49 GHz VLA D-array map in Gioia and Fabbiano (1987).]

NGC 3949.—Double core source resolved by the 1.465 GHz VLA C-array map in Hummel *et al.* (1985).

NGC 3953.—S does not include the $S_P = 0.9$ mJy source at $\alpha = 11^h51^m28^s.3$, $\delta = +52°39'17''$. Southern extension of radio peak on bright H II region? [1.465 GHz VLA C-array map in Hummel *et al.* (1985).]

NGC 3982.—[1.49 GHz VLA D-array map in Gioia and Fabbiano (1987).]

NGC 4013.—S does not include the $S_P = 1.7$ mJy source at $\alpha = 11^h56^m03^s.5$, $\delta = +44°11'53''$.

NGC 4027.—Radio peak at $\alpha = 11^h56^m57^s.3$, $\delta = -18°59'19''$. Asymmetric northwestern extension coincides with a large spiral arm. S does not include the $S_P = 1.3$ mJy source at $\alpha = 11^h56^m46^s.8$, $\delta = -18°59'15''$.

NGC 4038.—S includes NGC 4039 (optical position $\alpha = 11^h59^m20^s.2$, $\delta = -18°36'21''$) but not the two faint western peaks. [Partial–VLA maps at 1.465 and 4.885 GHz in Hummel and van der Hulst (1986).]

NGC 4041.—[1.465 GHz VLA C-array maps in Condon (1983) and Hummel *et al.* (1985).]

NGC 4051.—[1.465 GHz VLA C-array map in Hummel *et al.* (1985); 1465 and 4885 MHz VLA A-array maps of the core in Ulvestad and Wilson (1984).]

NGC 4088.—S does not include the $S_P = 4.1$ mJy source at $\alpha = 12^h02^m57^s.2$, $\delta = +50°46'41''$. [1.465 GHz VLA C-array map in Hummel *et al.* (1985).]

NGC 4136.—S does not include the $S_P = 1.1$ mJy source at $\alpha = 12^h06^m47^s.9$, $\delta = +30°14'31''$.

NGC 4145.—Low T_B, uncertain S. S includes all components shown in the contour map.

NGC 4151.—S does not include the $S_P = 13.3$ mJy source at $\alpha = 12^h08^m02^s.4$, $\delta = +39°43'24''$. [4.885 GHz VLA maps of the nucleus in Ulvestad, Wilson, and Sramek (1981) and Condon *et al.* (1982); 1485 and 4885 MHz partial–VLA maps of the nucleus in Johnston *et al.* (1982); 14.985 GHz VLA A-array map of the nucleus in Wilson and Ulvestad (1982);

1666 MHz MTRLI map of the core in Booler, Pedlar, and Davies (1982).]

NGC 4157.—S does not include the $S_I = 62.3$ mJy source at $\alpha = 12^h08^m42^s.3$, $\delta = +50°48'18''$. [1.49 GHz VLA D-array map in Gioia and Fabbiano (1987); 1.465 GHz VLA C-array map in Condon (1983).]

NGC 4178.—The $S_P = 5.9$ mJy radio peak at $\alpha = 12^h10^m09^s.9$, $\delta = +11°07'40''$ coincides with an optically bright knot at the southwest tip of the galaxy (cf. Schanberg 1972).

NGC 4214.—S includes the $S_P = 1.5$ mJy source at $\alpha = 12^h13^m05^s.2$, $\delta = +36°39'02''$ that appears to coincide with optically bright H II regions. [1419 MHz Cambridge Half-Mile Telescope map in Allsopp (1979).]

NGC 4216.—The radio peak is significantly east of the optical position.

NGC 4236.—Low T_B, very uncertain S. S includes the $S_P = 0.9$ mJy component at $\alpha = 12^h14^m03^s.9$, $\delta = +69°47'50''$ and the $S_P = 1.6$ mJy component at $\alpha = 12^h14^m43^s.9$, $\delta = +69°40'28''$.

NGC 4244.—Low T_B, very uncertain S. S includes the $S_P = 1.5$ mJy component at $\alpha = 12^h14^m39^s.8$, $\delta = +38°01'35''$ and the $S_P = 1.4$ mJy component at $\alpha = 12^h15^m18^s.9$, $\delta = +38°08'28''$.

NGC 4242.—Radio variable? $S = 8$ mJy in the 1.49 GHz VLA D-array map in Gioia and Fabbiano (1987) not centered on the optical galaxy.

NGC 4254.—S does not include the $S_P = 3.4$ mJy source at $\alpha = 12^h16^m22^s.7$, $\delta = +14°45'30''$. The $S_P = 22.6$ mJy peak at $\alpha = 12^h16^m13^s.5$, $\delta = +14°43'19''$ is probably caused by confusion (see the 1.465 GHz VLA C-array map in Condon 1983). [10.7 GHz 100 m telescope map in Urbanik, Klein, and Gräve (1986).]

NGC 4258.—Not observed. $S = [790]$ mJy estimated using $S = 0.83$ Jy at 1400 MHz from the NRAO 91 m telescope sky maps (Condon and Broderick 1985), converted to 1.49 GHz assuming $\alpha \approx +0.75$. [1412 MHz WSRT map in van Albada (1980); 610 MHz map in de Bruyn (1977*b*); 1.465 GHz VLA C-array map in Hummel *et al.* (1985); combined VLA and WSRT 1.48 GHz maps in van Albada and van der Hulst (1982); 4.75 and 10.7 GHz 100 m telescope maps in Krause, Beck, and Klein (1984); 10.7 GHz map in Klein and Emerson (1981).]

NGC 4274.—S does not include the $S_I = 3.8$ mJy source at $\alpha = 12^h17^m10^s.5$, $\delta = +29°52'44''$. [1.49 GHz VLA D-array map in Gioia and Fabbiano (1987).]

NGC 4303.—S does not include the $S_P = 11.5$ mJy source at $\alpha = 12^h19^m10^s.2$, $\delta = +04°46'13''$. [1.465 GHz VLA C-array map in Condon (1983).]

NGC 4314.—[1.49 GHz VLA D-array map in Gioia and Fabbiano (1987).]

NGC 4321.—$S = [340]$ mJy estimated using $S = 0.36$ Jy at 1400 MHz from the NRAO 91 m telescope sky maps (Condon and Broderick 1985), converted to 1.49 GHz assuming $\alpha \approx +0.75$. $S = 230$ mJy in the VLA map. The extension southeast of the nucleus produced by SN 1979C (Weiler *et al.* 1981) is resolved in the 1.465 GHz VLA C-array map in Hummel *et al.* (1985). [1415 MHz WSRT map in van der Kruit (1973*b*); 10.7 GHz 100 m telescope map in Urbanik, Klein, and Gräve (1986).]

NGC 4388.—[VLA $\lambda = 6$ cm map of the central region in Hummel, van Gorkom, and Kotanyi (1983).]

NGC 4395.—S does not include the $S_P = 28.1$ mJy confusing (?) source at $\alpha = 12^h23^m30^s.9$, $\delta = +33°50'20''$ that lies in an empty field on the POSS prints. [1.49 GHz VLA D-array map in Gioia and Fabbiano (1987).]

NGC 4414.—[1.465 GHz VLA C-array map in Condon (1983).]

NGC 4438.—Map degraded by sidelobe response to 3C 274. S does not include the $S_P = 10.8$ mJy source at $\alpha = 12^h25^m19^s.8$, $\delta = +13°20'16''$. [1.4 GHz WSRT map in Kotanyi and Ekers (1983); VLA $\lambda = 6$ cm map of the central region in Hummel, van Gorkom, and Kotanyi (1983).]

NGC 4449.—S does not include the $S_P = 4.9$ mJy source at $\alpha = 12^h25^m40^s.3$, $\delta = +44°18'25''$. The northern extension of the peak covers the supernova remnant shown in the VLA D-array $\lambda = 6$ cm map in Bignell and Seaquist (1983) as well as a complex of H II regions (Crillon and Monnet 1969). [2.7 GHz NRAO interferometer map in Seaquist and Bignell (1978); 24.5 GHz 100 m telescope map in Klein and Gräve (1986).]

NGC 4448.—[1.49 GHz VLA D-array map in Gioia and Fabbiano (1987).]

NGC 4450.—S does not include the faint eastern extension.

NGC 4490.—S includes NGC 4485, visible as the northern extension to the main source. [1.49 GHz VLA D-array map in Gioia and Fabbiano (1987); 1415 and 4995 MHz WSRT maps in Viallefond, Allen, and de Boer (1980); 1.465 GHz VLA C-array map in Condon (1983); 2.7 and 8.1 GHz NRAO interferometer maps in Seaquist, Davis, and Bignell (1978); 10.7 GHz 100 m telescope maps in Klein and Emerson (1981) and Klein, Gräve, and Wielebinski (1983); 24.5 GHz map in Klein (1983).]

NGC 4496.—The $S_P = 14.3$ mJy offset radio peak at $\alpha = 12^h29^m07^s.8$, $\delta = +04°12'11''$ coincides with an optically bright H II region.

NGC 4501.—S does not include the $S_P = 1.8$ mJy source at $\alpha = 12^h29^m25^s.3$, $\delta = +14°38'54''$ or the $S_P = 0.7$ mJy source at $\alpha = 12^h29^m38^s.7$, $\delta = +14°39'29''$. [10.7 GHz 100 m telescope map in Urbanik, Klein, and Gräve (1986).]

NGC 4504.—Not detected?

NGC 4517.—S does not include the $S_I = 4.1$ mJy source at $\alpha = 12^h30^m16^s.3$, $\delta = +00°24'52''$.

NGC 4527.—[1.465 GHz VLA C-array map in Hummel *et al.* (1985).]

NGC 4536.—S does not include the $S_P = 4.0$ mJy source at $\alpha = 12^h32^m02^s.6$, $\delta = +02°26'21''$ or the $S_P = 2.5$ mJy source at $\alpha = 12^h32^m07^s.2$, $\delta = +02°25'30''$. [1.465 GHz VLA C-array map in Hummel *et al.* (1985); 1413 MHz VLA A-array map of the central region in Condon *et al.* (1982).]

NGC 4548.—Detected? Confusion?

NGC 4559.—S does not include the $S_P = 2.1$ mJy source at $\alpha = 12^h33^m40^s.3$, $\delta = +28°14'22''$. [1.49 GHz VLA D-array map in Gioia and Fabbiano (1987).]

NGC 4565.—[1.49 GHz VLA D-array map in Gioia and Fabbiano (1987).] The 1414 MHz WSRT map of Broeils and Sancisi (1985) shows an unresolved 1.3 mJy central source at $\alpha = 12^h33^m52^s.1$, $\delta = +26°15'47''$. Both 610 and 1412 MHz

WSRT maps in Ekers and Sancisi (1977). A 1410 MHz WSRT map appears in Hummel, Sancisi, and Ekers (1984).

NGC 4568.—S includes NGC 4567 (optical position: $\alpha = 12^h34^m01^s.1$, $\delta = +11°32'01''$) but does not include the faint southeastern radio extension.

NGC 4569.—[10.7 GHz 100 m telescope map in Urbanik, Klein, and Gräve (1986).]

NGC 4579.—Map degraded by sidelobe response to 3C 274.

NGC 4593.—Badly confused by the $S_I = 18.4$ mJy source at $\alpha = 12^h37^m02^s.6$, $\delta = -05°05'23''$.

NGC 4596.—Not detected.

NGC 4605.—S includes only the main radio component centered on the galaxy.

NGC 4618.—The southern extension of the radio source coincides with an optically bright hooked arm. [1.49 GHz VLA D-array map in Gioia and Fabbiano (1987).]

NGC 4631.—[1.49 GHz VLA D-array map in Gioia and Fabbiano (1987); WSRT maps at 610 and 1412 MHz in Ekers and Sancisi (1977); 4995 MHz map in de Bruyn (1977*b*); 2.7 and 8.1 GHz NRAO interferometer maps in Duric, Crane, and Seaquist (1982); 327 MHz OSRT map in Sukumar and Velusamy (1985); 4800 MHz 100 m telescope map in Wielebinski and von Kap-herr (1977); 10.7 GHz map in Klein, Wielebinski, and Beck (1984*a*).]

NGC 4651.—Confused by the $S_I = 2.75$ Jy quasar 3C 275.1 at $\alpha = 12^h41^m27^s.4$, $\delta = +16°39'18''$ (cf. Sandage, Véron, and Wyndham 1965).

NGC 4654.—[1.465 GHz VLA C-array map in Condon (1983).]

NGC 4656.—S includes all components surrounded by the lowest contour enclosing the galaxy position. Gaussian fit to central component only. [1.49 GHz VLA D-array map in Gioia and Fabbiano (1987).]

NGC 4666.—[1.465 GHz VLA C-array map in Condon (1983).]

NGC 4689.—[1.465 GHz VLA C-array map in Hummel *et al.* (1985).]

NGC 4691.—S does not include the $S_I = 8.5$ mJy confusing source at $\alpha = 12^h45^m44^s.2$, $\delta = -03°04'18''$.

NGC 4698.—Detected? Confusion?

NGC 4725.—Low T_B, confused? S does not include the $S_P = 7.8$ mJy source at $\alpha = 12^h48^m13^s.6$, $\delta = +25°44'32''$. [1.49 GHz VLA D-array map in Gioia and Fabbiano (1987).]

NGC 4731.—S does not include the $S_P = 2.1$ mJy source at $\alpha = 12^h48^m34^s.4$, $\delta = -06°07'27''$.

NGC 4736.—S does not include the $S_P = 2.9$ mJy source at $\alpha = 12^h48^m13^s.5$, $\delta = +41°21'38''$. [1.49 GHz VLA D-array map in Gioia and Fabbiano (1987); WSRT maps at 610, 1415, and 4995 MHz in de Bruyn (1977*a*); partial–VLA map at 4885 MHz in van der Hulst, Crane, and Keel (1981); 10.7 GHz 100 m telescope map in Klein and Emerson (1981).]

NGC 4775.—S does not include the $S_I = 3.3$ mJy source at $\alpha = 12^h51^m03^s.5$, $\delta = -06°20'57''$.

NGC 4781.—S does not include the faint southern extension.

NGC 4826.—[1.49 GHz VLA D-array map in Gioia and Fabbiano (1987); 10.7 GHz 100 m telescope map in Klein and Emerson (1981).]

NGC 4866.—Not detected. Confused by the $S_I = 8.0$ mJy source at $\alpha = 12^h56^m51^s.5$, $\delta = +14°26'32''$.

NGC 4902.—S includes only the main Gaussian component.

NGC 4939.—[1.465 GHz VLA C-array map in Hummel *et al.* (1985).]

NGC 4981.—[1.465 GHz VLA C-array map in Hummel *et al.* (1985).]

NGC 5005.—S does not include the faint eastern or western extensions. 1.465 GHz VLA C-array map in Hummel *et al.* (1985).

NGC 5023.—Not detected.

NGC 5033.—S does not include the $S_P = 2.1$ mJy source at $\alpha = 13^h10^m52^s.1$, $\delta = +36°50'35''$.

NGC 5055.—$S = [390]$ mJy estimated using $S = 0.42$ Jy at 1400 MHz from the NRAO 91 m telescope sky maps (Condon and Broderick 1985), converting to 1.49 GHz assuming $\alpha \approx +0.75$, and subtracting the $S_I = 11.9$ mJy confusing (?) source at $\alpha = 13^h13^m50^s.3$, $\delta = +42°18'33''$. $S = 332$ mJy appears in the VLA map. [1.465 GHz VLA C-array map in Hummel *et al.* (1985); WSRT maps at 610 and 1410 MHz in Hummel and Bosma (1982); 1415 MHz WSRT map in van der Kruit (1973*a*); 10.7 GHz 100 m telescope map in Klein and Emerson (1981).]

NGC 5054.—S does not include the faint southern extension. [1.465 GHz VLA C-array map in Hummel *et al.* (1985).]

NGC 5068.—The radio peaks appear to coincide with bright H II complexes (cf. Hodge 1969).

NGC 5101.—S does not include the $S_P = 1.3$ mJy confusing source at $\alpha = 13^h18^m57^s.7$, $\delta = -27°08'56''$.

NGC 5112.—S does not include the $S_P = 0.7$ mJy source at $\alpha = 13^h19^m32^s.6$, $\delta = +39°01'27''$.

NGC 5170.—S includes all components enclosed in the lowest contour containing the galaxy position.

NGC 5194.—The total flux density $S = [1490]$ mJy was estimated using $S = 1.57$ Jy at 1400 MHz from the NRAO 91 m telescope sky maps (Condon and Broderick 1985) and converting to 1.49 GHz assuming $\alpha \approx +0.75$. $S = 1234$ mJy in the VLA map includes NGC 5195 (optical position $\alpha = 13^h27^m52^s.4$, $\delta = +47°31'48''$), visible as the $S_P = 47.4$ mJy peak at $\alpha = 13^h27^m53^s.8$, $\delta = +47°31'09''$ on the map, but not the $S_P = 24.9$ mJy confusing source at $\alpha = 13^h28^m09^s.5$, $\delta = +47°25'52''$. [1.465 GHz VLA C-array map in Condon (1983); WSRT maps at 610 and 1415 MHz in Segalovitz (1977*a*); VLA maps of the core at 6 and 20 cm in Ford *et al.* (1985); 10.7 GHz 100 m telescope map in Klein and Emerson (1981); 14.7 and 22.8 GHz maps in Klein, Wielebinski, and Beck (1984*b*).]

NGC 5236.—[1.465 GHz VLA C-array map in Condon (1983); 843 MHz MOST map in Harnett (1984); 1465 MHz VLA B + C-array map and 4885 MHz C-array map of the bar region in Ondrechen (1985); 1413 MHz VLA A-array map of the central region in Condon *et al.* (1982).]

NGC 5248.—Confused by the $S_I = 123$ mJy source at $\alpha = 13^h35^m00^s.1$, $\delta = +09°10'14''$. [1.465 GHz VLA C-array map in Hummel *et al.* (1985).]

NGC 5247.—The $S_P = 3.3$ mJy component at $\alpha = 13^h35^m15^s.8$, $\delta = -17°39'13''$ coincides with optically bright knots in the southwestern spiral arm. S does not include the $S_P = 1.6$ mJy source at $\alpha = 13^h35^m14^s.1$, $\delta = -17°34'07''$ or the $S_P = 1.9$ mJy source at $\alpha = 13^h35^m19^s.5$, $\delta = -17°35'01''$. 1.465 GHz VLA C-array map in Hummel *et al.* (1985).

NGC 5334.—Badly confused by the $S_P = 7.9$ mJy source at $\alpha = 13^h50^m27^s.1$, $\delta = -00°51'09''$.

NGC 5371.—S does not include the $S_P = 1.7$ mJy source at $\alpha = 13^h53^m34^s.3$, $\delta = +40°45'08''$. The lowest radio contours twist to match the optical major-axis P.A. 0°. Asymmetric central component resolved by the 1.465 GHz VLA C-array map in Hummel *et al.* (1985).

NGC 5364.—Badly confused. S includes only the component centered on the galaxy position.

NGC 5457.—The total flux density $S = [750]$ mJy was estimated using $S = 0.77$ Jy at 1400 MHz from the NRAO 91 m telescope sky maps (Condon and Broderick 1985) and converting to 1.49 GHz with $\alpha \approx +0.4$ (Israel, Goss, and Allen 1975). [1.49 GHz VLA D-array map in Gioia and Fabbiano (1987); 610 and 1415 MHz WSRT maps in Israel, Goss, and Allen (1975).]

NGC 5474.—The radio source lies on the bright "eccentric nucleus" (Nilson 1973) at the northern edge of the galaxy.

NGC 5566.—S does not include the $S_P = 7.6$ mJy source at $\alpha = 14^h17^m45^s.2$, $\delta = +04°06'56''$.

NGC 5585.—Not detected?

NGC 5584.—Off-nuclear peak at $\alpha = 14^h19^m51^s.7$, $\delta = -00°09'47''$ coincides with a bright H II region?

NGC 5643.—[VLA A/B-array maps at 1.49 and 4.86 GHz in Morris *et al.* (1985).]

NGC 5669.—S does not include the $S_P = 0.7$ mJy source at $\alpha = 14^h30^m07^s.6$, $\delta = +10°06'37''$.

NGC 5676.—S does not include the faint northern extension, which is resolved into two background (?) sources by the 1.465 GHz VLA C-array maps in Condon (1983) and Hummel *et al.* (1985).

NGC 5701.—Not detected.

NGC 5713.—[1.465 GHz VLA C-array map in Condon (1983).]

NGC 5746.—Badly confused by the $S_P = 34.4$ mJy source at $\alpha = 14^h42^m24^s.4$, $\delta = +02°12'17''$ and the $S_P = 25.1$ mJy source at $\alpha = 14^h42^m26^s.0$, $\delta = +02°13'27''$.

NGC 5907.—Confused by the $S_I = 34.5$ mJy source at $\alpha = 15^h14^m44^s.8$, $\delta = +56°27'09''$ and the $S_I = 29.1$ mJy source at $\alpha = 15^h14^m45^s.7$, $\delta = +56°27'57''$. [1410 MHz WSRT map in Hummel, Sancisi, and Ekers (1984).]

NGC 5921.—[1.465 GHz VLA C-array map in Hummel *et al.* (1985).]

NGC 5985.—S includes only the main radio component on the galaxy position. [1.49 GHz VLA D-array map in Gioia and Fabbiano (1987).]

NGC 6015.—S does not include the $S_P = 1.0$ mJy source at $\alpha = 15^h50^m27^s.8$, $\delta = +62°27'47''$.

NGC 6118.—Confused?

NGC 6140.—Not detected?

NGC 6217.—S does not include the faint southwestern extension. [1.465 GHz VLA C-array map in Hummel *et al.* (1985); 4.885 GHz VLA A-array map of the core in Hummel, van der Hulst, and Dickey (1984).]

NGC 6340.—Not detected. Confused by the $S_I = 7.0$ mJy unresolved (< 0'.2 FWHM) source at $\alpha = 17^h11^m14^s.7$, $\delta = +72°21'24''$.

NGC 6384.—S does not include the faint southeastern extension.

NGC 6503.—Near the $S_I = 1212$ mJy point source 1749+70.1 at $\alpha = 17^h49^m03^s.6$, $\delta = +70°06'40''$ identified with a BL Lac object (Arp *et al.* 1976).

NGC 6643.—S does not include the $S_P = 2.1$ mJy source at $\alpha = 18^h20^m24^s.5$, $\delta = +74°32'19''$

NGC 6822.—The $S_I = 11.7$ mJy extended (1'.2 × 0'.5 in P.A. 122°) source centered on $\alpha = 19^h41^m43^s.3$, $\delta = -14°49'27''$ covers Hodge's (1977) H II regions 2 and 4. The $S_I = 20.2$ mJy source at $\alpha = 19^h42^m02^s.9$, $\delta = -14°50'30''$ coincides with his H II region No. 9 and the $S_I = 8.8$ mJy source at $\alpha = 19^h42^m15^s.5$, $\delta = -14°50'38''$ with No. 14. The faint ($S_I = 2.1$ mJy) source at $\alpha = 19^h42^m06^s.9$, $\delta = -14°55'45''$ is close to H II region 12 (optical position $\alpha = 19^h42^m06^s.1$, $\delta = -14°55'49''$) and may be a supernova remnant (cf. Dickel, D'Odorico, and Silverman 1985). S does not include any of the remaining discrete sources visible in the contour map. [10.7 GHz 100 m telescope map in Klein, Gräve, and Wielebinski (1983); 4.75 GHz map in Klein and Gräve (1986).]

NGC 6907.—[1.465 GHz VLA C-array map in Hummel *et al.* (1985).]

NGC 6946.—[VLA D-array maps at 1.49 and 4.86 GHz in Gioia and Fabbiano (1987); WSRT maps at 610, 1415, and 4995 MHz in van der Kruit, Allen, and Rots (1977); VLA maps with 1" resolution at 6 and 2 cm of core in Turner and Ho (1985); 10.7 GHz 100 m telescope map in Klein *et al.* (1982).]

NGC 7184.—Double-peaked brightness distribution.

NGC 7217.—S does not include the faint southwestern extension. 1.49 GHz VLA D-array map in Gioia and Fabbiano (1987).

NGC 7314.—[1.465 GHz VLA C-array map in Hummel *et al.* (1985).]

NGC 7331.—The radio core is resolved in the 1.465 GHz VLA C-array map in Hummel *et al.* (1985). [1415 MHz WSRT map in van der Kruit (1973*b*); WSRT maps at 610 and 1410 MHz in Hummel and Bosma (1982); 10.7 GHz 100 m telescope map in Klein, Wielebinski, and Beck (1984*a*).]

NGC 7418.—S does not include the $S_P = 0.8$ mJy source at $\alpha = 22^h53^m44^s.7$, $\delta = -37°15'38''$.

NGC 7424.—Low T_B, very uncertain S. S does not include the $S_P = 40.6$ mJy source at $\alpha = 22^h54^m39^s.9$, $\delta = -41°18'46''$.

NGC 7479.—S does not include the $S_P \approx 8.9$ mJy confusing (?) source at $\alpha = 23^h02^m24^s.8$, $\delta = +12°04'48''$. The southwest radio extension corresponds to a large spiral arm.

NGC 7496.—S does not include the $S_I = 2.3$ mJy source at $\alpha = 23^h06^m57^s.7$, $\delta = -43°39'55''$.

NGC 7541.—[1.465 GHz VLA C-array map in Hummel *et al.* (1985).]

NGC 7552.—[1415 MHz FST map in Ward *et al.* (1980).]

NGC 7582.—[1415 MHz FST map in Ward *et al.* (1980); 1465 and 4885 MHz VLA A-array maps of the core in Ulvestad and Wilson (1984).]

NGC 7606.—S does not include the $S_P = 4.8$ mJy source at $\alpha = 23^h16^m30^s.5$, $\delta = -08°48'23''$.

IC 5332.—Detected?

NGC 7713.—S includes the main radio component on the galaxy position only.

NGC 7723.—S includes the main radio component on the galaxy position only.

NGC 7741.—S does not include the $S_P = 1.0$ mJy source at $\alpha = 23^h41^m19\overset{s}{.}4$, $\delta = +25°50'12''$. [1.49 GHz VLA D-array map in Gioia and Fabbiano (1987).]

NGC 7793.—S does not include the $S_P = 5.1$ mJy source at $\alpha = 23^h54^m55\overset{s}{.}6$, $\delta = -32°54'10''$ or the $S_P = 2.0$ mJy source at $\alpha = 23^h55^m10\overset{s}{.}9$, $\delta = -32°55'49''$. [843 MHz MOST map in Harnett (1986).]

DDO 221.—Low T_B, very uncertain S.

REFERENCES

Allen, R. J., Baldwin, J. E., and Sancisi, R. 1978, *Astr. Ap.*, **62**, 397.
Allsopp, N. J. 1979, *M.N.R.A.S.*, **188**, 765.
Arp, H. 1968, *Astrofisika*, **4**, 59.
______. 1970, *Ap. Letters*, **5**, 257.
Arp, H., and Sulentic, J. W. 1979, *Ap. J.*, **229**, 496.
Arp, H., Sulentic, J. W., Willis, A. G., and de Ruiter, H. R. 1976, *Ap. J.* (*Letters*), **207**, L13.
Baars, J. W. M., Genzel, R., Pauliny-Toth, I. I. K., and Witzel, A. 1977, *Astr. Ap.*, **61**, 99.
Baker, J. R., Haslam, C. G. T., Jones, B. B., and Wielebinski, R. 1977, *Astr. Ap.*, **59**, 261.
Balick, B., and Heckman, T. 1981, *Astr. Ap.*, **96**, 271.
Bash, F. N., and Kaufman, M. 1986, *Ap. J.*, **310**, 621.
Beck, R., Biermann, P., Emerson, D. T., and Wielebinski, R. 1979, *Astr. Ap.*, **77**, 25.
Bignell, R. C., and Seaquist, E. R. 1983, *Ap. J.*, **270**, 140.
Booler, R. V., Pedlar, A., and Davies, R. D. 1982, *M.N.R.A.S.*, **199**, 229.
Broeils, A. H., and Sancisi, R. 1985, *Astr. Ap.*, **153**, 281.
Burstein, D., Condon, J. J., and Yin, Q. F. 1987, *Ap. J.* (*Letters*), **315**, L99.
Condon, J. J. 1974, *Ap. J.*, **188**, 279.
______. 1983, *Ap. J. Suppl.*, **53**, 459.
Condon, J. J., and Broderick, J. J. 1985, *A.J.*, **90**, 2540.
______. 1986, *A.J.*, **91**, 1051.
Condon, J. J., Condon, M. A., Gisler, G., and Puschell, J. J. 1982, *Ap. J.*, **252**, 102.
Condon, J. J., and Dressel, L. L. 1978, *Ap. J.*, **221**, 456.
Condon, J. J., Yin, Q. F., and Burstein, D. 1987, *Ap. J. Suppl.*, **65**, 543.
Crillon, R., and Monnet, G. 1969, *Astr. Ap.*, **1**, 449.
de Bruyn, A. G. 1977*a*, *Astr. Ap.*, **54**, 491.
______. 1977*b*, *Astr. Ap.*, **58**, 221.
de Bruyn, A. G., and Hummel, E. 1979, *Astr. Ap.*, **73**, 196.
Dennison, B., Balonek, T. J., Terzian, Y., and Balick, B. 1975, *Publ. A.S.P.*, **87**, 83.
de Vaucouleurs, G., de Vaucouleurs, A., and Corwin, H. G. 1976, *Second Reference Catalogue of Bright Galaxies* (Austin: University of Texas Press) (RC2).
Dickel, J. R., D'Odorico, S., and Silverman, A. 1985, *A.J.*, **90**, 414.
Dressel, L. L., and Condon, J. J. 1976, *Ap. J. Suppl.*, **31**, 187.
Duric, N., Crane, P. C., and Seaquist, E. R. 1982, *A.J.*, **87**, 1671.
Duric, N., and Seaquist, E. R. 1986, *Canadian J. Phys.*, **64**, 531.
Duric, N., Seaquist, E. R., Crane, P. C., Bignell, R. C., and Davis, L. E. 1983, *Ap. J.* (*Letters*), **273**, L11.
Duric, N., Seaquist, E. R., Crane, P. C., and Davis, L. E. 1986, *Ap. J.*, **304**, 82.
Ekers, R. D., and Sancisi, R. 1977, *Astr. Ap.*, **54**, 973.
Ford, H. C., Crane, P., Jacoby, G. H., Lawrie, D. G., and van der Hulst, J. M. 1985, *Ap. J.*, **293**, 132.
Gallouët, L., Heidmann, N., and Dampierre, F. 1975, *Astr. Ap. Suppl.*, **19**, 1.
Gioia, I. M., and Fabbiano, G. 1987, *Ap. J. Suppl.*, **63**, 771.
Harnett, J. I. 1984, *M.N.R.A.S.*, **210**, 13.
______. 1986, *Proc. Astr. Soc. Australia*, **6**, 235.
Harnett, J. I., and Reynolds, J. E. 1985, *M.N.R.A.S.*, **215**, 247.
Hodge, P. W. 1969, *Ap. J. Suppl.*, **18**, 73.
______. 1977, *Ap. J. Suppl.*, **33**, 69.
Hummel, E. 1980, *Astr. Ap. Suppl.*, **41**, 151.
Hummel, E., and Bosma, A. 1982, *A.J.*, **87**, 242.
Hummel, E., Dettmar, R.-J., and Wielebinski, R. 1986, *Astr. Ap.*, **166**, 97.
Hummel, E., Pedlar, A., van der Hulst, J. M., and Davies, R. D. 1985, *Astr. Ap. Suppl.*, **60**, 293.
Hummel, E., Sancisi, R., and Ekers, R. D. 1984, *Astr. Ap.*, **133**, 1.
Hummel, E., Smith, P., and van der Hulst, J. M. 1984, *Astr. Ap.*, **137**, 138.
Hummel, E., and van der Hulst, J. M. 1986, *Astr. Ap.*, **155**, 151.
Hummel, E., van der Hulst, J. M., and Dickey, J. M. 1984, *Astr. Ap.*, **134**, 207.
Hummel, E., van Gorkom, J. H., and Kotanyi, C. G. 1983, *Ap. J.* (*Letters*), **267**, L5.
Israel, F. P., Goss, W. M., and Allen, R. J. 1975, *Astr. Ap.*, **40**, 421.
Johnston, K. J., Elvis, M., Kjer, D., and Shen, B. S. P. 1982, *Ap. J.*, **262**, 61.
Klein, U. 1983, *Astr. Ap.*, **121**, 150.
Klein, U., Beck, R., Buczilowski, U. R., and Wielebinski, R. 1982, *Astr. Ap.*, **108**, 176.
Klein, U., and Emerson, D. T. 1981, *Astr. Ap.*, **94**, 29.
Klein, U., and Gräve, R. 1986, *Astr. Ap.*, **161**, 155.
Klein, U., Gräve, R., and Wielebinski, R. 1983, *Astr. Ap.*, **117**, 332.
Klein, U., Urbanik, M., Beck, R., and Wielebinski, R. 1983, *Astr. Ap.*, **127**, 177.
Klein, U., Wielebinski, R., and Beck, R. 1984*a*, *Astr. Ap.*, **133**, 19.
______. 1984*b*, *Astr. Ap.*, **135**, 213.
Kotanyi, C. G., and Ekers, R. D. 1983, *Astr. Ap.*, **122**, 267.
Kraan-Korteweg, R. C., and Tammann, G. A. 1979, *Astr. Nach.*, **300**, 181.
Krause, M., Beck, R., and Klein, U. 1984, *Astr. Ap.*, **138**, 385.
Kronberg, P. P., and Biermann, P. 1981, *Ap. J.*, **243**, 89.
Kronberg, P. P., Biermann, P., and Schwab, F. R. 1981, *Ap. J.*, **246**, 751.
______. 1985, *Ap. J.*, **291**, 693.
Lauberts, A. 1982, *The ESO/Uppsala Survey of the ESO (B) Atlas* (Garching: ESO).
Mitchell, K. J., and Condon, J. J. 1985, *A.J.*, **90**, 1957.
Morris, S., Ward, M., Whittle, M., Wilson, A. S., and Taylor, K. 1985, *M.N.R.A.S.*, **216**, 193.
Nilson, P. 1973, *Uppsala General Catalogue of Galaxies* (Uppsala: Uppsala Astronomical Observatory).
Ondrechen, M. P. 1985, *A.J.*, **90**, 1474.
Ondrechen, M. P., and van der Hulst, J. M. 1983, *Ap. J.* (*Letters*), **269**, L47.
Pedlar, A., Booler, R. V., Spencer, R. E., and Stewart, O. J. 1983, *M.N.R.A.S.*, **202**, 647.
Reynolds, J. E., and Harnett, J. I. 1983, *Proc. Astr. Soc. Australia*, **5**, 235.
Rupen, M. P., van Gorkom, J. H., Knapp, G. R., Gunn, J. E., and Schneider, D. P. 1987, *A.J.*, **94**, 61.
Sandage, A. 1971, *Ap. J.*, **186**, 13.
Sandage, A., and Tammann, G. A. 1974, *Ap. J.*, **190**, 525.
______. 1981, *A Revised Shapley-Ames Catalog of Bright Galaxies* (Washington, DC: Carnegie Institution of Washington) (RSA).
Sandage, A., Tammann, G. A., and Yahil, A. 1979, *Ap. J.*, **232**, 352.
Sandage, A., Véron, P., and Wyndham, J. D. 1965, *Ap. J.* (*Letters*), **142**, 1307.
Sandqvist, A., Jörsäter, S., and Lindblad, P. O. 1982, *Astr. Ap.*, **110**, 336.
Schanberg, B. C. 1972, *Ap. J. Suppl.*, **26**, 115.
Schlickeiser, R., Werner, W., and Wielebinski, R. 1984, *Astr. Ap.*, **140**, 277.
Seaquist, E. R., Bell, M. B., and Bignell, R. C. 1985, *Ap. J.*, **294**, 546.
Seaquist, E. R., and Bignell, R. C. 1976, *Astr. Ap.*, **48**, 421.
______. 1977, *Astr. Ap.*, **55**, 163.
______. 1978, *Ap. J.* (*Letters*), **226**, L5.
Seaquist, E. R., Davis, L., and Bignell, R. C. 1978, *Astr. Ap.*, **63**, 199.
Segalovitz, A. 1977*a*, *Astr. Ap.*, **54**, 703.
______. 1977*b*, *Astr. Ap.*, **55**, 203.
Sukumar, S., and Velusamy, T. 1985, *M.N.R.A.S.*, **212**, 367.
Turner, J. L., and Ho, P. T. P. 1983, *Ap. J.* (*Letters*), **268**, L79.
______. 1985, *Ap. J.* (*Letters*), **299**, L77.
Ulvestad, J. S., and Wilson, A. S. 1984, *Ap. J.*, **285**, 439.
Ulvestad, J. S., Wilson, A. S. and Sramek, R. A. 1981, *Ap. J.*, **247**, 419.
Urbanik, M., Gräve, R., and Klein, U. 1985, *Astr. Ap.*, **152**, 291.
Urbanik, M., Klein, U., and Gräve, R. 1986, *Astr. Ap.*, **166**, 107.
van Albada, G. D. 1980, *Astr. Ap. Suppl.*, **39**, 283.
van Albada, G. D., and van der Hulst, J. M. 1982, *Astr. Ap.*, **115**, 263.
van der Hulst, J. M., Crane, P. C., and Keel, W. C. 1981, *A.J.*, **86**, 1175.
van der Hulst, J. M., Hummel, E., and Dickey, J. M. 1982, *Ap. J.* (*Letters*), **261**, L59.
van der Kruit, P. C. 1973*a*, *Astr. Ap.*, **29**, 231.
______. 1973*b*, *Astr. Ap.*, **29**, 249.
van der Kruit, P. C., Allen, R. J., and Rots, A. H. 1977, *Astr. Ap.*, **55**, 421.
van der Kruit, P. C., and de Bruyn, A. G. 1976, *Astr. Ap.*, **48**, 373.

Viallefond, F., Allen, R. J., and de Boer, J. A. 1980, *Astr. Ap.*, **82**, 207.
Viallefond, F., Goss, W. M., van der Hulst, J. M., and Crane, P. C. 1986, *Astr. Ap. Suppl.*, **64**, 237.
von Kap-herr, A., Berkhuijsen, E. M., and Wielebinski, R. 1978, *Astr. Ap.*, **62**, 51.
Walterbos, R. A. M., Brinks, E., and Shane, W. W. 1985, *Astr. Ap. Suppl.*, **61**, 451.
Ward, M., Penston, M. V., Blades, J. C., and Turtle, A. J. 1980, *M.N.R.A.S.*, **193**, 563.
Weiler, K. W., van der Hulst, J. M., Sramek, R. A., and Panagia, N. 1981, *Ap. J. (Letters)*, **243**, L151.
Wells, D. C., Greisen, E. W., and Harten, R. H. 1981, *Astr. Ap. Suppl.*, **44**, 363.
Wielebinski, R., and von Kap-herr, A. 1977, *Astr. Ap.*, **59**, L17.
Wilson, A. S., and Ulvestad, J. S. 1982, *Ap. J.*, **263**, 576.
______. 1983, *Ap. J.*, **275**, 8.
Wolstencroft, R. D., Tully, R. B., and Perley, R. A. 1984, *M.N.R.A.S.*, **207**, 889.
Wynn-Williams, C. G., and Becklin, E. E. 1985, *Ap. J.*, **290**, 108.
Wynn-Williams, C. G., Becklin, E. E., and Scoville, N. Z. 1985, *Ap. J.*, **297**, 607.

J. J. CONDON: National Radio Astronomy Observatory, Edgemont Road, Charlottesville, VA 22903-2475